7th International Conference on
New Developments In Photodetection

Tours, France, June 30th to July 4th **2014**

NDIP

Tutorial SiPMs

Véronique PUILL

cnrs IN2P3 Les deux infinis

LABORATOIRE DE L'ACCÉLÉRATEUR LINÉAIRE

Faculté des sciences d'Orsay

Outline

- The photodetection process in Silicon devices
- The main Si detector characteristics
- From the PIN photodiode to the SiPM
- Caracteristics of SiPM
- Quick look on some other structures:

digital SiPM, Resistor embedded in the bulk

Basic principle of the Photodetection

Goal of the Photodetection: convert Photons into a detectable electrical signal

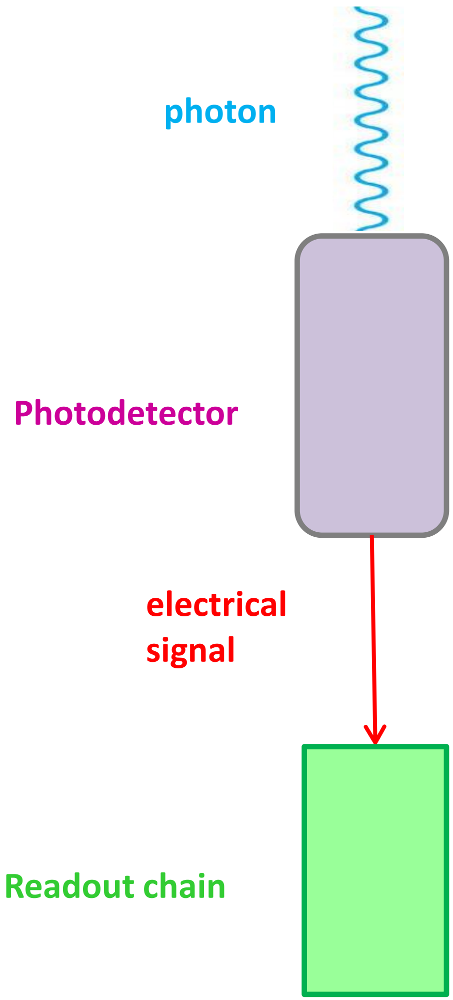

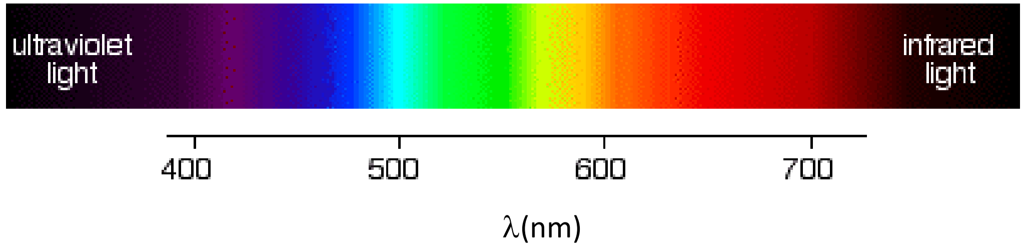

1. Photoconversion: photoelectric effect

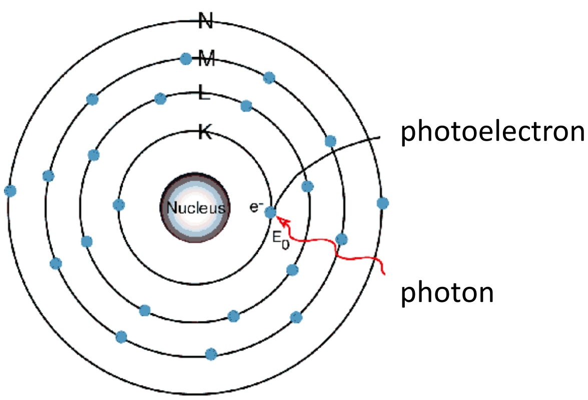

2. Photo-electron collection

3. Signal multiplication

Phase 1 : the Photoconversion in Si

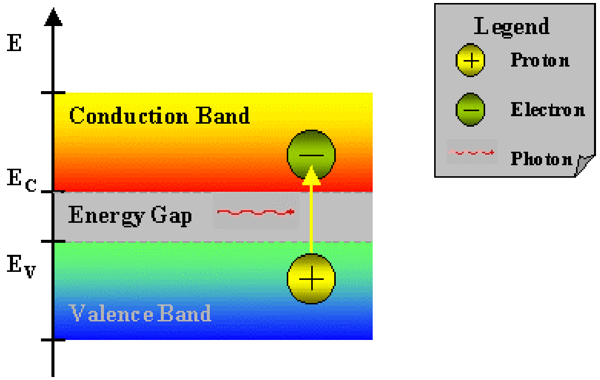

Band gap (T=300K) = 1.12 eV (~1100 nm)

Step 1: Absorption of the photon (γ) in the material and generation of electrons

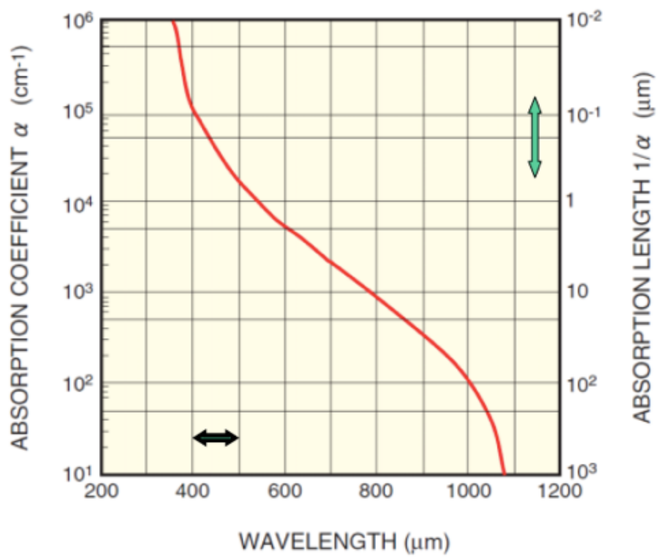

Beer-Lambert law

$$I(\lambda, z) = I(\lambda) e^{-\alpha(\lambda) z}$$

$I(\lambda)$: initial photon flux
$I(\lambda,z)$: photon flux on the distance z from SiPM surface
$\alpha(\lambda)$: optical absorption coefficient
z : penetrated thickness in Si

Most of the photon absorption (63%) occurs over a distance $1/\alpha$ (it is called **penetration depth** δ)

If $E_\gamma > E_g$, electrons are lifted to conduction band → for Si-photodetector this leads to a photocurrent: internal photoelectric effect

Phase 2: the Photoelectron collection

Once created, the electron/hole pair can be lost (absorption, recombination)

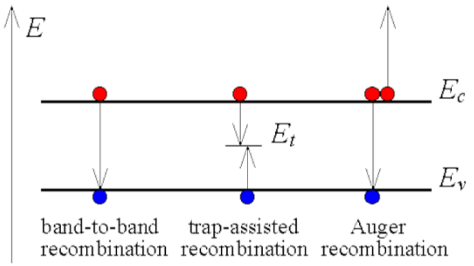

Need of a good **collection efficiency (C_E)**: probability to transfer the primary p.e or e/h to the readout channel or the amplification region

Phase 3: the signal multiplication

The primary electron/hole pair is amplified (photodetector with **internal gain**)

Some photodetectors incorporate internal gain mechanisms so that the photoelectron current can be physically amplified within the detector and thus make the signal more easily detectable.

The main Si detector characteristics

- Sensitivity
- Noise
- Gain
- Linearity
- Time response

Sensitivity

Probability that the incident photon (Nγ) generates a photoelectron (Npe) that contributes to the detector current

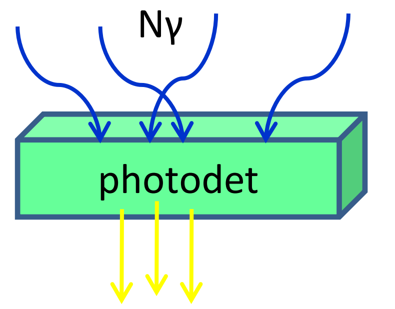

Sensitivity x Gain x Npe

Quantum efficiency

$$Q\varepsilon[\%] = \frac{N_{pe}}{N_{\gamma}}$$

Radiant sensitivity

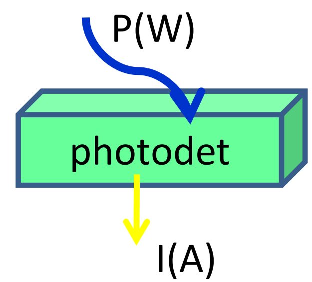

$$S[mA/W] \approx \frac{Q\varepsilon[\%] x \lambda[nm] x qe}{hxc} = \frac{Q\varepsilon[\%] x \lambda[nm]}{124}$$

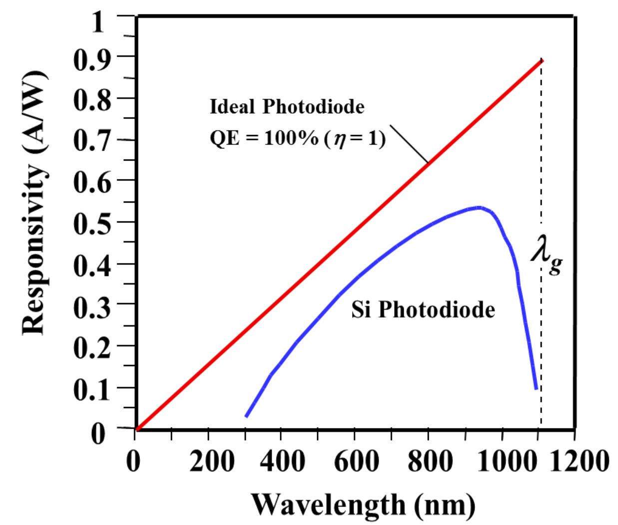

Photo detection efficiency (SiPM)

$$PDE\ [\%] = \mathcal{E}geom\ [\%] \times Q\varepsilon[\%] \times Ptrig\ [\%]$$

$\mathcal{E}geom$: geometrical factor

Ptrig: triggering probability

Gain and its fluctuations

In high electric field ($\approx 10^5\ \mathrm{V \cdot cm^{-1}}$) the carriers are accelerated and can rich an energy higher than the ionization energy of valent electrons → impact ionisation process → multiplication

Gain (G): charge of the pulse when one photon is detected divided by the electron charge

$$G = \frac{Q_{signal}}{q_e}$$

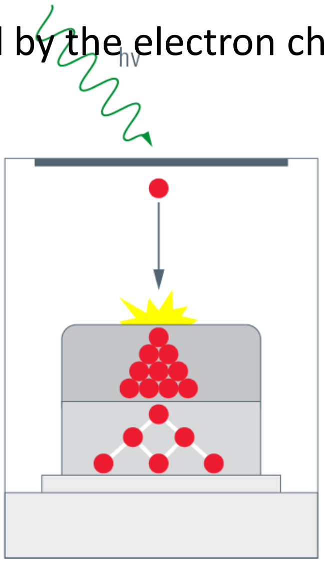

The photodetector output current fluctuates.
The noise in this signal arises from 2 sources:

- randomness in the photon arrivals
- randomness in the carrier multiplication process

The statistical fluctuation of the avalanche multiplication which widen the response of a photodetector to a given photon signal beyond what would be expected from simple photoelectron statistics (Poisson) is characterized by the **excess noise factor ENF**

$$ENF = 1 + \frac{\sigma_G^2}{G^2}$$

ENF
- ❖ impacts the photon counting capability for low light measurements
- ❖ deteriorates the stochastic term in the energy resolution of a calorimeter

Photodetector noise

Principal noises associated with photodetectors :

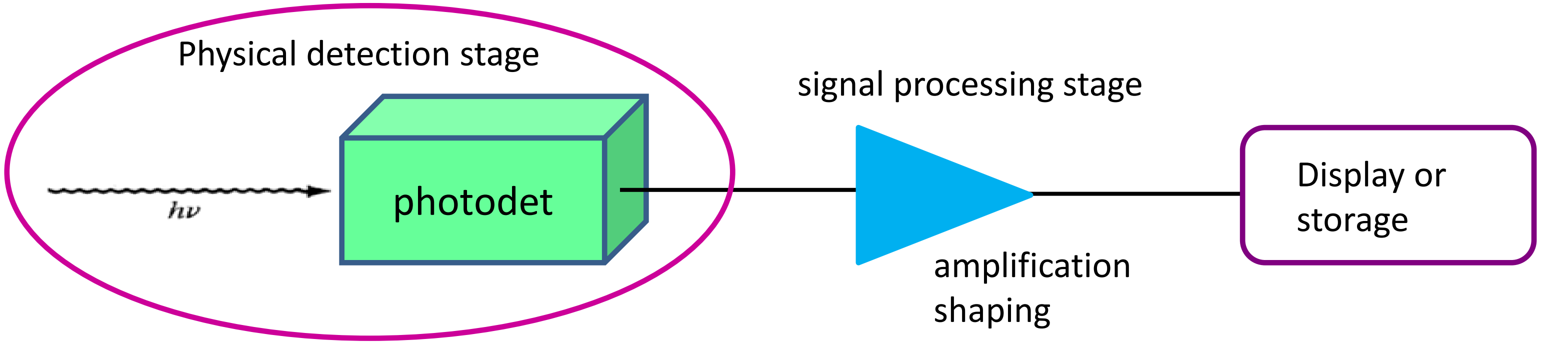

Shot noise:

statistical nature of the production and collection of photo-generated electrons upon optical illumination (the statistics follow a Poisson process)

Dark current noise:

the current that continues to flow through the bias circuit in the absence of the light :

- **bulk dark current** due to thermally generated charges
- **surface dark current** due to surface defects

The dark noise depends a lot on the threshold → not a big issue when we want to detect hundreds or thousands of photons but crucial in the case of very weak incident flux ….

Linearity

Ideally, the photocurrent response of the photodetector is linear with incident radiation over a wide range. Any variation in responsivity with incident radiation represents a variation in the linearity of the detector

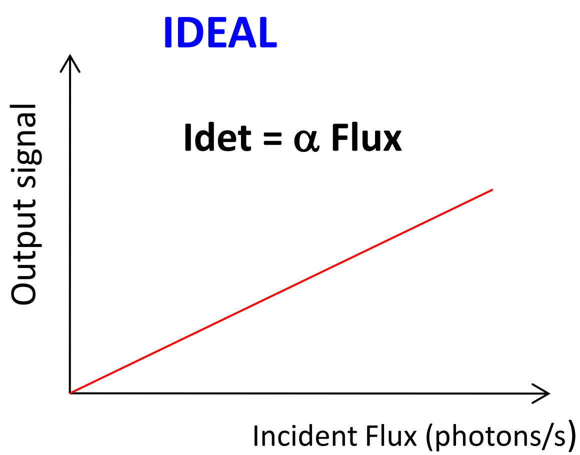

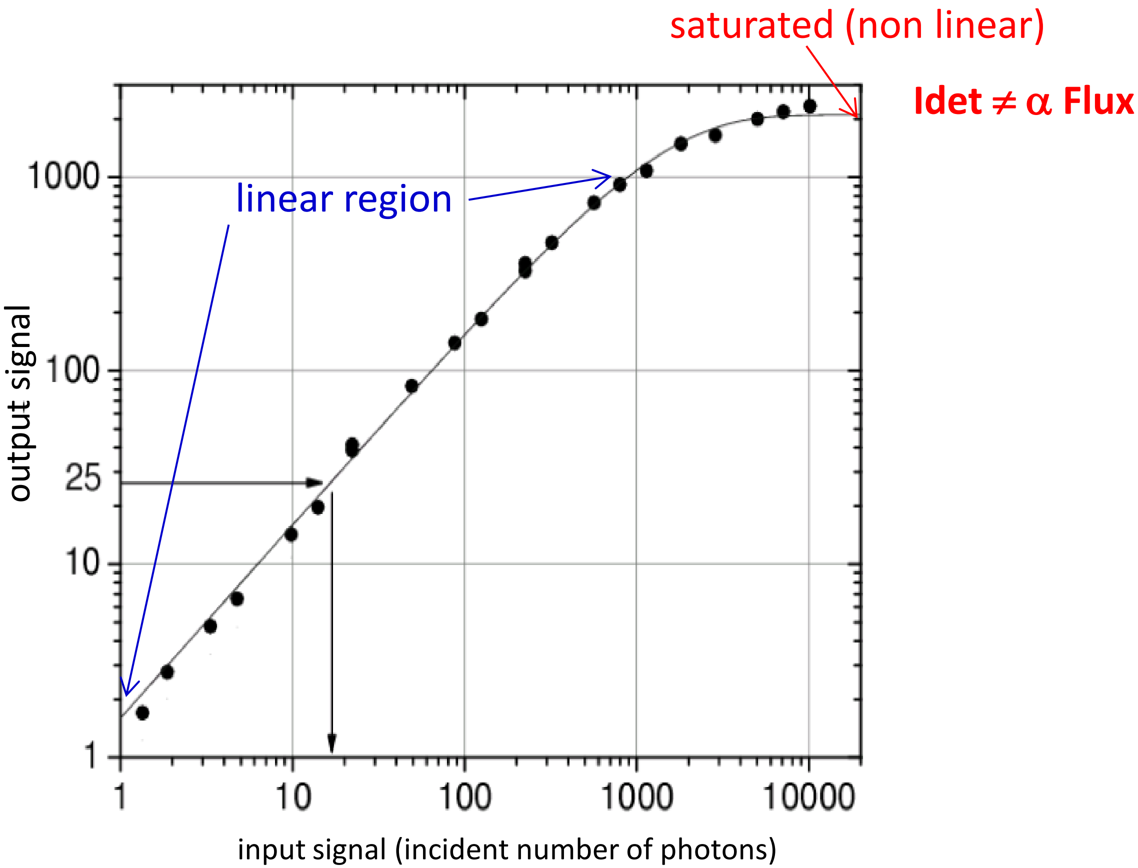

Saturation: issue for the measurement of large number of photons (calorimeter)

Time response

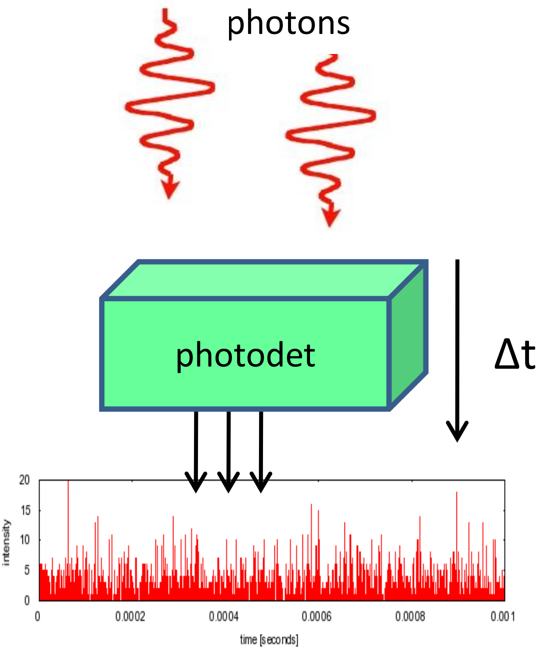

Electrical signal

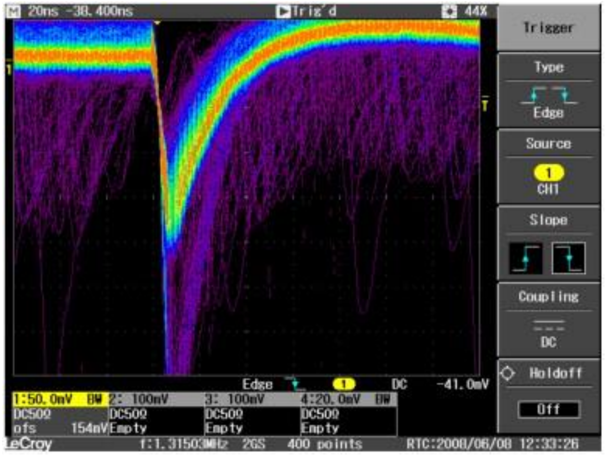

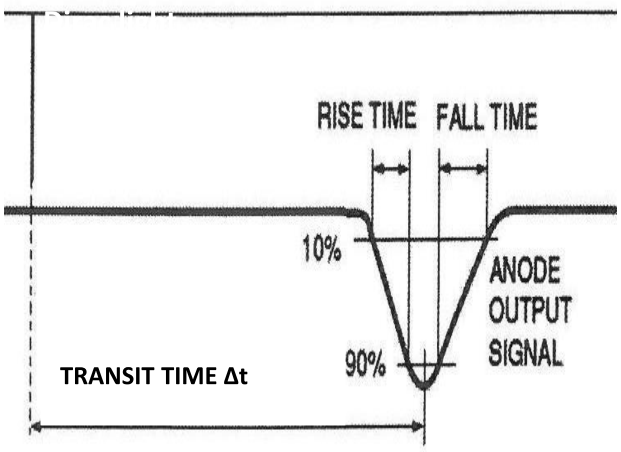

Timing parameters of the signal:

- Rise time, fall time (or decay time)
- Duration
- Transit time (Δt): time between the arrival of the photon and the electrical signal
- Transit time spread (TTS): transit time variation between different events

→ timing resolution

From the PIN photodiode to SiPM

Schematic structure of an idealized PIN PD

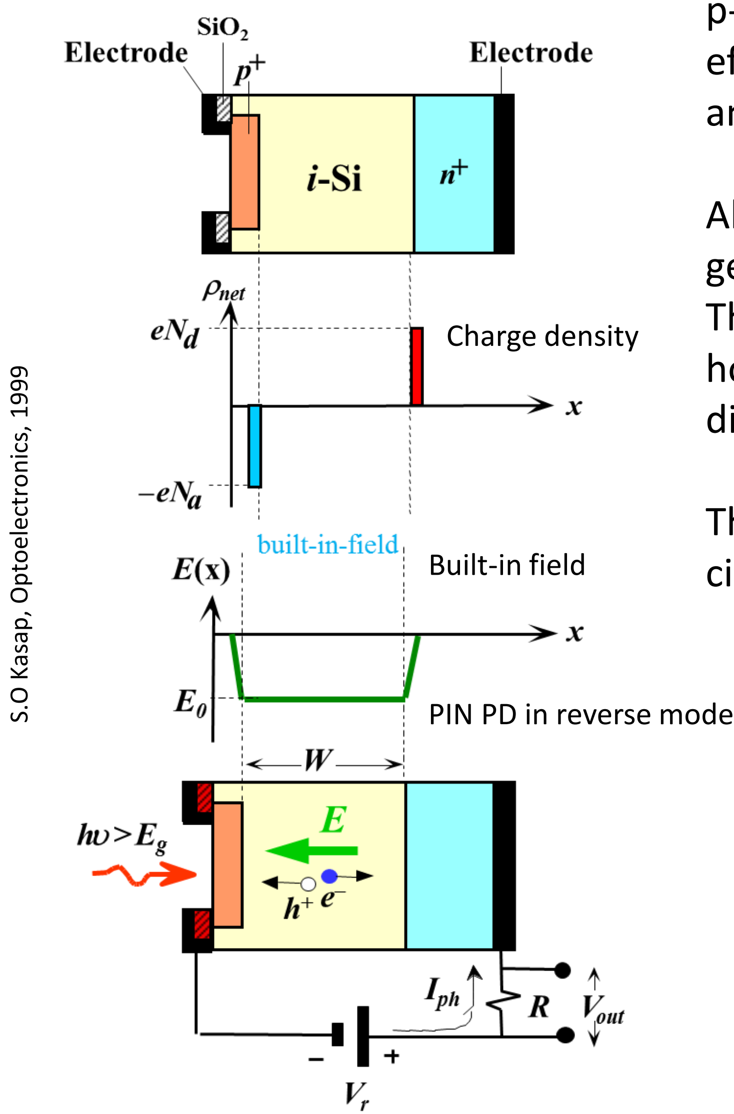

p-i-n junction structure based on the internal photoelectric effect: intrinsic region sandwiched between heavily doped p+ and n+ layers

Absorption of photon in the depletion layer (1 – 3 µm) → generation of e- and holes
The internal electric field sweeps the e- to the n+ side and the hole to the p+ side → a drift current that flows in the reverse direction from the n+ side (cathode) to the p+ side (anode)

This transport process induces an electric current in the external circuit.

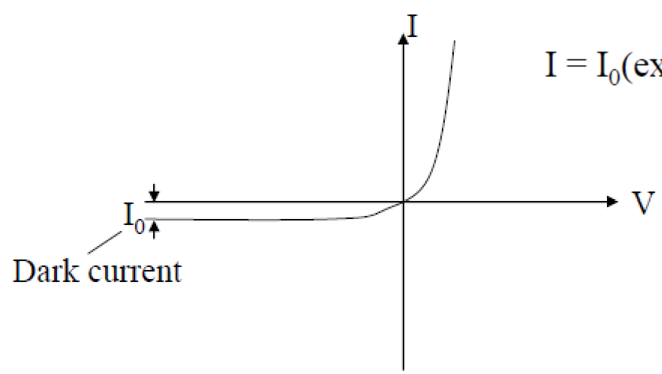

$$I = I_0(\exp(eV/k_BT) - 1)$$

I_0 : thermal-generated free carriers which flow through the junction

The PIN photodiode

PIN photodiodes first large scale application of Si sensors for low light level detection.
They were developed to find a replacement for PMTs in high HEP experiments (high magnetic fields)

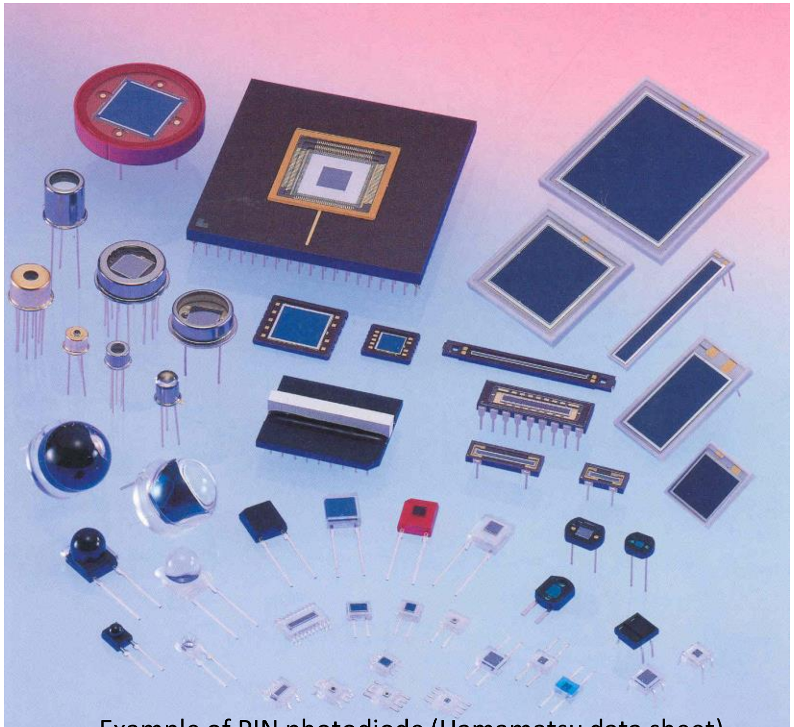

Example of PIN photodiode (Hamamatsu data sheet)

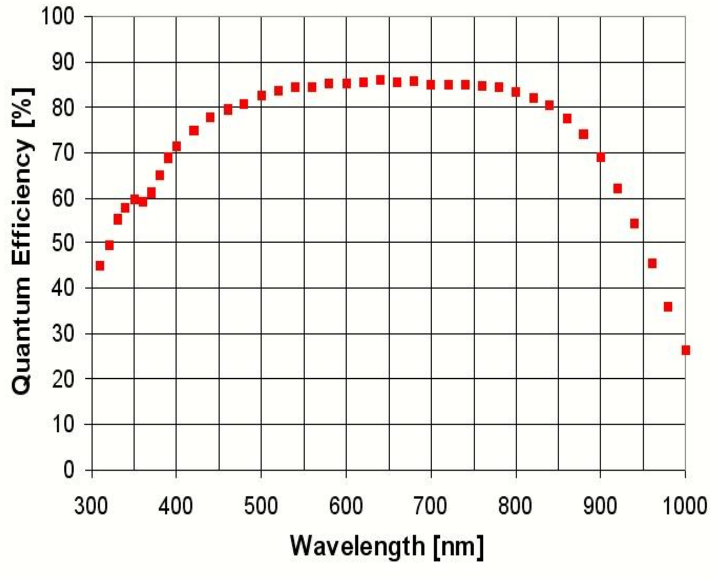

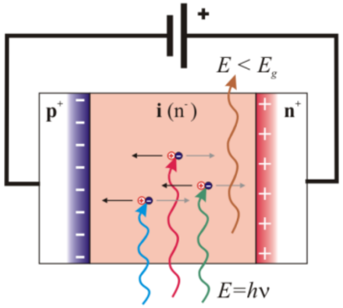

- high QE (80% @ 700nm)
- Gain = 1

The Avalanche Photodiode

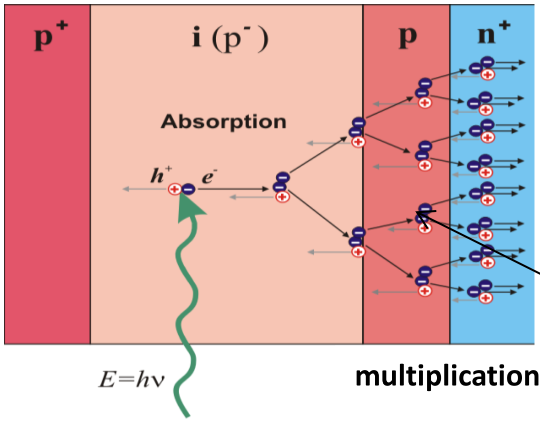

1. large reverse bias across the junction (50 - 200 V)

2. high electric field (≈ 10^5V/ cm) in the depletion-layer

3. the generated e- and holes may acquire sufficient energy to liberate more e- and holes within this layer by a process of impact ionization

Ionization coefficients α for electrons and β for holes

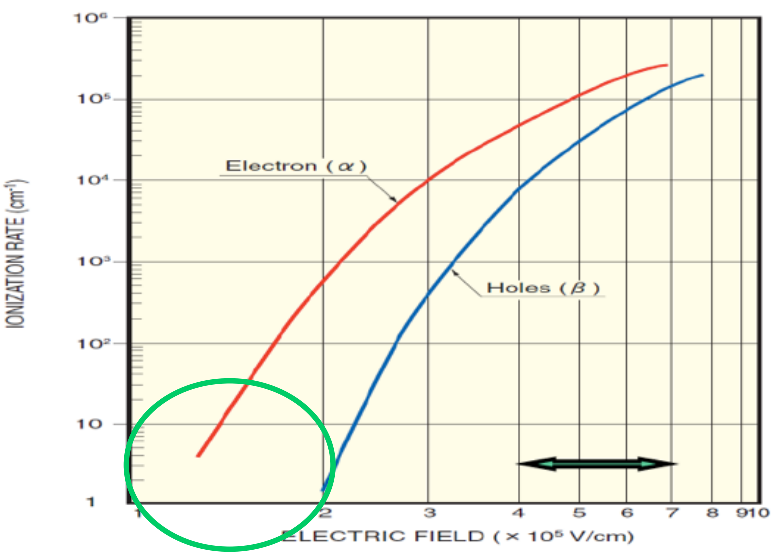

Ionization coffient for avalanche Multiplication

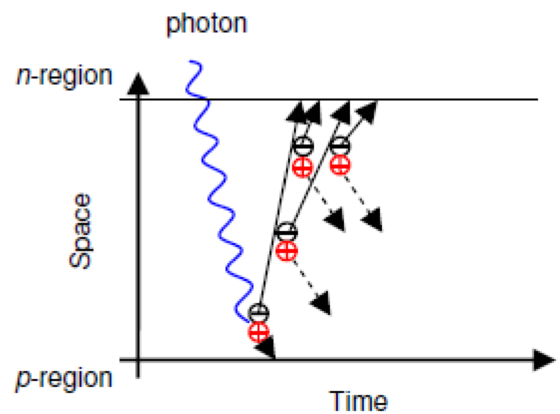

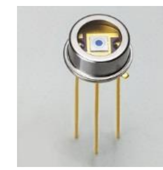

The avalanche process is one directional and self quenched when carriers reach the border of depleted area.

avalanche process created only by the e-

The Avalanche Photodiode

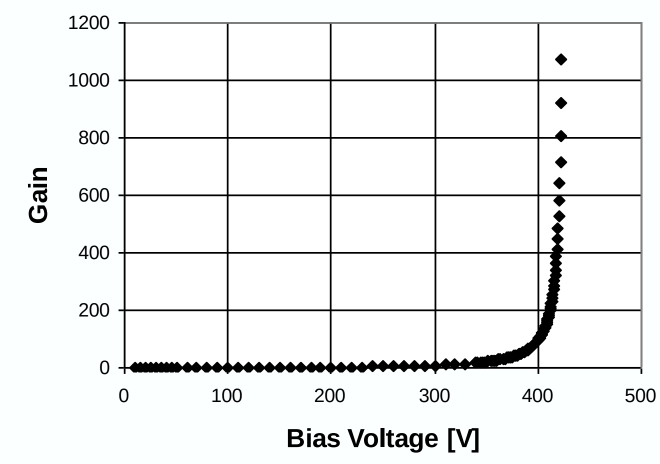

D. Renker, 2009 JINST 4 P04004

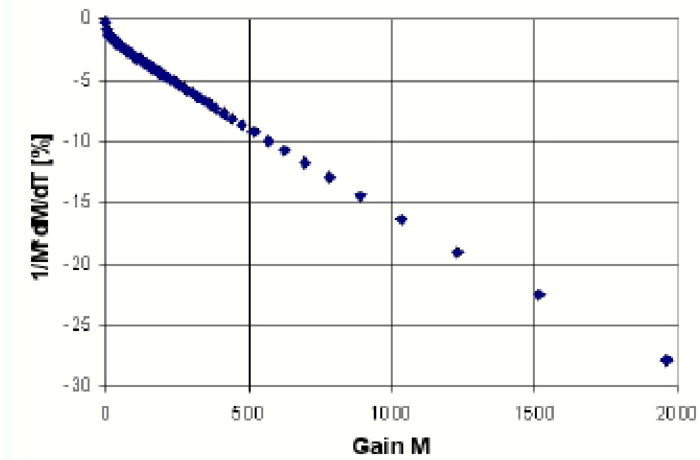

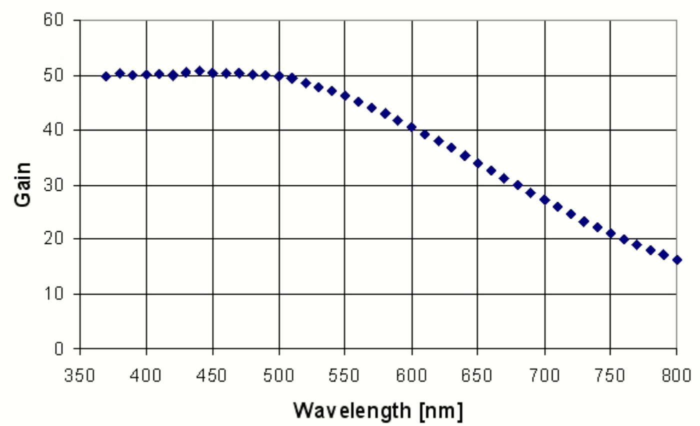

APDs (≈ 120000) in the ECAL of CMS

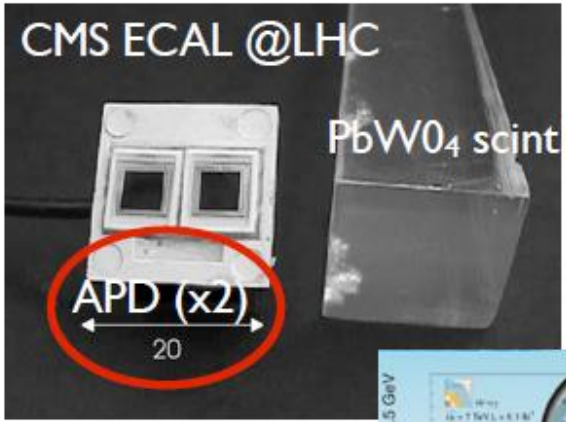

working gain ~ 50
Vbias ~70V

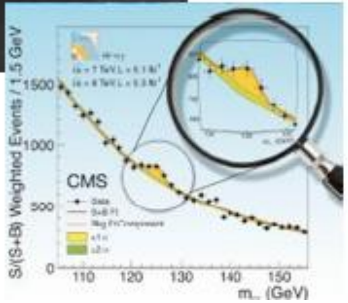

Bias voltage : 50 – 200 V

- high QE (80% @ 700nm)
- Gain = 50 – 100
- high variation with temp. and bias voltage : ΔG = 3.1%/V and -2.4 %/°C (gain= 50)

From PIN photodiode to Geiger mode APD

Geiger mode -APD

- $V_{bias} > V_{BD}$
- G ⇨ ∞
- single photon level

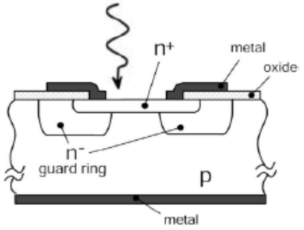

R.H. Haitz.,, J. Appl. Phys. 35 (1964)

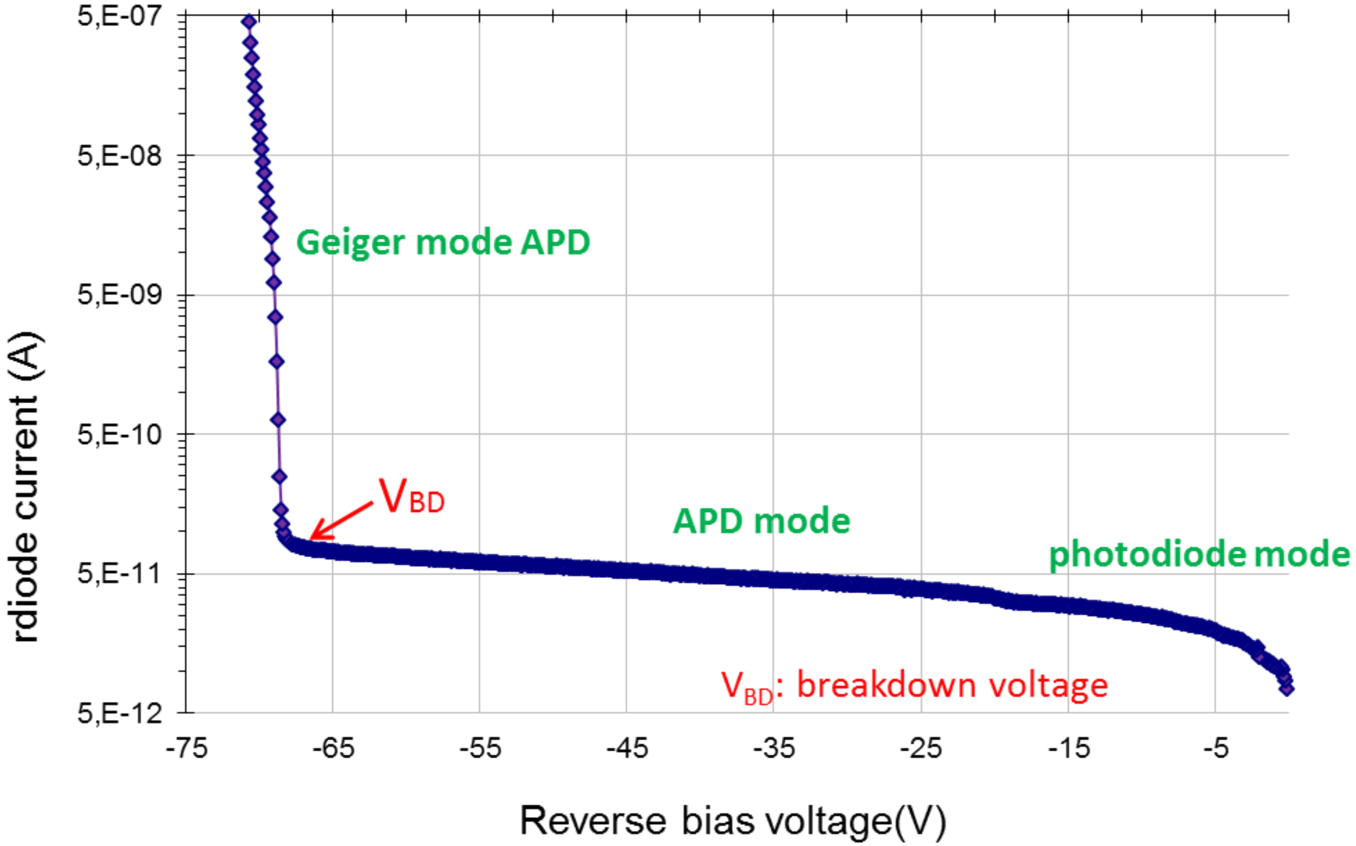

APD

- $V_{APD} < V_{bias} < V_{BD}$
- G = M (50 - 100)
- Linear-mode operation

Photodiode

- $0 < V_{bias} < V_{APD}$ (few volts)
- G = 1
- Operate at high light level (few hundreds of photons)

The Geiger mode APD

Schematic structure of a G-M APD

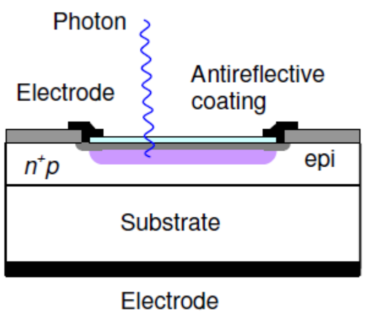

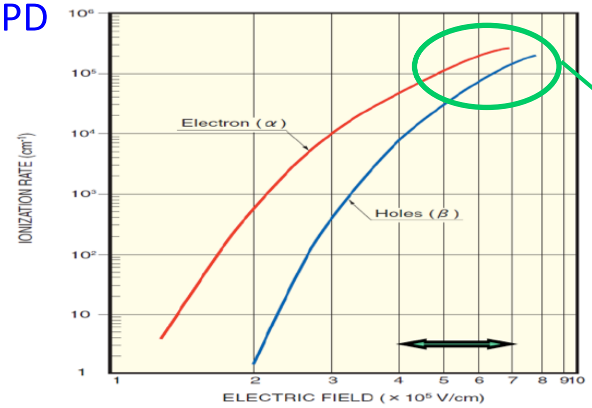

Ionization coffient for avalanche Multiplication

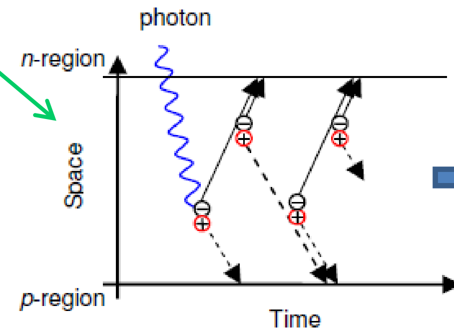

→ breakdown

Valeri Saveliev, ISBN 978-953-7619-76-3

$G = 10^5 - 10^6$

both type of carriers participate in the avalanche process → creation of a self-sustaining avalanche → current rises exponentially with time and reach the breakdown condition. No internal "turn-off" → the avalanche process must be quenched by the voltage drop across a serial resistor : quenching resistor

equivalent electrical circuit

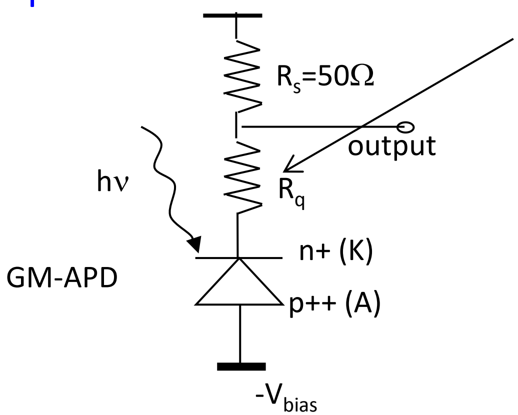

output signal

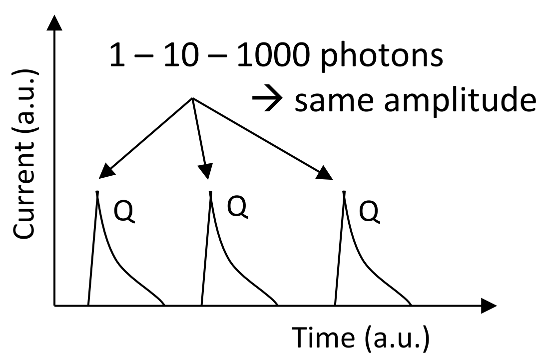

→ output charge is not proportional to the number of of incident photons

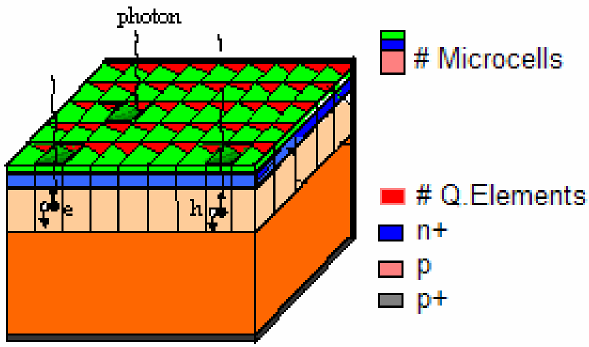

Valeri Saveliev, ISBN 978-953-7619-76-3

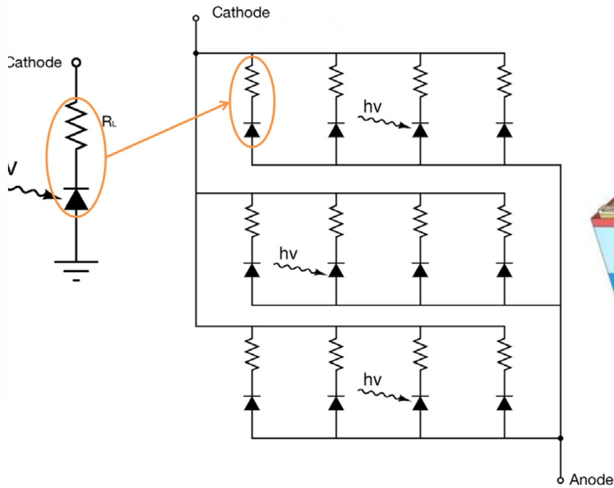

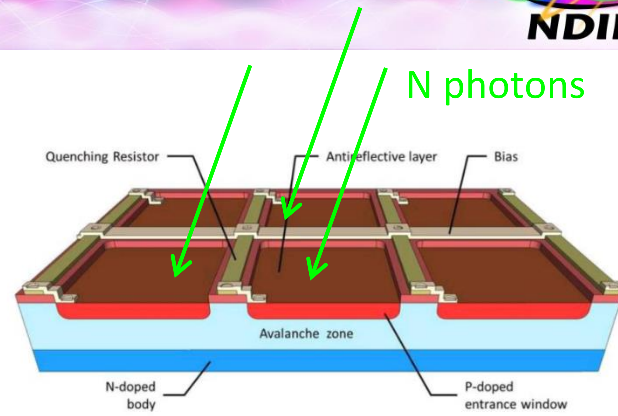

KETEK web site

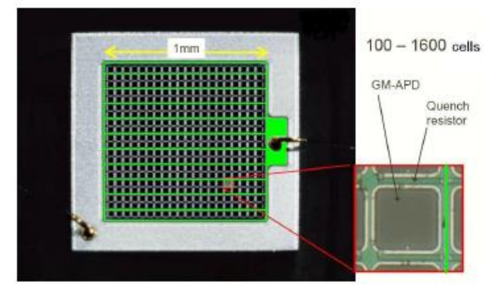

✓ GM-APDs (cell) connected in parallel (few hundreds/mm²)

✓ Each cell is reverse biased above breakdown

✓ Self quenching of the Geiger breakdown by individual serial resistors

Each element is independent and gives the same signal when fired by a photon

⇓

output charge is proportional to the number of of incident photons

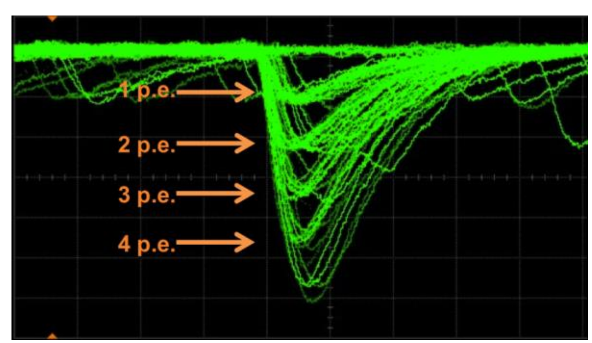

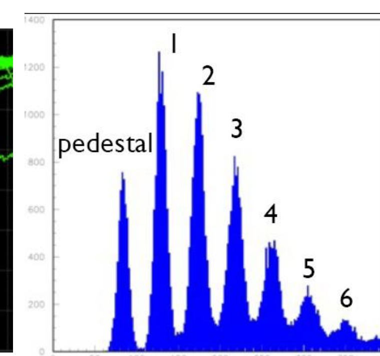

overlap display of pulse waveforms

G. Bisogni, RESMDD10

equivalent electrical circuit of a SiPM cell

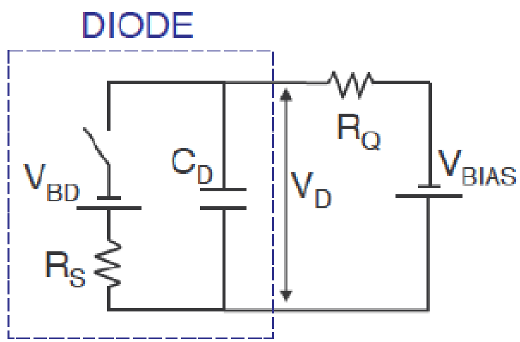

V_{BD} : breakdown voltage
R_Q : quenching resistance
R_S : Si subtrate serie resistance
C_D : diode capacitance
V_{BIAS} : bias voltage

Vbias > Vbd

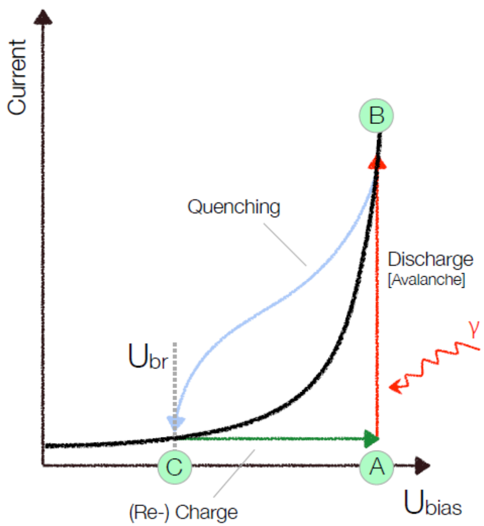

quiescient mode, switch opened
If no photon or no dark event, the current stay stable

A → B : avalanche triggered, switch closed
C_D **discharges** to V_{BD} with the time constant
$\tau = R_S \times C_D$ → asymptotic grows of the current

B→ C : avalanche quenched, switch open

C→ A : reset of the system
C_D **recharges** with the time constant $\tau' = R_Q \times C_D$

Time sequence

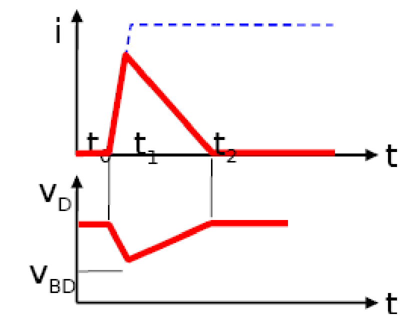

t=0: carrier initiates the avalanche

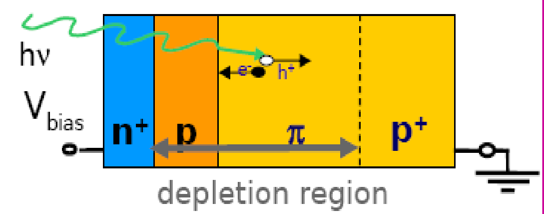

0<t<t1: avalanche spreading

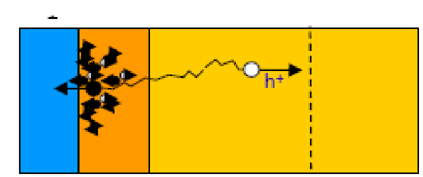

t1<t: self-sustaining current limited by series R

G.Collazuol, LIGHT11

Characteristics of SiPM

Important photodetectors parameters

Photodetectors parameters

- Photon Detection Efficiency
- Dark noise rate
- Correlated noise
- Timing capability
- Signal shape
- Gain
- Radiation hardness
- Geometry
- Temperature dependence
- Packaging

System requirements

- ◆Large dynamic range (Calo, Astro, ..)
- ◆Timing Resolution (TOF PID, PET, …)
- ◆Energy resolution (Calo, PET, ..)
- ◆Large or complicated systems (HEP, Astro, medical appli, …)

Important photodetectors parameters

Photodetectors parameters | **System requirements**

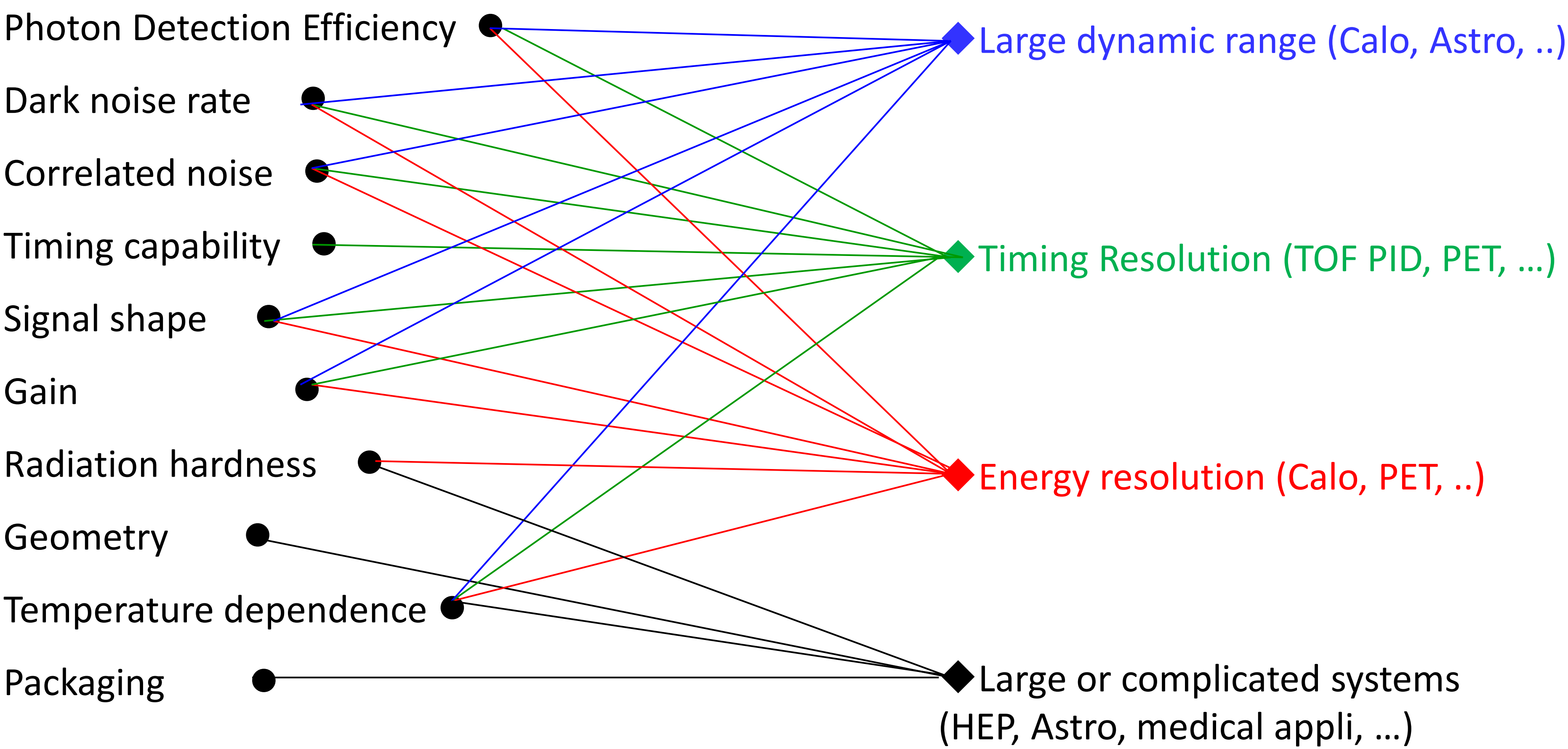

What does it look like?


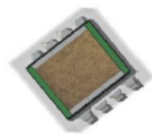
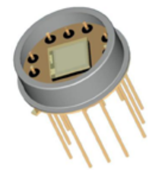
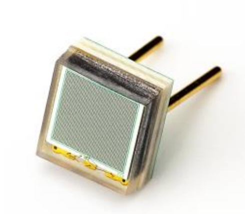
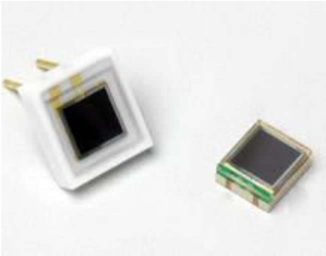

Dimensions: 1 mm² to 16 mm²

Cell size: 15 µm, 25, …, 100 µm

Matrixes: 4 to 256 channels

Packaging: metal (TO8), ceramic, plastic, with pins, surface mount type, matrix


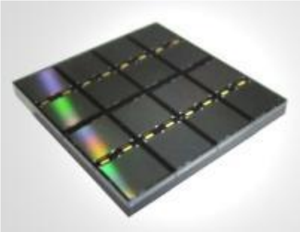
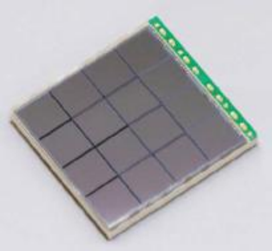

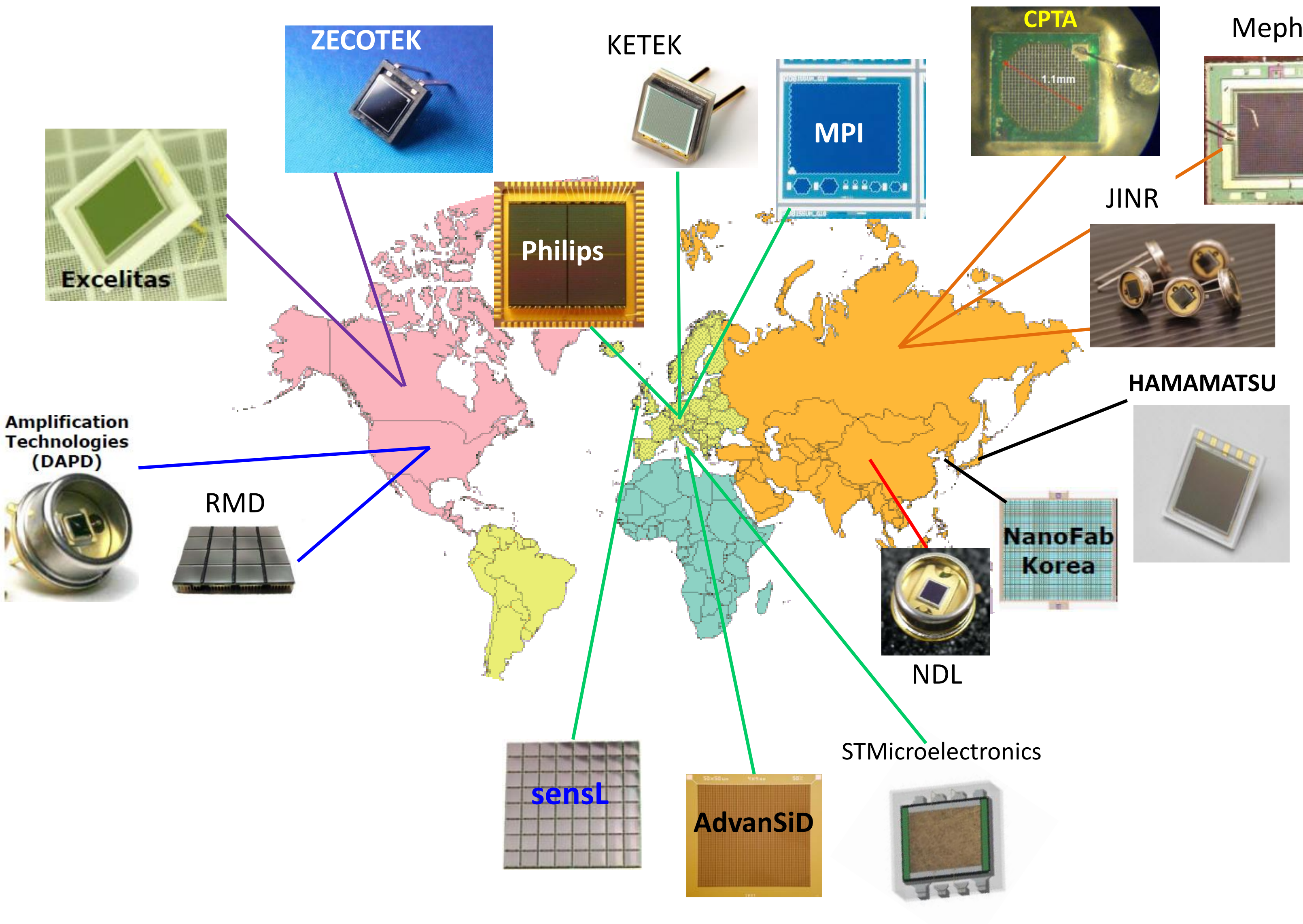
ZECOTEK
KETEK
MPI
CPTA
1.1mm
Mephi
Excelitas
Philips
JINR
HAMAMATSU
Amplification
Technologies
(DAPD)
RMD
NanoFab
Korea
NDL
STMicroelectronics
sensL
AdvanSiD

Signal pulse shape

Fast rise time: hundreds of ps

$T_R = R_S C_D$

Recovery time: tens to hundreds of ns

Time to recharge a cell after a breakdown : $\tau = R_Q C_D$

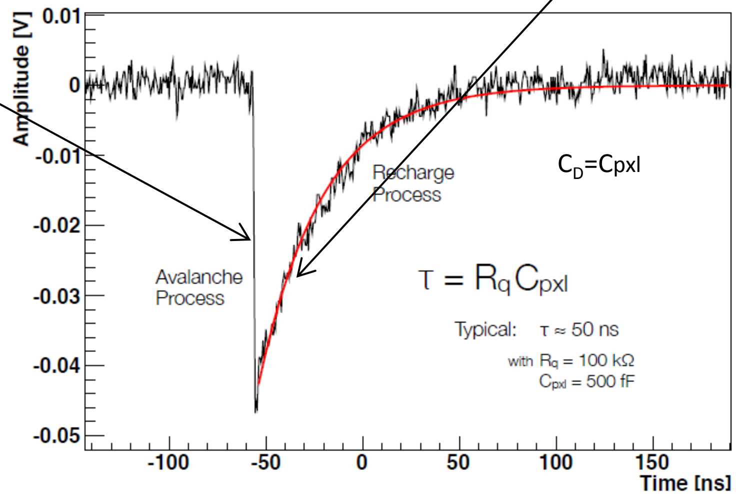

Polysilicon are temperature dependent → strong dependence of the recovery time with the temperature

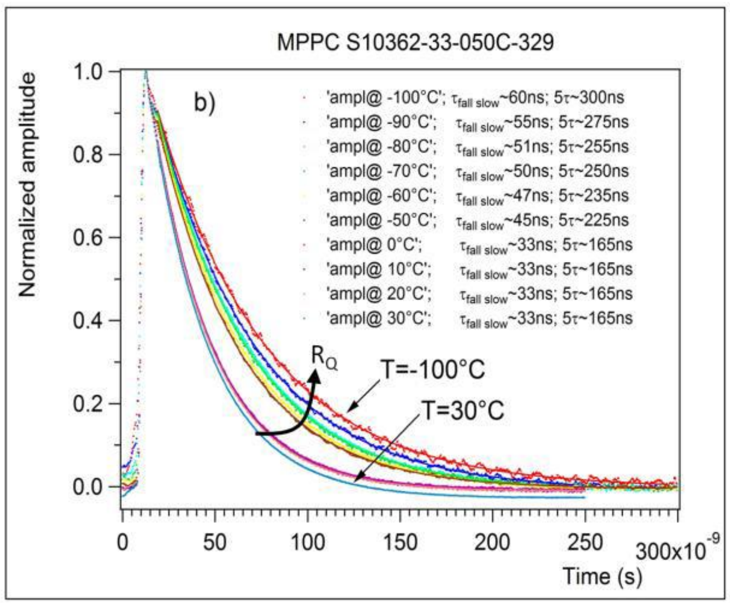

Dinu, IEEE NSS 2010

Solution: Metal Quenching Resistor (MQR)

T. Nagano, IEEE NSS 2013

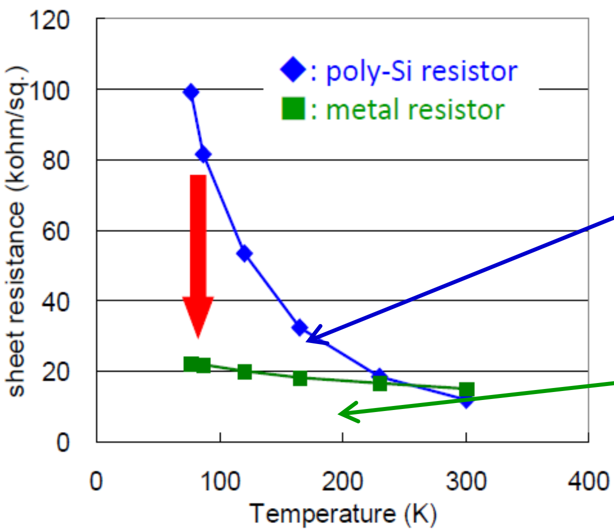

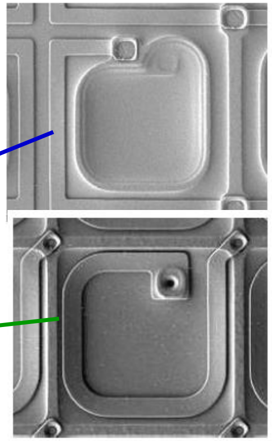

MQR with high transmittance → directly on the photosensitive surface → higher fill factor

Gain

Defined as the charge developed in one cell by a primary carrier

$$Gain = \frac{Q_{cell}}{e} = \frac{C_{cell} \times (V_{bias} - V_{BD})}{e}$$

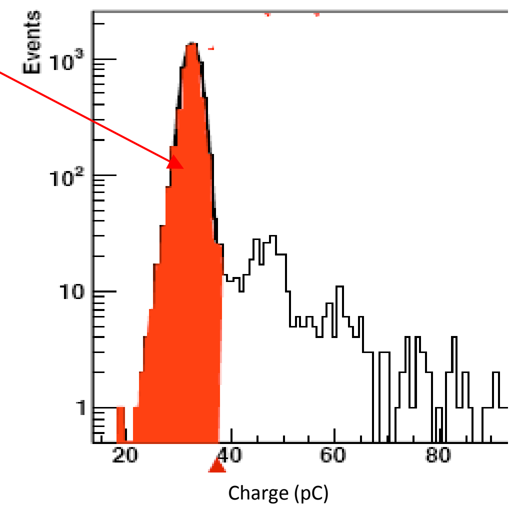

V_{BD}: bias at which occurs the breakdown

$\Delta V = V_{bias} - V_{BD}$

Gain of 1 mm² SiPM (25°C)

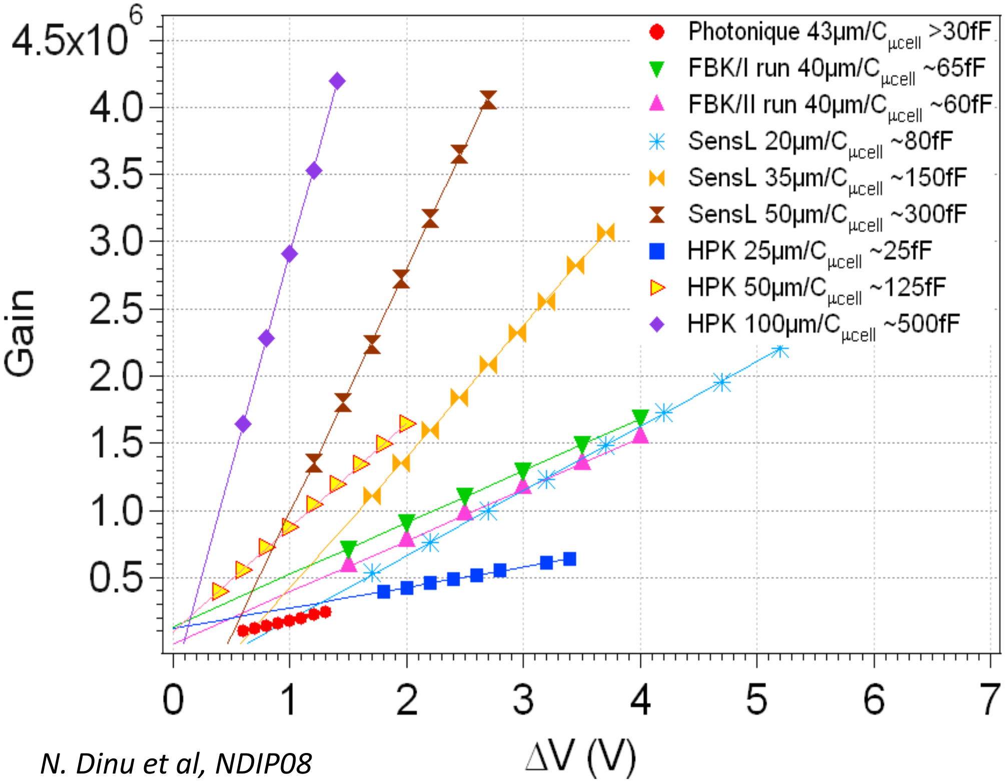

N. Dinu et al, NDIP08

10^5 < Gain < 10^6

- linear increase of the gain with Vbias
- slope of the linear fit of G as a function of Vbias → cell capacitance (tens to hundreds of fF)
- increase of the gain with the cell dimensions

Variation of the gain with the temperature

Temperature coefficients as a function of Vbias

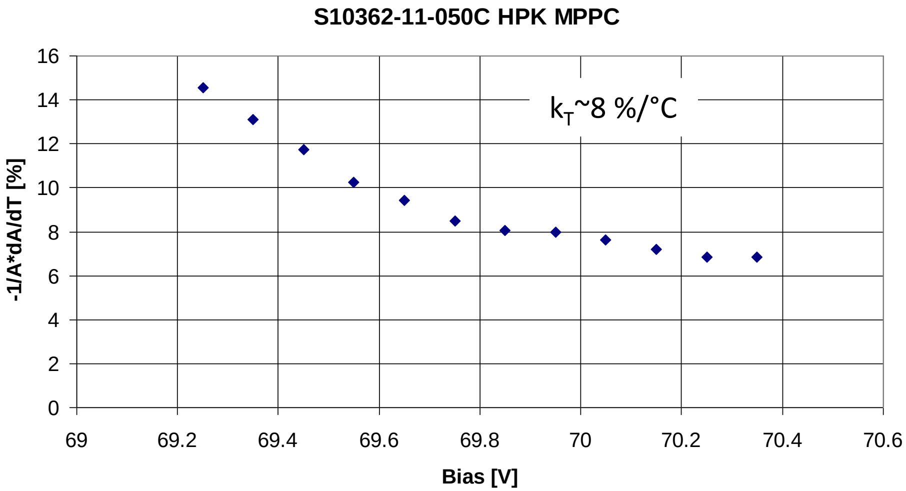

Y. Musienko PoS(PD07)012

Gain independent of the temperature at fixed ΔV

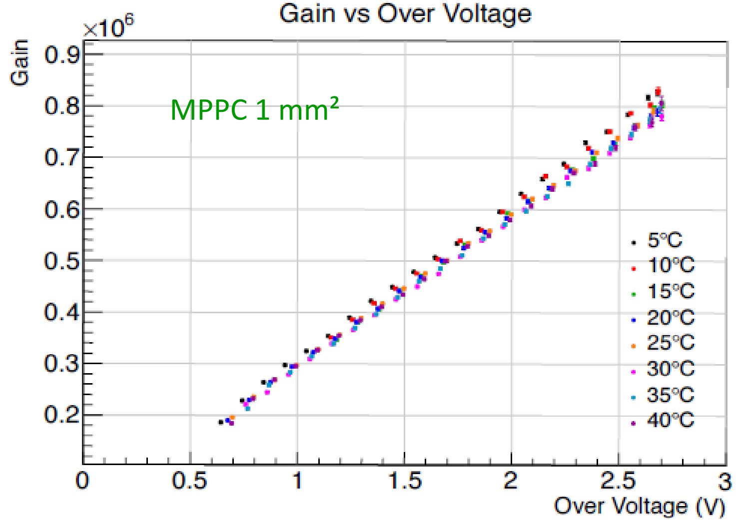

H. Tajima, 2013 CTA SiPM meeting

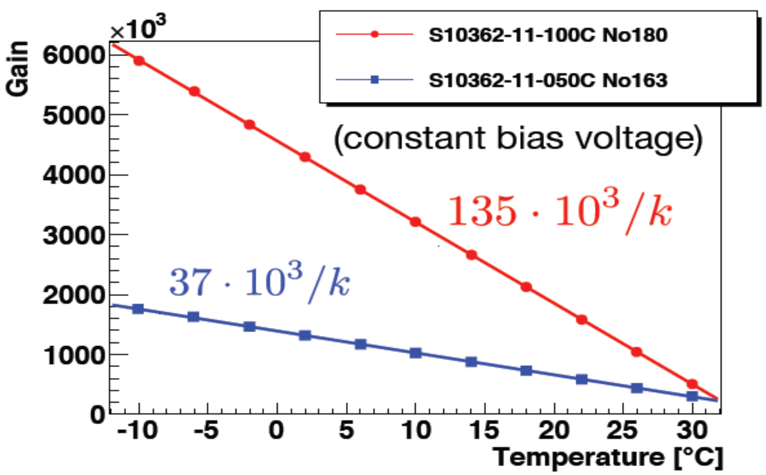

A. Tadday (UniHei)

For a stable operation:

✓ the temperature needs to be controlled with a precision of a degree

✓ the over voltage as to be kept constant

The dependence of the gain with the temperature is larger with a bigger cell

Single photon detection performance

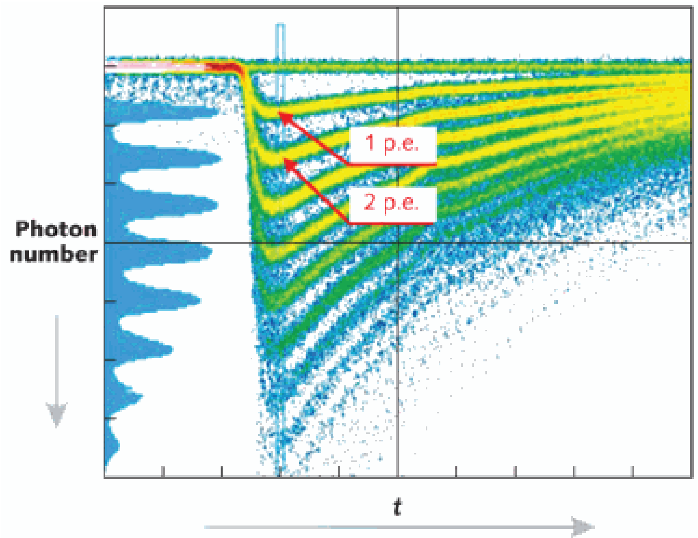

Signal distribution of the detecting the low photon flux by SiPM at room temperature

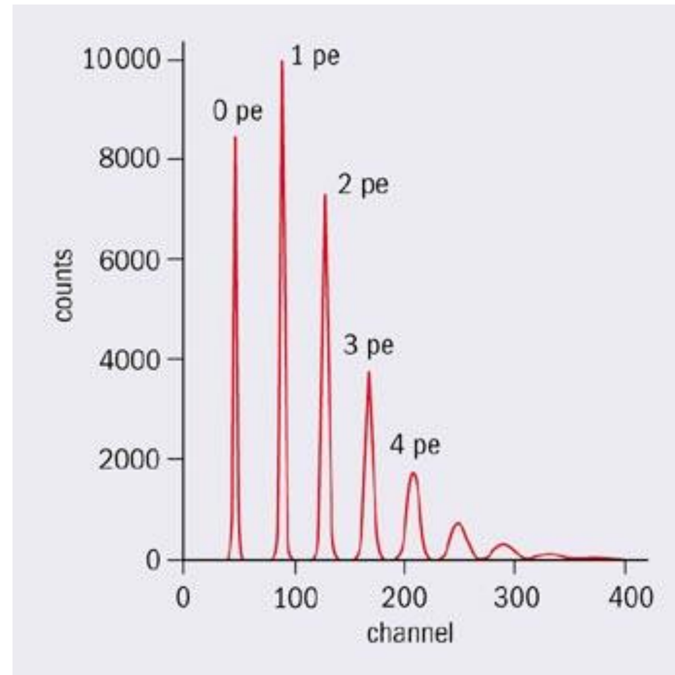

100c-69.7V-1.0%

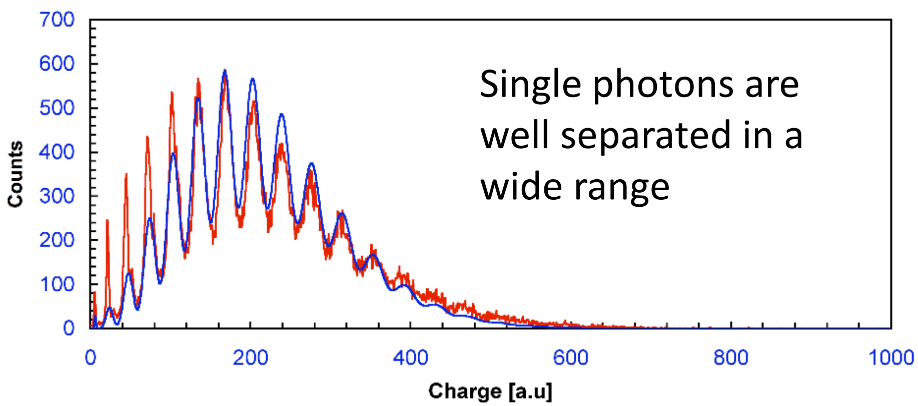

Single photons are well separated in a wide range

The resolution of SiPM allows very precise analysis of the detecting photon flux up to single photon

29

Photo Detection Efficiency (PDE - Qε)

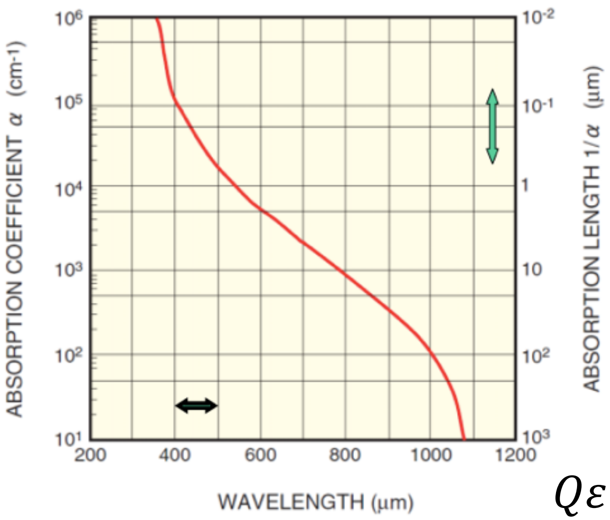

$$PDE = Q_{\varepsilon} \cdot P_{trig} \cdot \varepsilon_{geom}$$

Qε: carrier Photo-generation

probability for a photon to generate a carrier that reaches the high field region in a cell

$$Q\varepsilon = (1 - R)\,\xi\,[1 - e^{-\alpha d}\,]$$

fraction of the photon flux absorbed in the depleted layer (sensitive region). The device should have a sufficiently large value d to maximize this factor.

effect of reflection at the surface of the device.
reflection can be reduced by the use of antireflection coatings

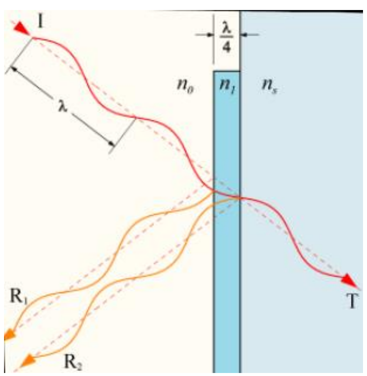

fraction of e-/h pairs that successfully avoid recombination at the material surface and contribute to the useful photocurrent

R : reflection Frenell coefficient = 0,3 for Si

Photo Detection Efficiency (PDE - P_{trig})

$$PDE = Q_\varepsilon \cdot P_{trig} \cdot \varepsilon_{geom}$$

Ptrig : avalanche triggering: probability for a carrier traversing the high-field to generate the avalanche
Depends on the position when the primary e/h pair is generated

e- directly collected at the n+ electrode → only the holes contribute to the trig proba

Hole directly collected at the p+ electrode → only the e- contribute to the trig proba

W.Oldham , IEEE TED (1972)

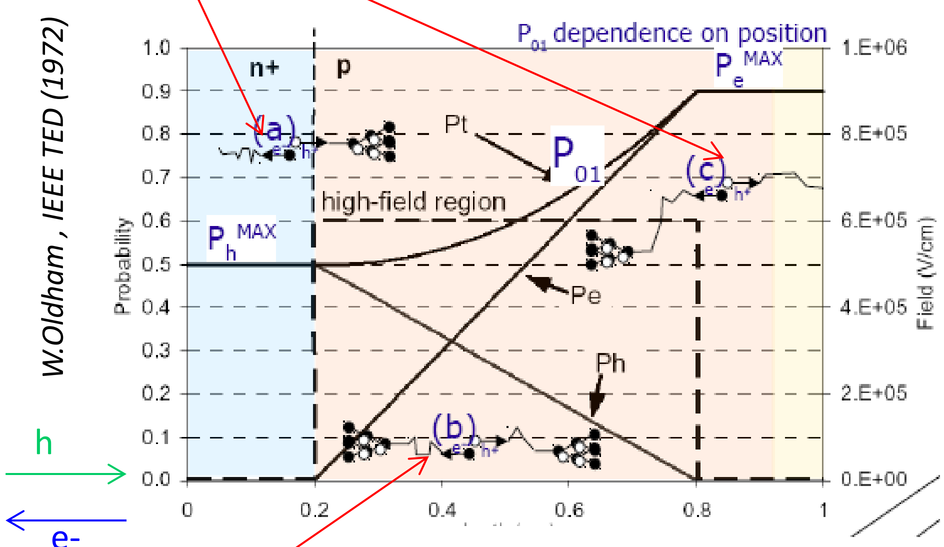

both carriers contribute to the trig proba

Ionization coefficients α for electrons and β for holes

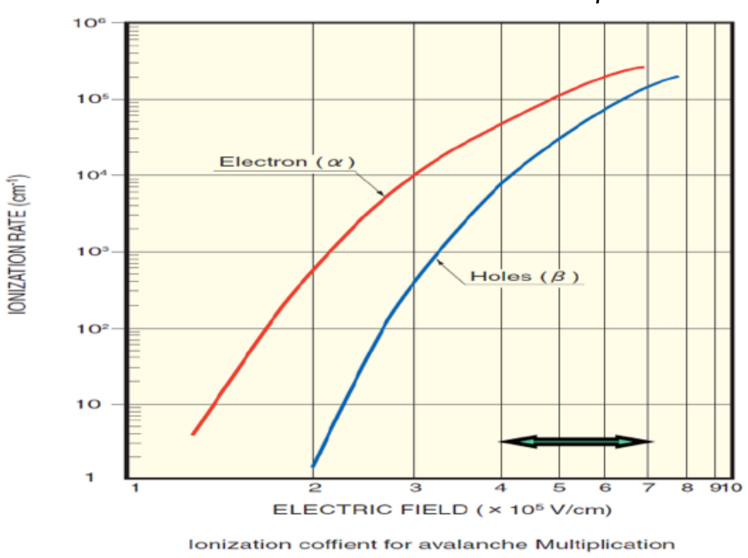

Ionization coefficient of e- > coeff of holes → the triggering probability is max when the charge carriers generation happens in the p side of the junction → the e- pass through the high field region

Photo Detection Efficiency (PDE - ε_{geom})

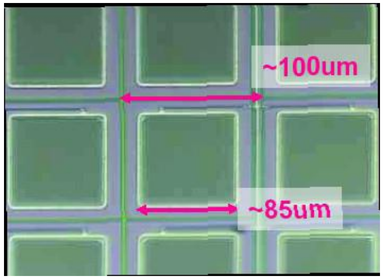

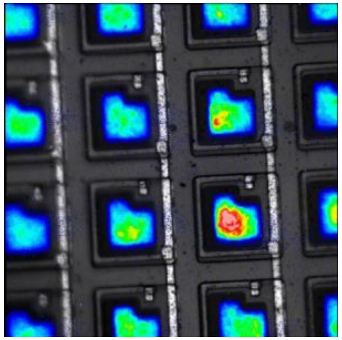

$$PDE = Q_{\varepsilon} \cdot P_{trig} \cdot \varepsilon_{geom}$$

ε_{geom} : geometrical Fill Factor

fraction of the sensitive to insensitive area. Only part of the area occupied by the cell is active and the rest is used for the quenching resistor and other connections

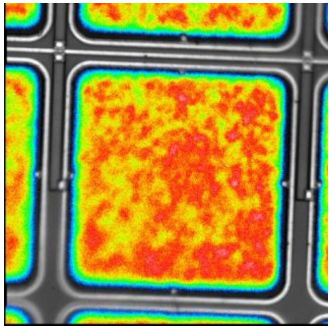

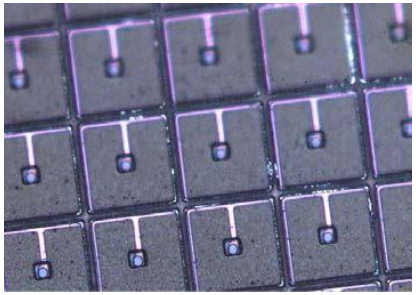

PDE of SiPMs: p-on-n structure

p-on-n SiPM with shallow junction exhibits higer PDE value in the blue region (e- trigger avalanches at short λ)

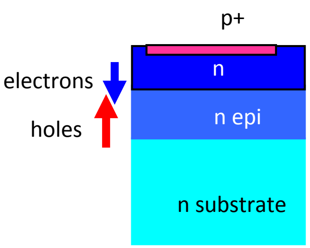

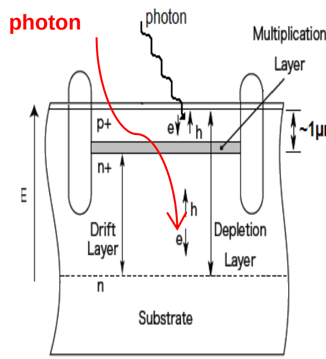

Otte, PD09

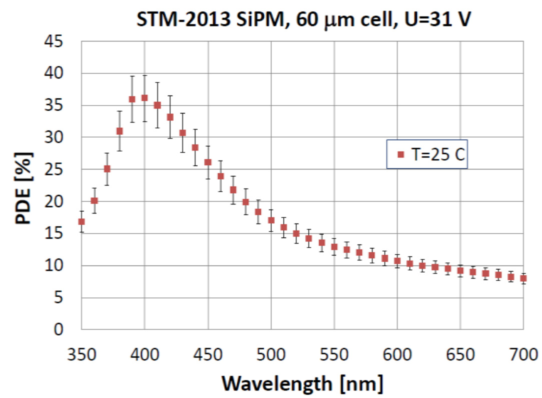

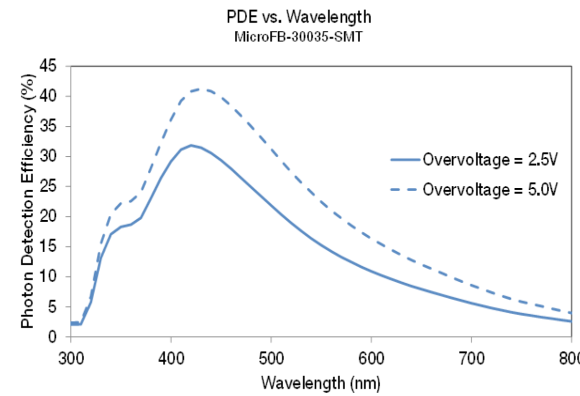

Y. Musienko, INSTR14

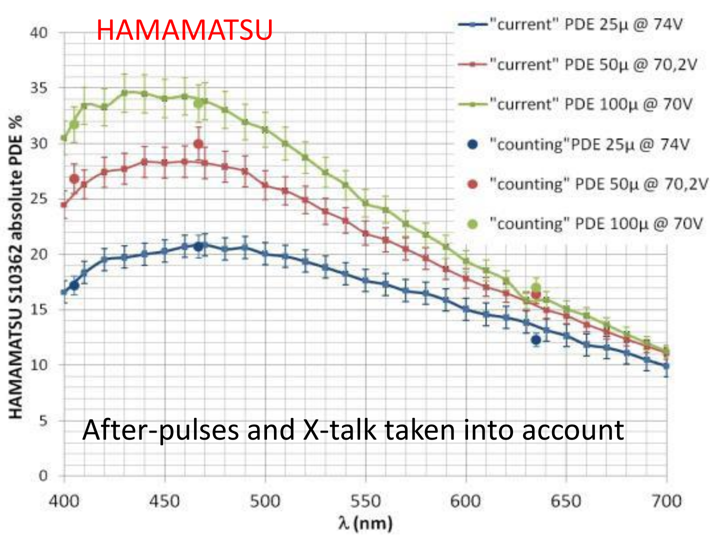

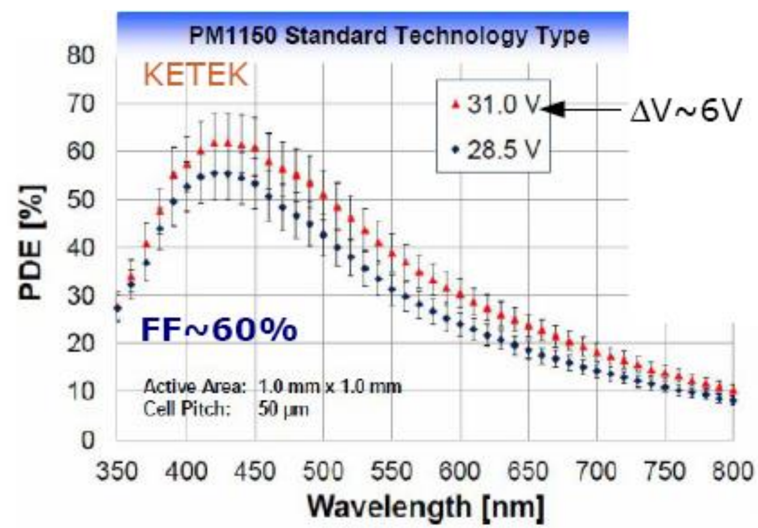

V. Chaumat, PoS (PhotoDet 2012) 058

F.Wiest – AIDA 2012

PDE of SiPMs: n-on-p structure

n-on-p SiPM with larger depletion depth have higher sensitivity in the red

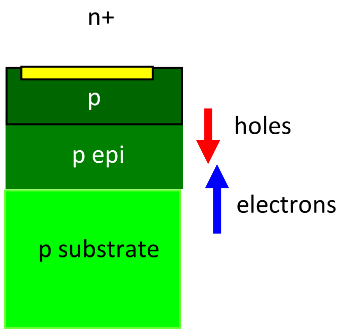

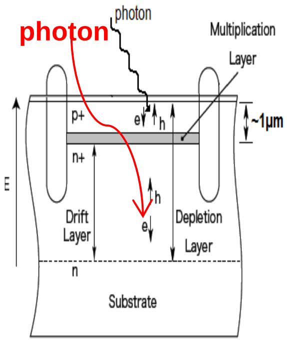

Otte, PD09

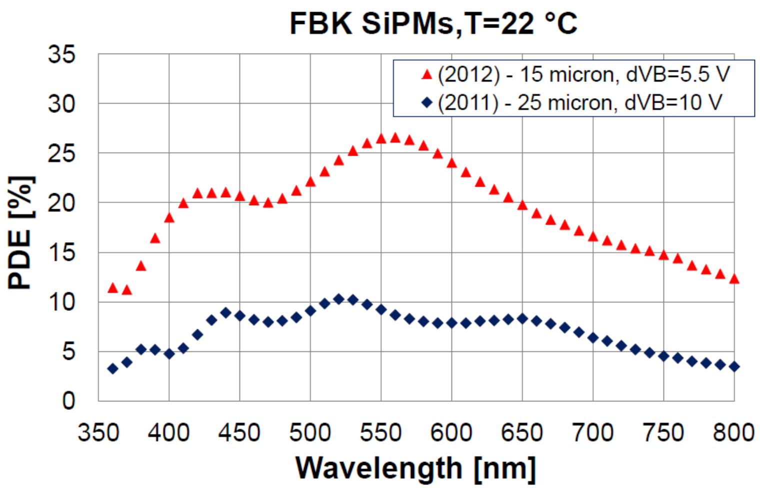

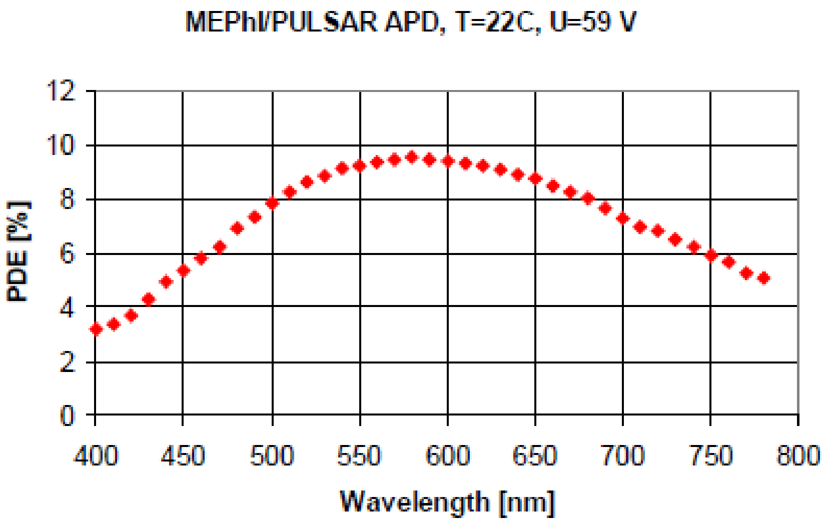

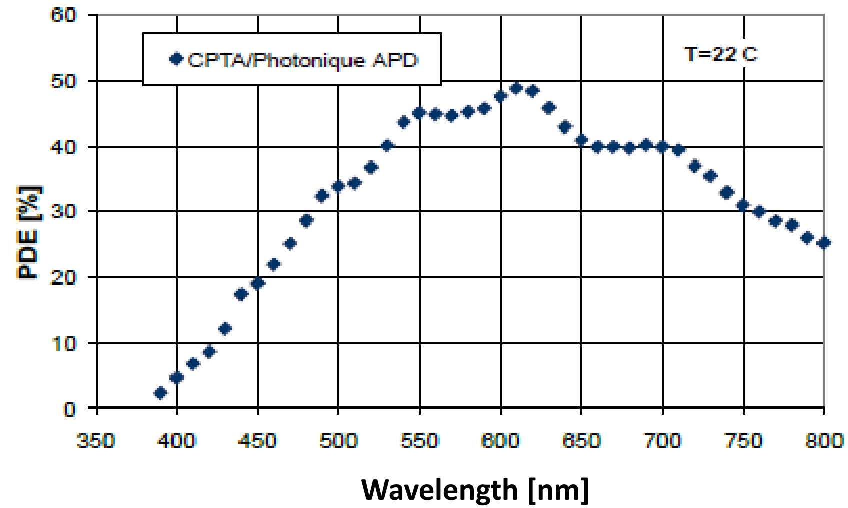

Y. Musienko, INSTR14

VUV SiPMs

Almost no detection of the UV light → limitation of the suitability of SiPMs for Noble-gas detectors

PDE for VUV is ≈ 0 for commercial devices because of the low transmission for VUV of the sensitive layer due to:

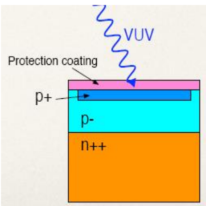

- protection coating (epoxy resin/silicon rubber)
- insensitive layer (p+ contact layer with ~zero field)
- absorption length in Si for VUV photon: ~5nm
- high reflectivity for VUV on Si surface

Possible solutions:

- Remove protection coating
- Thinner p+ contact layer
- Optimize reflection/refractive index on sensor surface

HAMAMATSU

UV-enhanced MPPC under development (collaboration between Hamamatsu, ICEPP and KEK) : removal of the protection coating and optimization of the MPPC parameters → currently sensor size: 12×12mm² (cell size = 50 µm)

- PDE (175 nm) = 17 % (best sample)
- Gain ≈ 10^6 @ 165 K
- DCR = 0 @ 165 K
- decay time ≈ 30 -60 ns

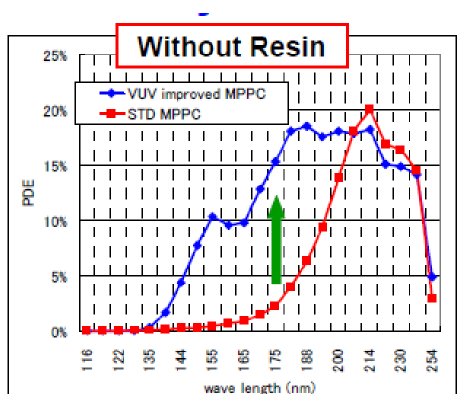

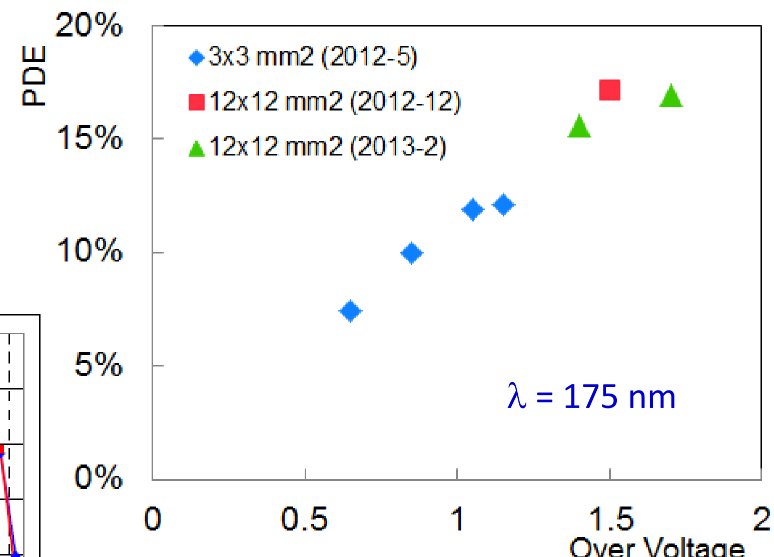

D. Kaneko at al, IEEE NSS 2013 Proceedings

NUV SiPMs

FBK NUV-SiPM (Near-UV SiPM)

1x1mm^2 50x50 µm^2 cell

Designs available: 1x1, 2x2, 3x3, 4x4mm^2

Results (FBK measurements):

- PDE (350 nm) = 20 %
- DCR = 4 MHz @ 20°C (ΔV = 5V)

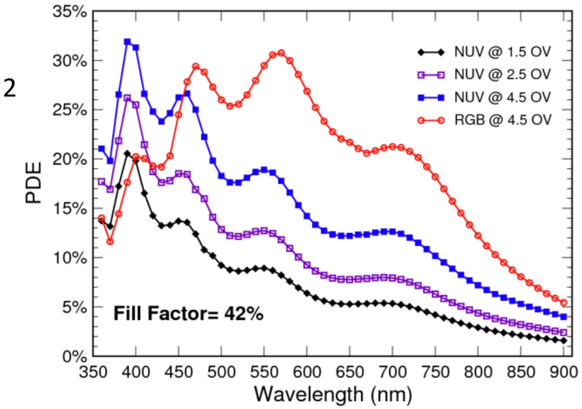

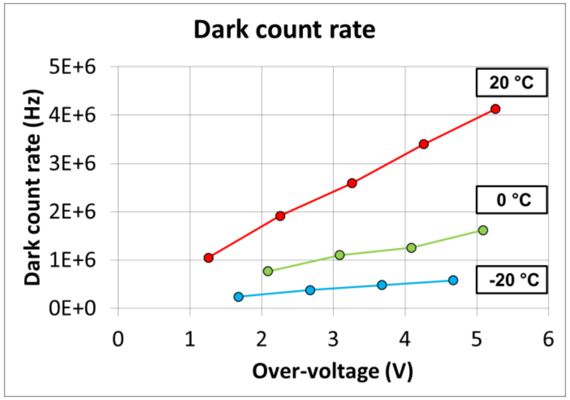

A. Ferri, NIMA 718 (2013)

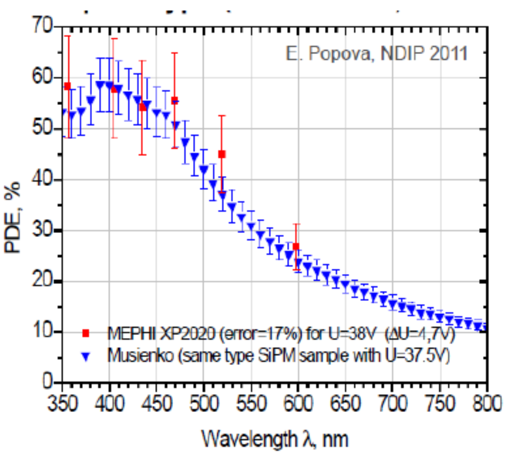

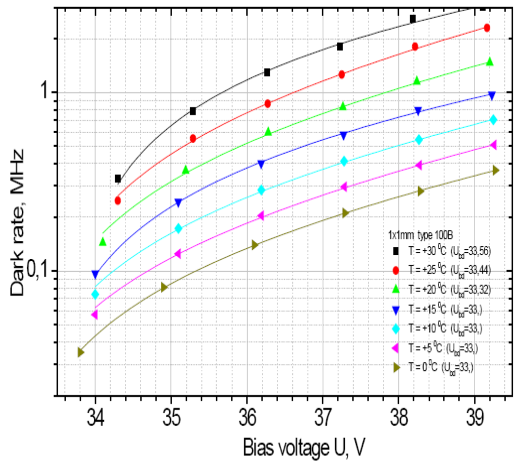

E. Popova, NDIP2011

Excelitas

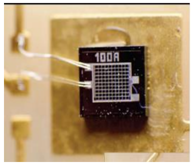

Collaboration between Excelitas, MEPHI and MPI : 1×1 mm^2 (cell size = 100 µm)

- PDE (350 nm) = 50 %
- DCR = 800 kHz @ 20 °C (ΔV = 4V)

Noise sources of a SiPM

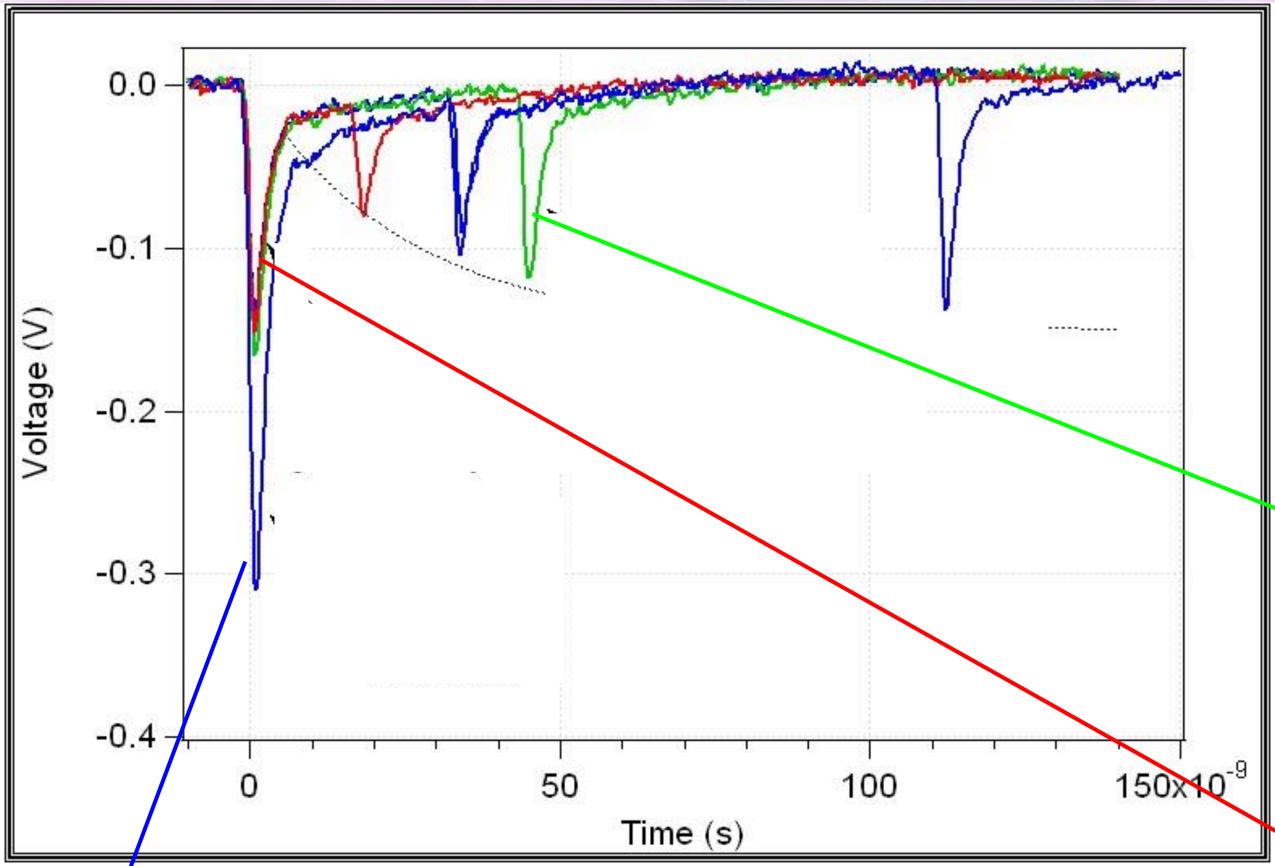

After-pulses

carriers trapped during the avalanche can produce delayed secondary pulses

Dark counts

pulses triggered by non-photo-generated carriers (thermal / tunneling generation in the bulk or in the surface depleted region around the junction)

Cross-talk : amplitude = 2 p.e

avalanche in one cell → proba that a photon triggers another avalanche in a neighboring cell without delay

Dark Count rate (DCR)

Average frequency of the thermally generated avalanches breakdown process that result in a current pulse indistinguishable from a pulse produced by the detection of a photon.

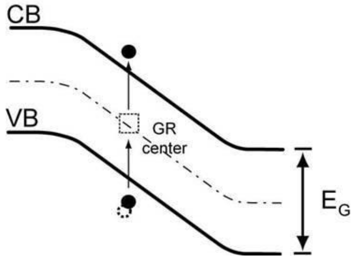

Few 100kHz/mm² < DCR < 1 MHz/mm² till 2013

DCR of most recent devices ≈ few 10 kHz/mm²

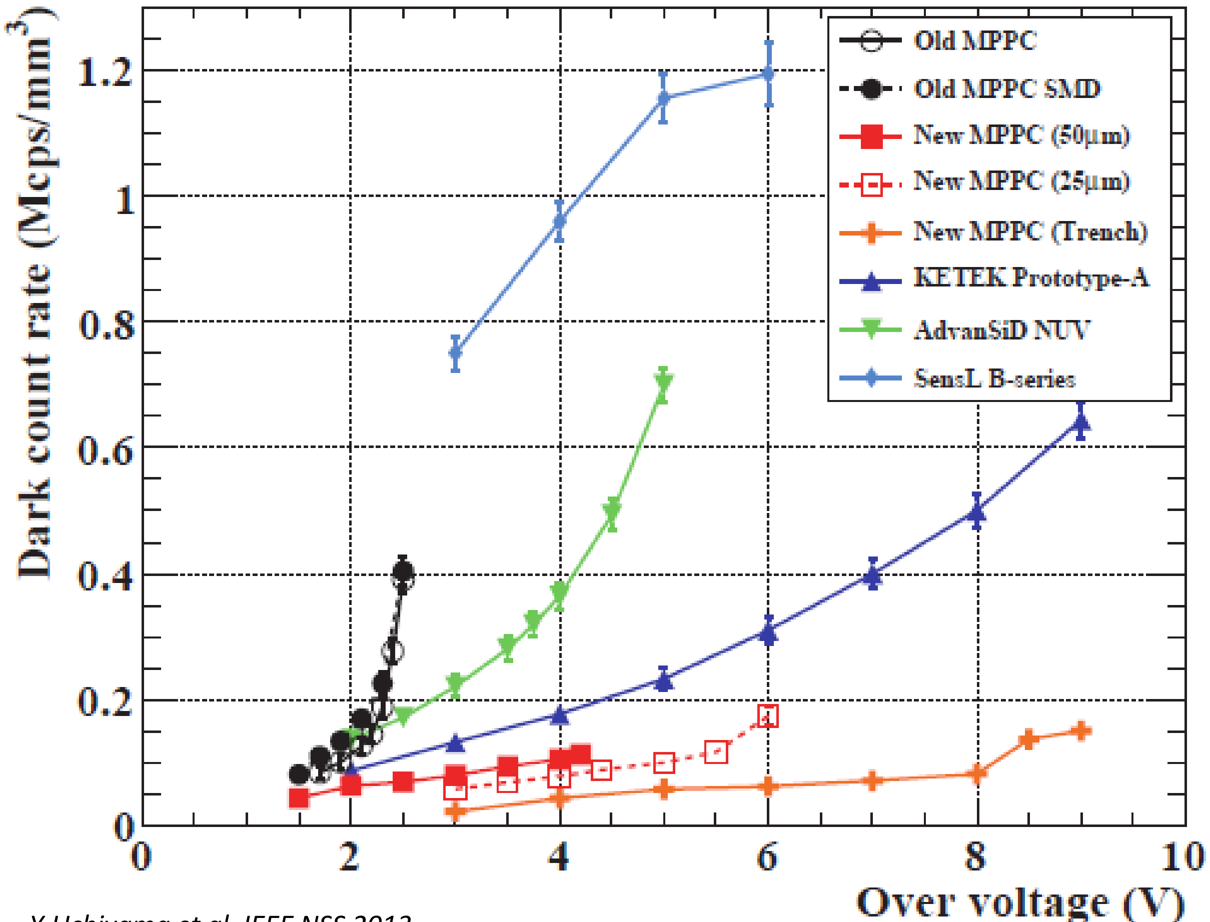

Y.Uchiyama et al, IEEE NSS 2013

Variation with the bias voltage and the temperature

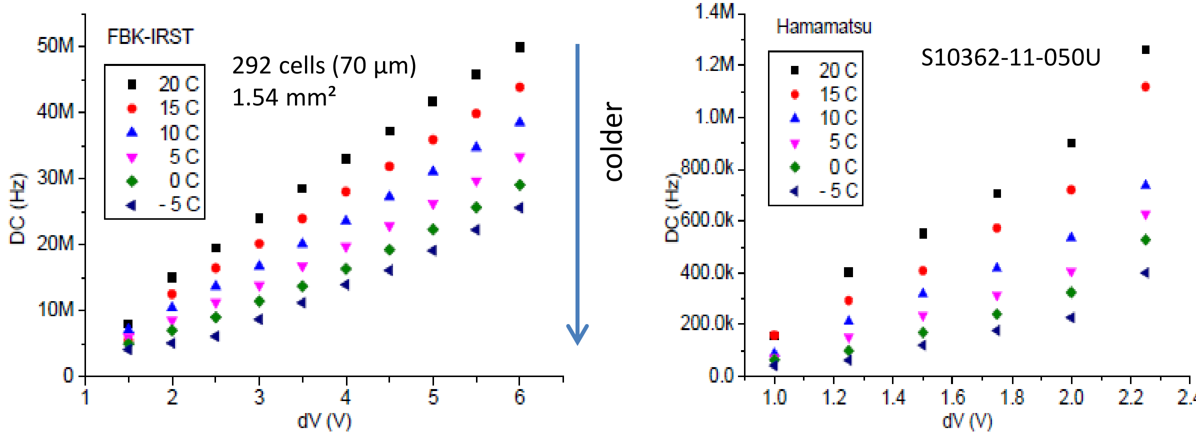

O. Starodubtsev, PoS 2012

9 mm²

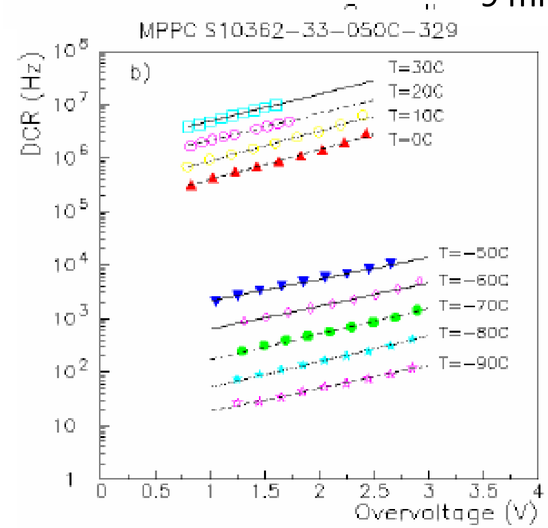

N. Dinu, IEEE NSS 2010

Increase of the DCR with the increase of the bias voltage and the temperature

Best way to decrease the Dark Count rate:

✓ operate the SiPM at lower voltage

✓ cooling (factor ≈ 2 reduction of the dark counts every 8°C)

After-pulses

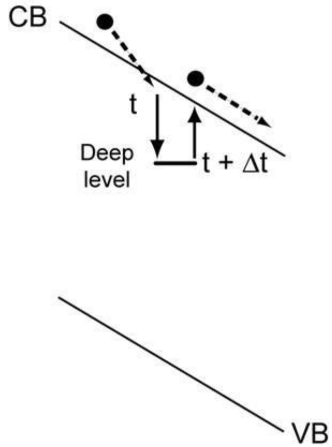

Breakdown → production of a large number of charge carriers → some of them are trapped in deep trap levels

These carriers may be released at some time and trigger a new breakdown avalanche event : afterpulse (described in term of probability)

$$P_{afterpulse}(t) = P_{trig} \times P_{capture} \frac{e^{-t/\tau}}{\tau}$$

$P_{capture}$: trap capture proba

P_{trig}: avalanche triggering proba

τ: trap lifetime

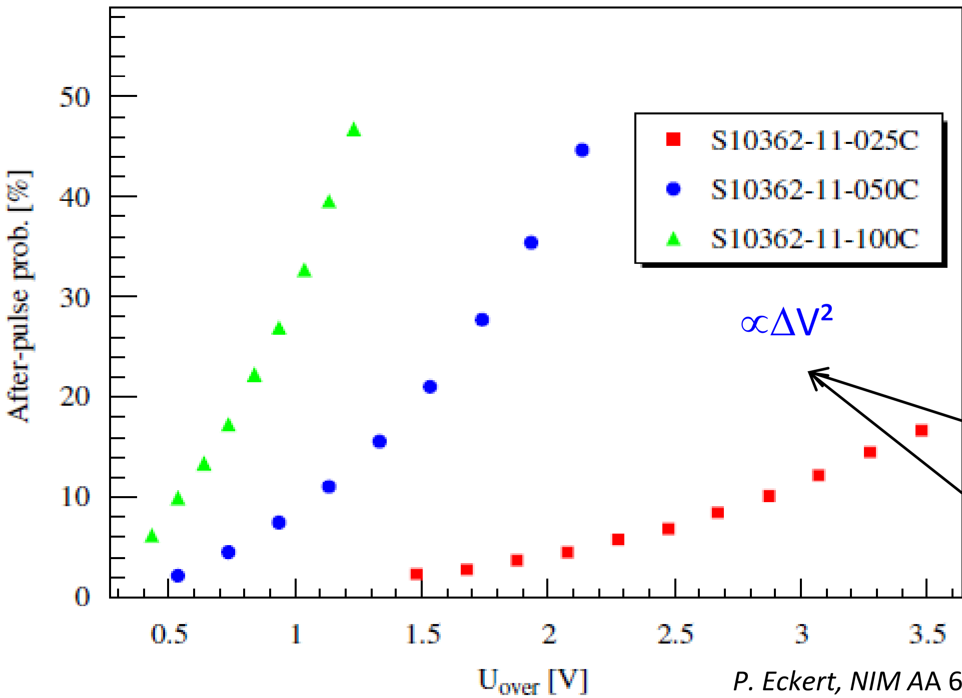

P. Eckert, NIM AA 620 (2010)

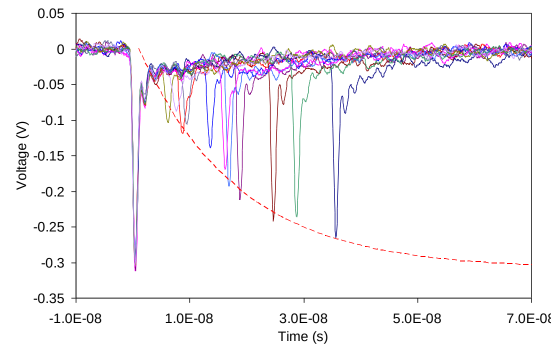

Number of carriers produced in the avalanche ∝ ΔV

Triggering proba ∝ ΔV

How to decrease the afterpulsing ?

Impurities (Iron, Gold) and defects (point, dislocation) create deep levels in the band gap

⇓

Minimization of the amount of impurities in the avalanche region employing pure Si wafers and new process conditions.

before

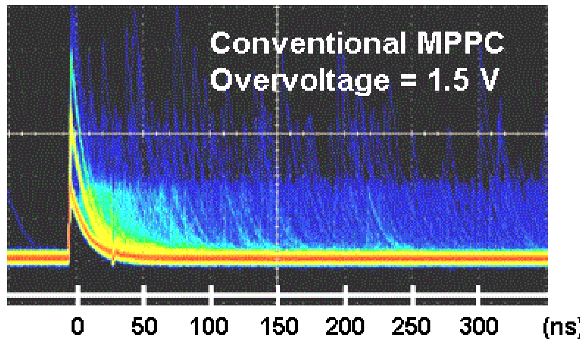

after

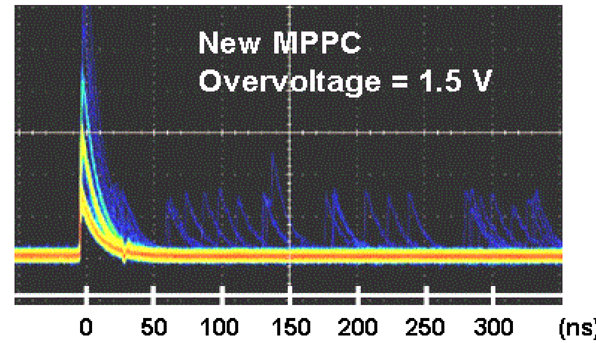

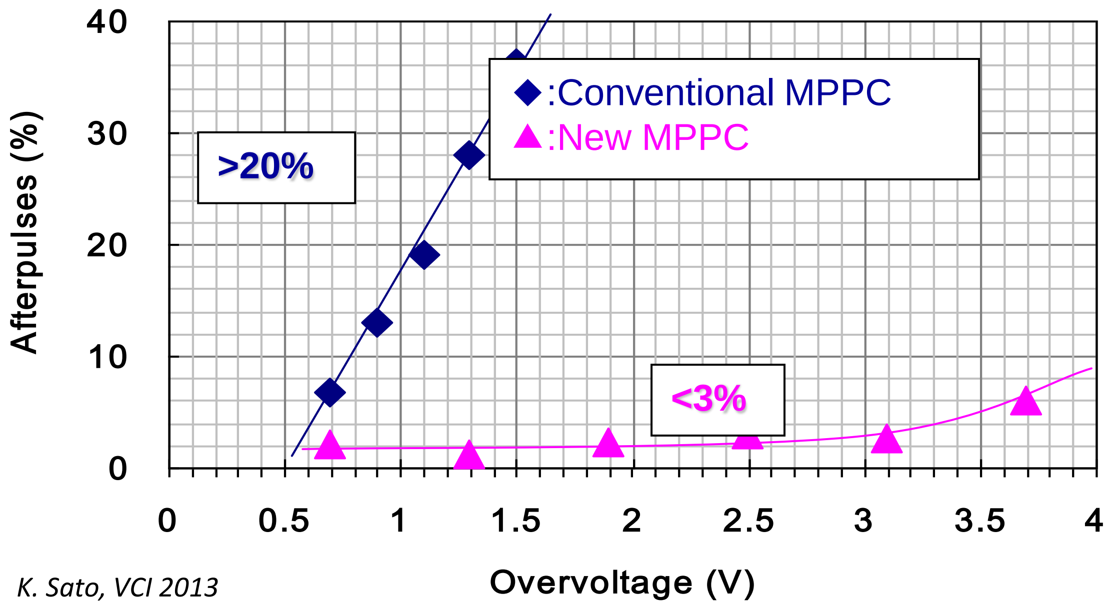

K. Sato, VCI 2013

Cross-talk

avalanche in one cell probability than 1 carrier emits ≈ 3.10^{-5} photons with E > 1.12 eV

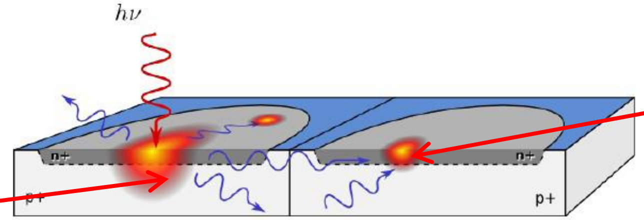

A. Lacaita, et al., IEEE Trans. Electron Devices ED-40 (1993) 577

these photons (≈ 30 for a gain of 10^6) can trigger another avalanche in a neighboring cell without delay

Cross-talk is responsible for the high rate at thresholds >1.5 p.e.

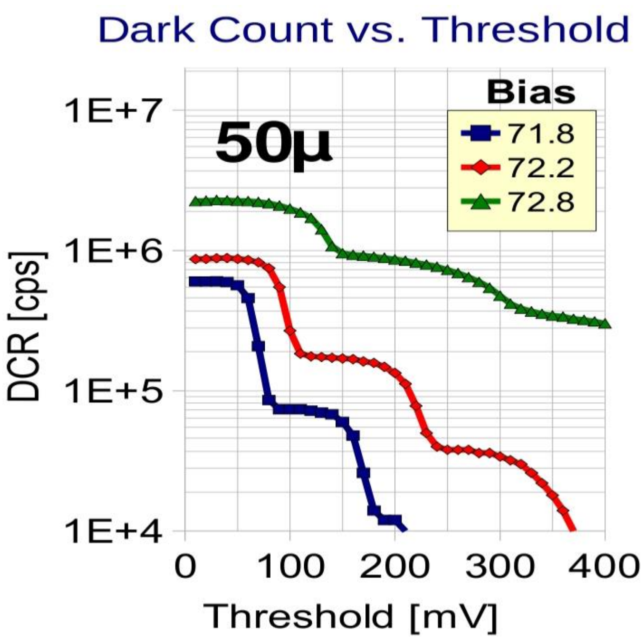

S. Gundacker, PhotoDet 2012

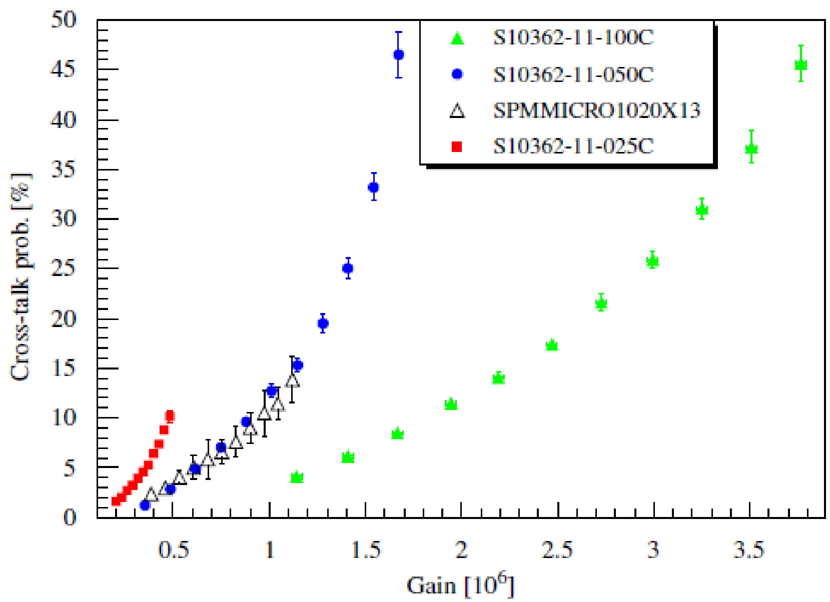

P. Eckert, NIM AA 620 (2010)

- Increases with the dimension of the cell (higher gain which depends on the junction capacitance)
- increase with the bias voltage (number of produced charge carriers)

How to decrease the Cross-talk

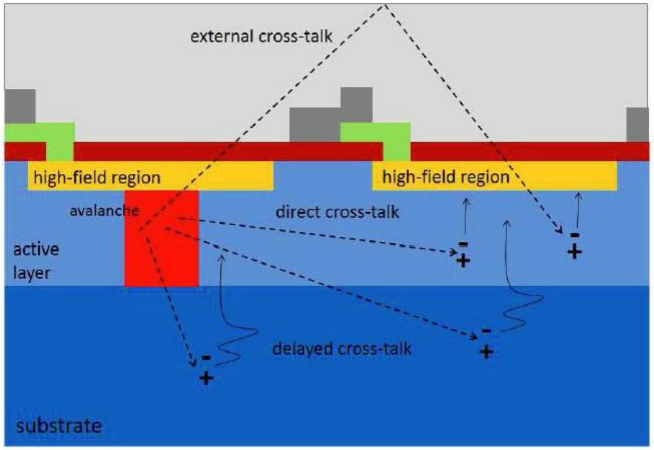

A. Ferri, IPRD13

One solution to decrease the optical isolation between the cells: etching trenches filled with opaque material

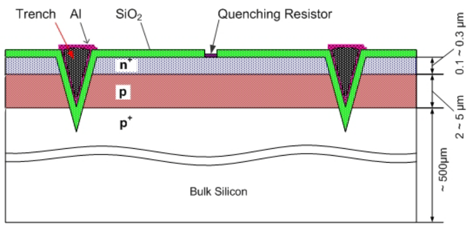

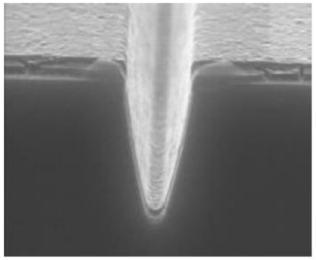

D. McNally, G-APD workshop (2009)

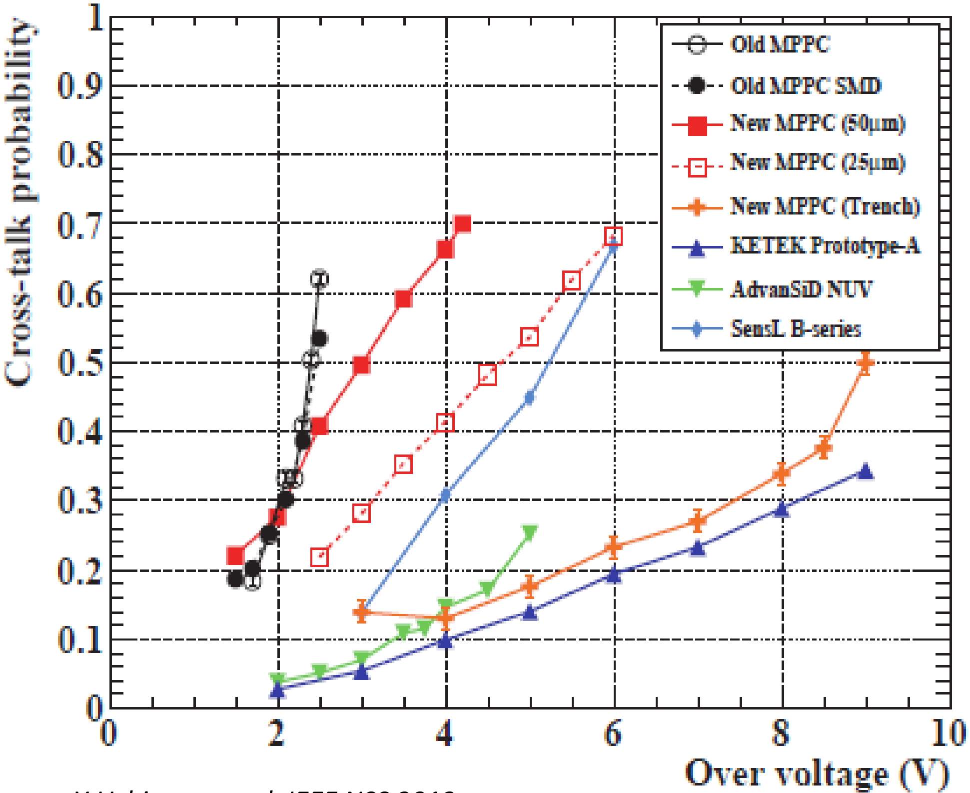

Y.Uchiyama et al, IEEE NSS 2013

Active layer is very thin (few µm) → breakdown development is very fast + big charge → we can expect very good timing properties even for single photons

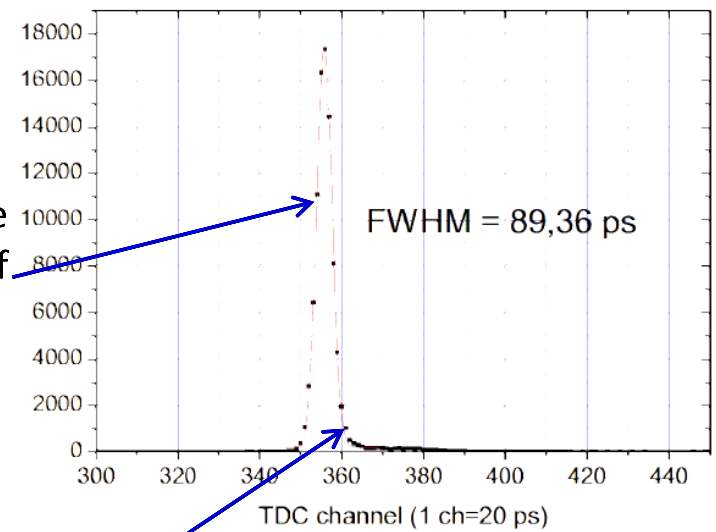

E. Popova, SiPM Advanced Workshop 2013

fast component of Gaussian shape with 50 ps< σ < 150ps
The fluctuation are due to the variance of the transverse diffusion speed and the variance of transverse position of photo-generation.

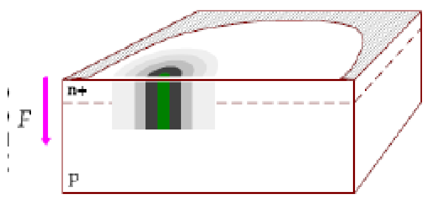

Transverse multiplication

slow component: minor non Gaussian tail with time scale of several ns due to minority carriers, photo-generated in the neutral regions beneath the depletion layer that reach the junction by diffusion.

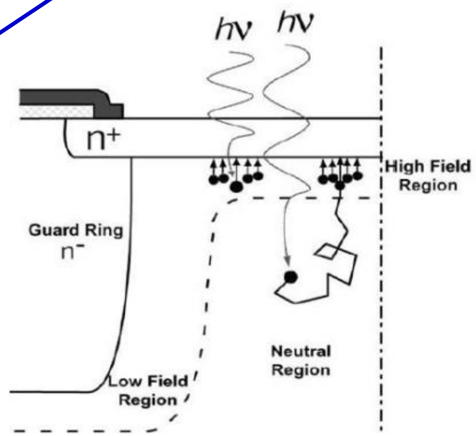

Variation of the timing resolution

Timing resolution as a function of the incident number of photons

SPTR as a function of the temperature

G. Collazuol, NIM A 581 (2007)

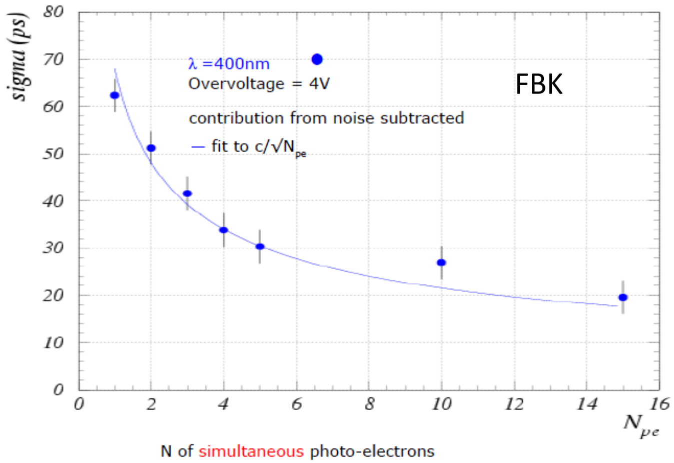

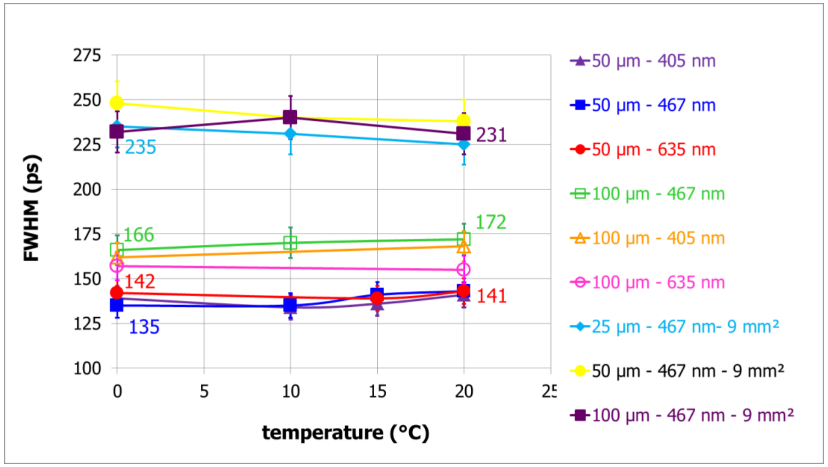

V. Puill, NIMA 695, 2012

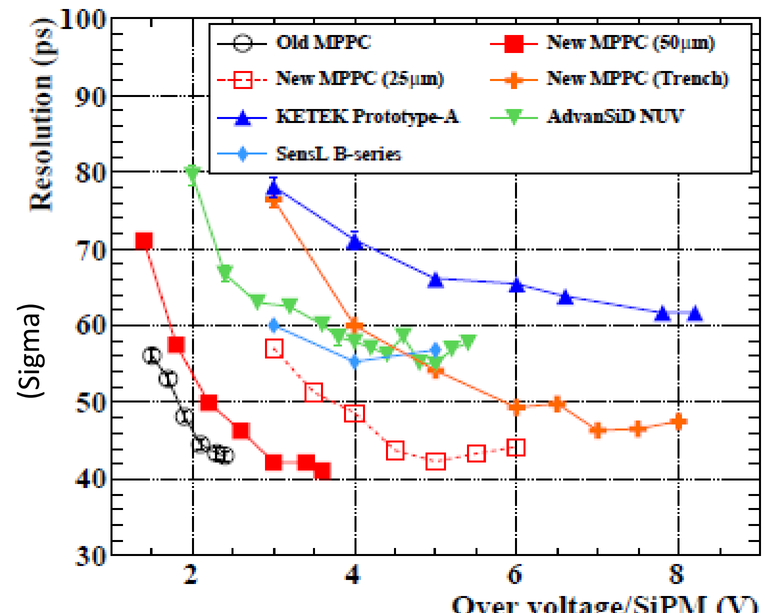

P.W Cattaneo, arXiv:1402.1404v1

Dynamic range and linearity

Detection of photons: statistical process based on the probability of detecting randomly distributed photons by the limited number of cells: the dynamic range is determined by the PDE and the total number of cells

$$A \approx N_{firedcells} = N_{total} \cdot \left(1 - e^{-\frac{N_{photon} \cdot PDE}{N_{total}}}\right)$$

$N_{firedcells}$: number of excited cells
N_{total}: total number of cells
N_{photon}: number of incident photons in a pulse

SiPM response as a function of the number of instantaneous incident photons

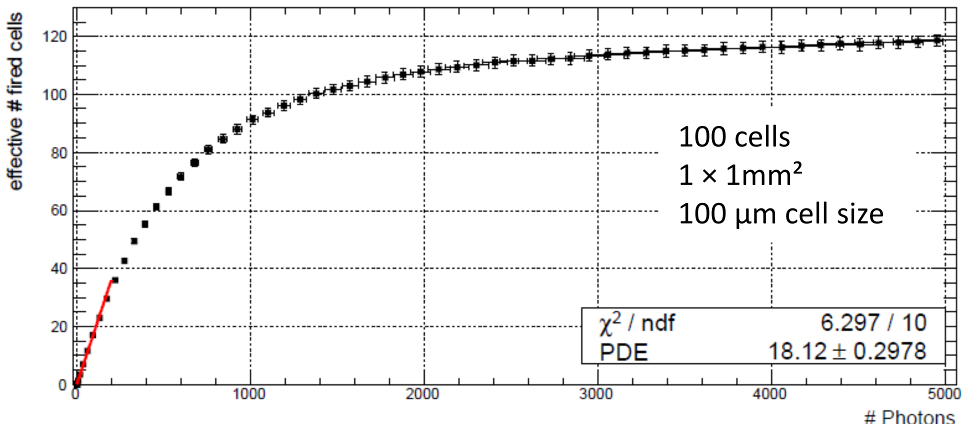

T. Kowalew Thesis

2 or more photons in 1 cell look exactly like 1 single photon

Output signal: proportional to the number of fired cells as long as

N_{photon} x PDE << N_{total}

The saturation is a limiting factor for the use of SiPM where large dynamic range of signal (5000 – 10000 photons/pulse) has to be detected (calorimetry)

Solution to the saturation: large number of cells

high density SiPM : device with more than 1000 cells/mm² + short recovery time

HAMAMATSU

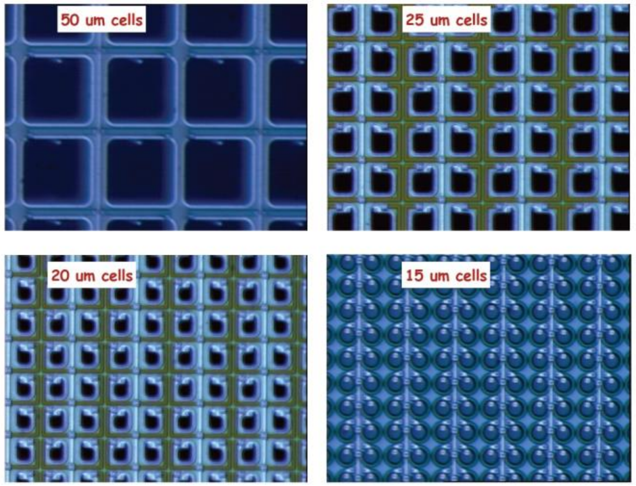

1 mm²
4489 cells
cell size : 15 µm
gain = 2×10^5

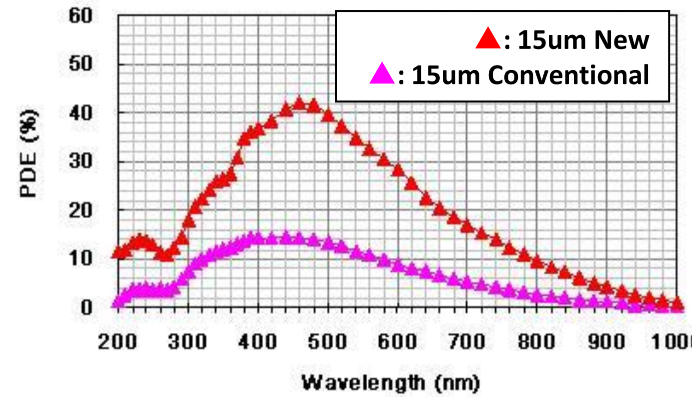

HPK, private communication

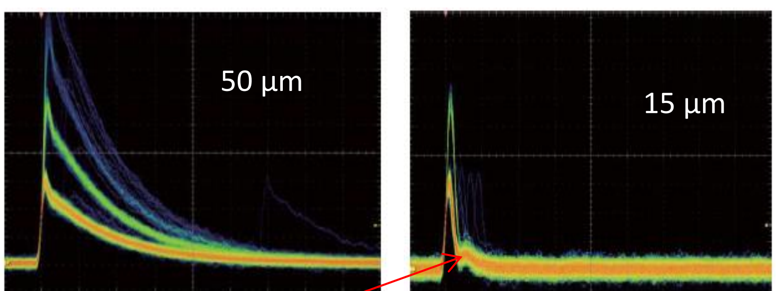

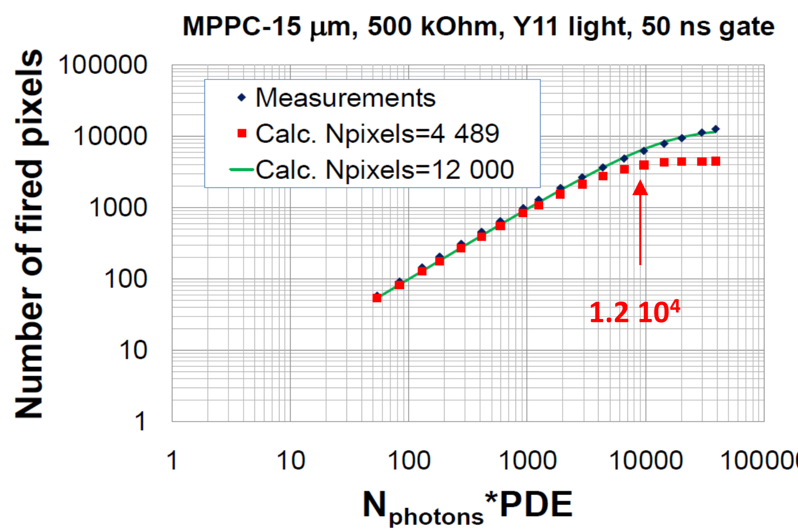

Y. Musienko, NDIP-2011

fast cell recovery time (~4ns) → the linearity for Y11 (WLS fiber) light of 4489 cells/mm² MPPC corresponds to a SiPM with ~ 12000 cells/mm²

Solution to the saturation: large number of cells

KETEK

high density SiPM : device with more than 1000 cells/mm²

MP15 V6 W8:
1.2x1.2 mm²
Cell size = 15 µm
12800 cells

MP20 V4 W12:
3x3 mm²
Cell size = 20 µm
22500 cells

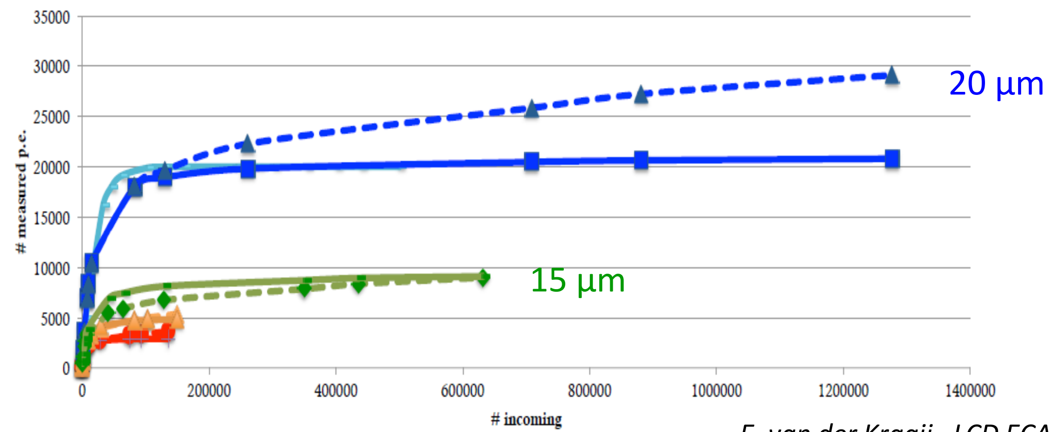

E. van der Kraaij, LCD ECAL meeting 2014

FBK

RGB-SiPM-HD

2.2 x 2.2 mm²
gain = 8x10^5
DCR = 2MHz/mm²
recovery time = 9 ns

Active area: **2.2x2.2 mm²**
cell size: **15x15 µm²**
cells: ~ 21300
Fill factor = 48%

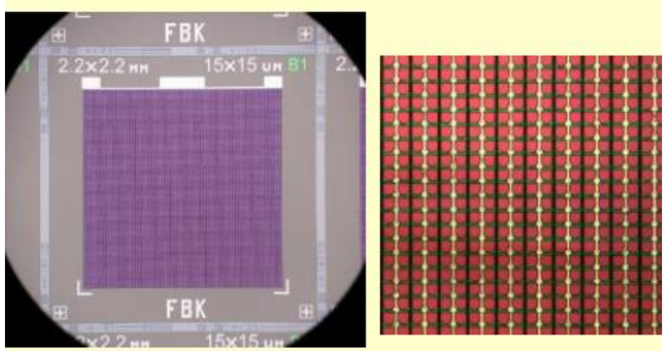

A. Ferri

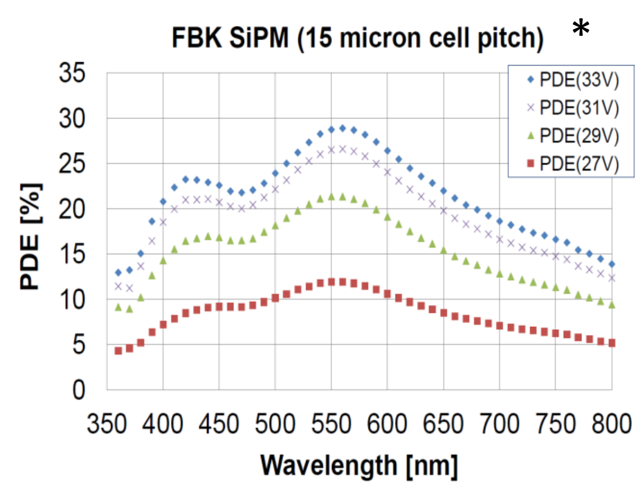

** measurements by Y.Musienko @ CERN*

Solution to the saturation: very large number of cells

ZECOTEK MAPD-3N

Special design: both the matrix of avalanche regions and the individual quenching elements are created inside the Si substrate with a special distribution of the inner electric field

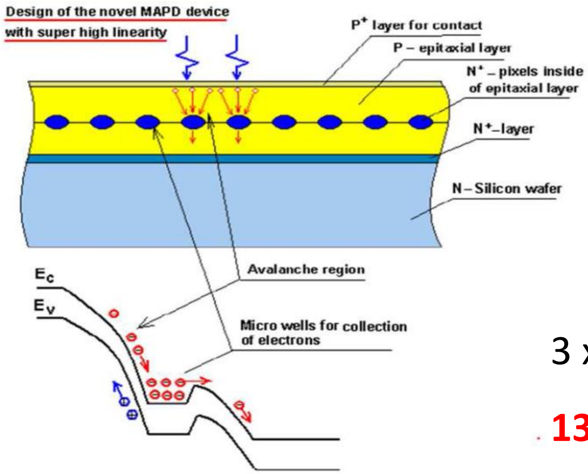

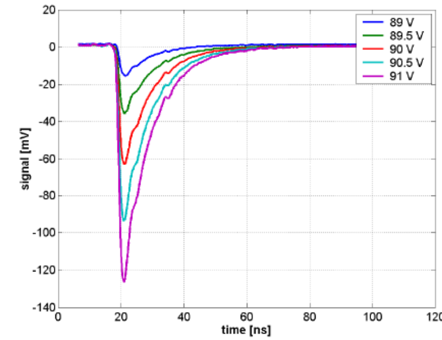

A. Rychter, Proc. of SPIE Vol. 8454

3 x 3 mm²

1350000 cells (15000/mm²)

gain = 10^5

slow cell recovery time : 80 ns

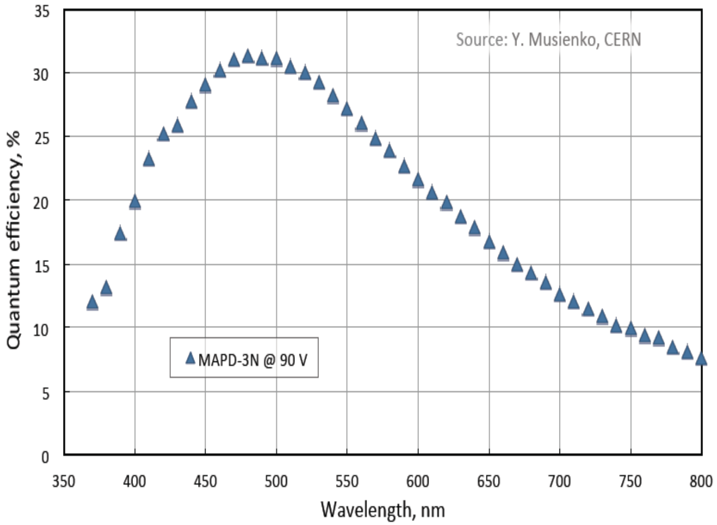

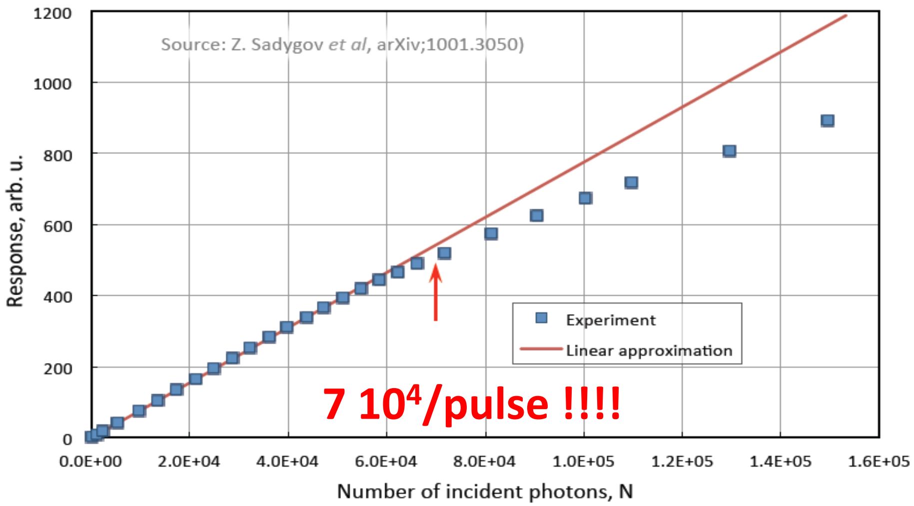

Radiation-hardness of SiPMs

protons / neutrons

bulk damages caused by lattice defects

γ-rays, X-rays

creation of trapped charges near the Si-insulator interface

Radiation hardness, an issue for photodetector in Calorimeters

- increase of the dark current and the DCR
- change of the breakdown voltage
- change of the gain and PDE dependence as a function of bias voltage

- limitation of the low light detection capability
- destruction of the device

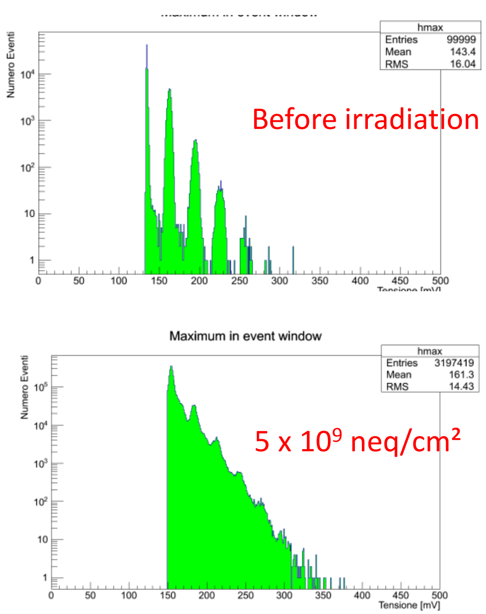

W. Baldini, TIPP 2014

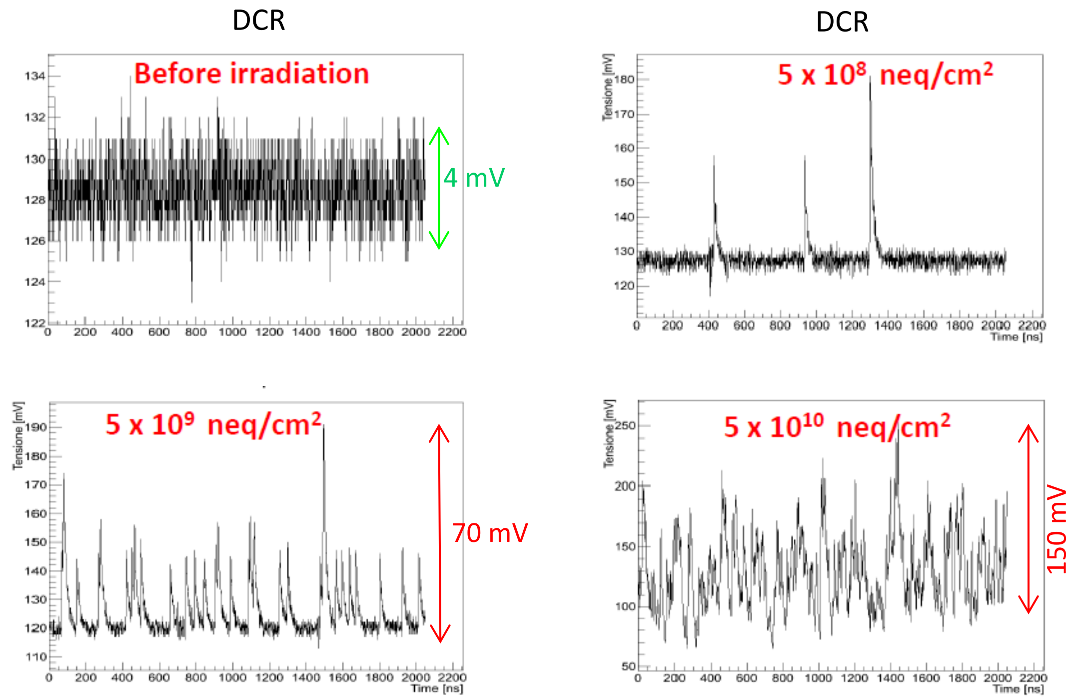

Good resistance to neutron irradiation

HAMAMATSU , NDL, ZECOTEK, KETEK developed devices with improved radiation hardness:

The best at the moment:

- 15 µm cell size MPPC (1 mm²)
- 10 µm cell size NDL (0.25 mm²) SiPM

which **survived 10^{13} n/cm² 1 MeV equivalent neutron flux** (10^{8} n/cm² 3 years ago)

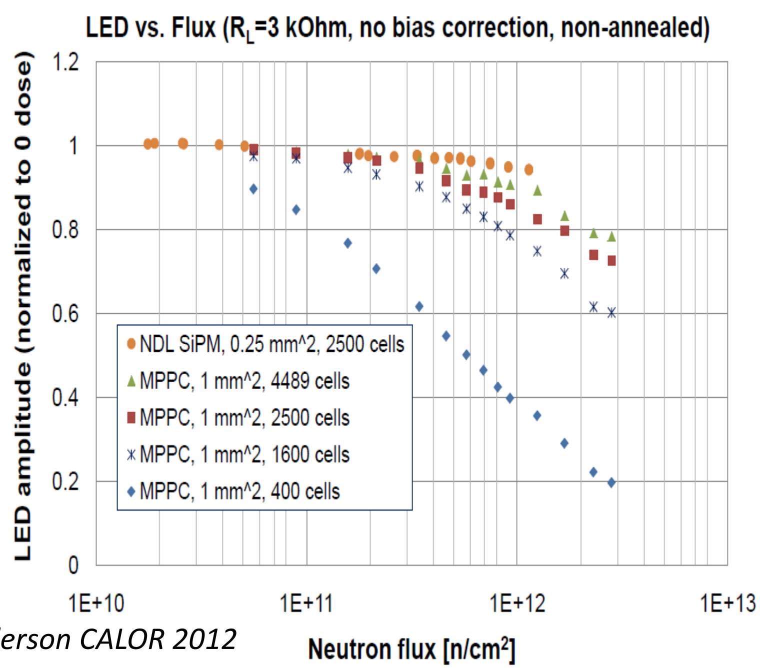

J. Anderson CALOR 2012

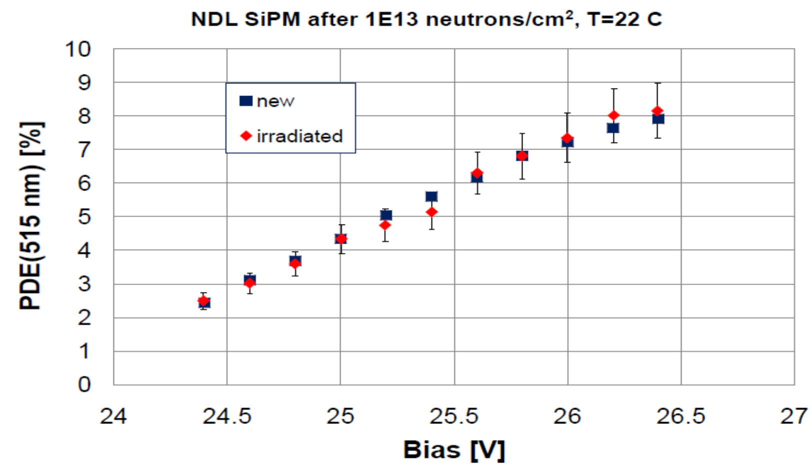

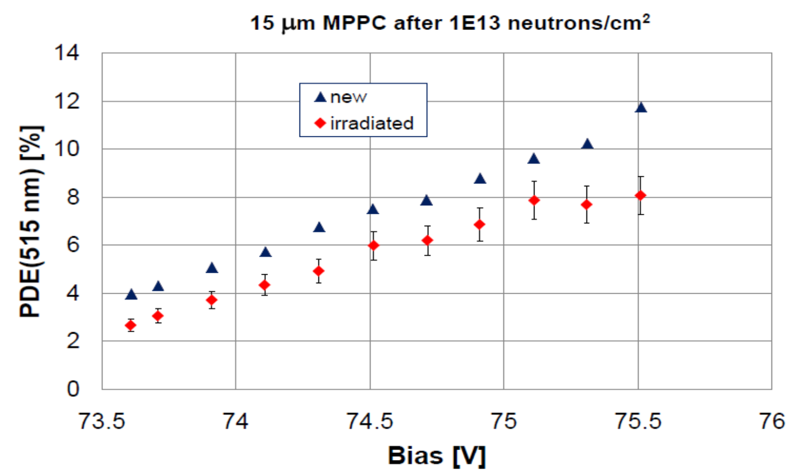

Y. Musienko, NDIP 2011

Large SiPMs: large sensitive area but high DCR …

Excelitas C30742-66

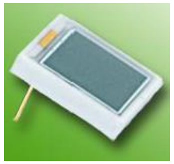

ASD-SiPM4S

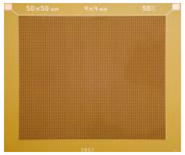

sensL C-series

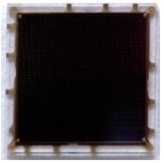

HAMAMATSU S10985

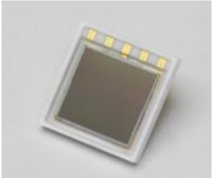

KETEK PM6060

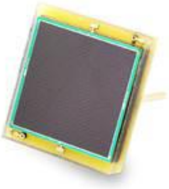

STMicroelectronics

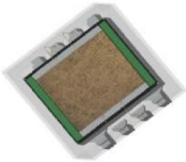

Producer	Reference	Area (mm²)	PDE max @ 25 °C *	Dark Count Rate max (Hz) @ 25°C *	Gain *
EXCELITAS	C30742	6 x 6	30% @ 420 nm	$10 .10^6$	$1.5\ 10^6$
FBK - AdvanSiD	ASD-SiPM4S	4 x 4	30% @ 480 nm	$9.5\ 10^7$	$4.8\ 10^6$
HAMAMATSU	S10985-50C	6 x 6	50% @ 440 nm (includes afterpulses & crosstalk)	10.10^6	$7.5\ 10^5$
SensL	C-series	6 x 6	40 % @ 420 nm	$4.5\ 10^6$ (21 °C)	$3\ 10^6$
KETEK	PM6060	6 x 6	40% @ 420 nm	18.10^6	10^7
STMicrolectronics	SPM35AN	3,5 x 3,5	16% @ 420 nm	$7.5\ 10^6$	$3.2\ 10^6$

** 2013-2014 datasheet data*

Segmentation of the light detection + need of larger active area → SiPM matrix

FBK

ASD-SiPM4S-P-4×4T-50

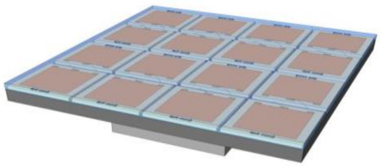

4x4 channels
1 channel = 4x4 mm²
6400 cells (50 x 50 µm²) /channel

Zecotek

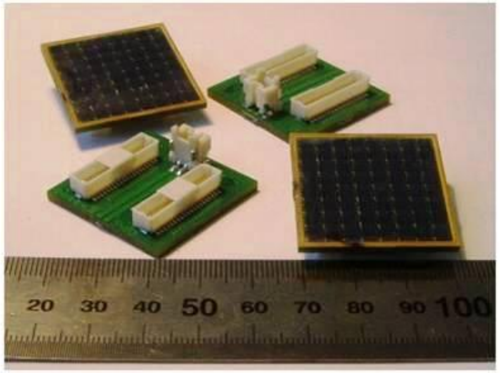

8x8 channels
1 channel = 3x3 mm²
15000 cells /channel

HAMAMATSU

S11834-3388DF

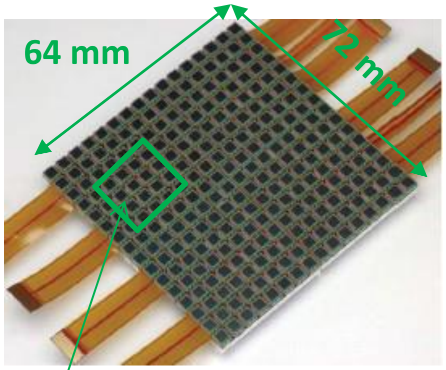

S11064-025

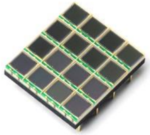

4x4 channels
1 channel= 3 x 3 mm²
14400 cells (25 x 25 µm²) /channel

Excelitas Ketek

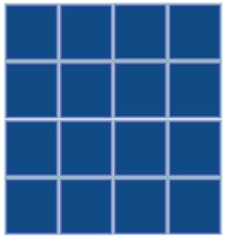

R&D in progress

Matrixes of 16 channels with 3 x 3 or 6 x 6mm²

SiPMs discrete arrays

Sensl

ArraySL-4p9-30035

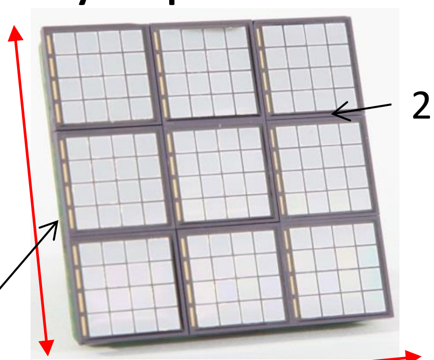

SL-4-30035-CER

4x4 channels
1 channel= 3 x 3 mm²
4774 cells (35 x 35 µm²) /channel

ArrayB-600XX-64P

8x8 channels
1 channel= 6 x 6 mm²
18980 cells /channel
new surface mount package

Sungkyunkwan University (Korea)

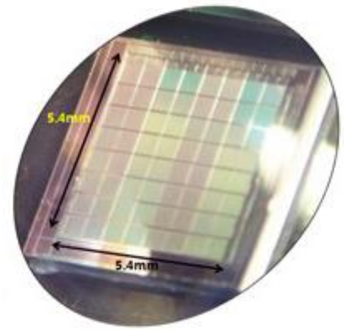

8x8 channels
1 channel= 0.5 x 0.5 mm²
1024 cells (32 x 32 µm²)/channel

Philips Digital Photon Counting

DLS-6400-22-44

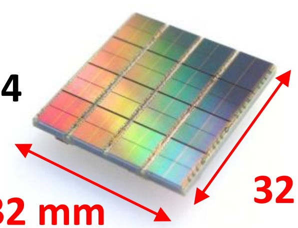

8x8 channels
1 channel = 3.9 x 3.2 mm²
6396 cells (59 x 32 µm²) /channel
Electronics embedded

Requirements for the SiPM matrixes:

- improvement of the spatial resolution and PDE
- simplification of the assembly for the building of detectors with large surface and large active area

✓ Important efforts on the packaging: matrix tileable on almost all their sides + small dead space between them

✓ Development of monolithic SiPM matrices: all the channels are on the same substrate → small dead spaces, simplification of the assembly

Discrete Array

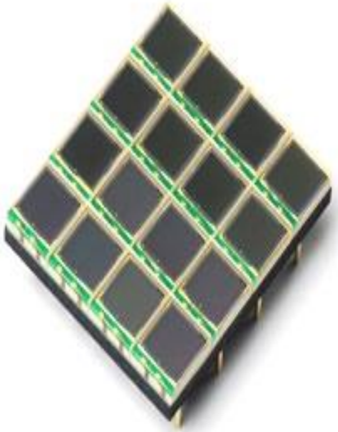

Monolithic Array

3-side buttable Tiling

SiPMs monolithic arrays

HAMAMATSU

4x4 channels

1 channel = 3x3 mm²

3600 cells (50x50 µm²)/channel

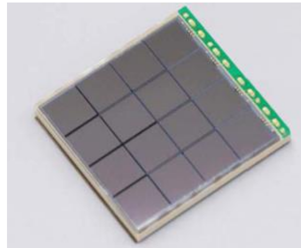

S11828-3344

Kato et al, NIMA 638 (2011) 83–91

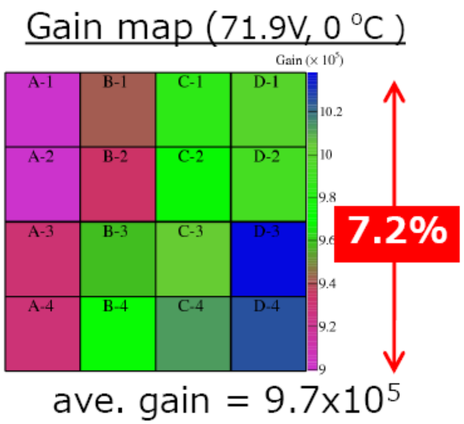

3 sides tileable

1 cathode – 16 anodes

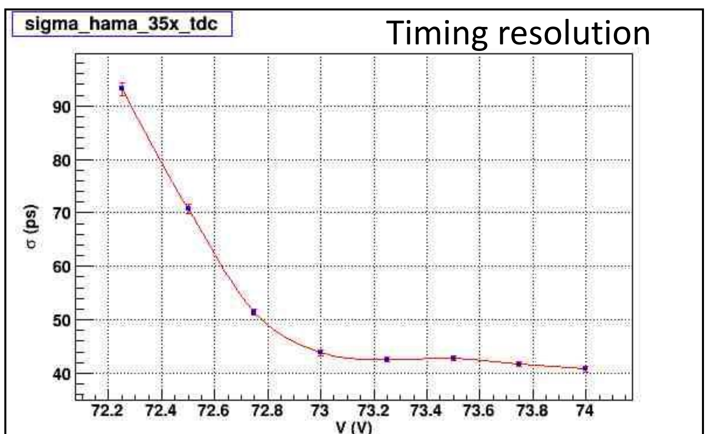

M. Bonesini, IPRD13

FBK - AdvanSiD

ASD-SiPM3S-P-4x4A

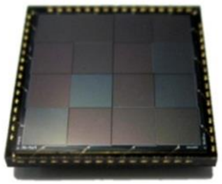

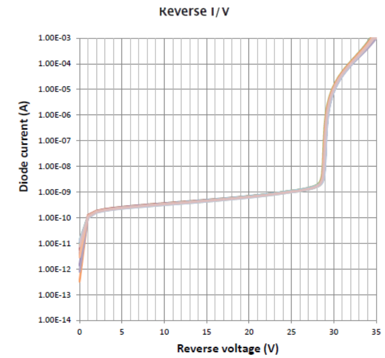

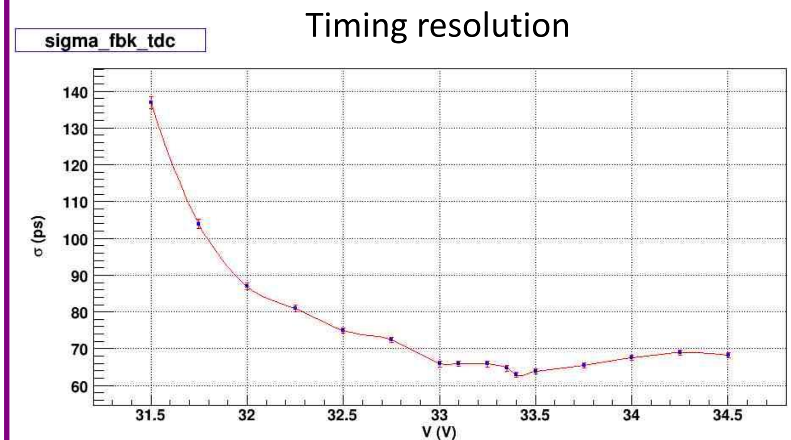

M. Bonesini, IPRD13

ASD-RGB1.5S-P-8x8A

NEW

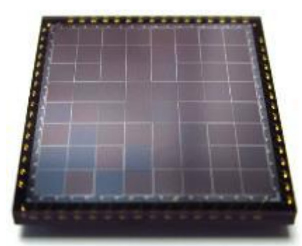

8 x 8 channels

4 sides tileable

Discret array with TSV technology

HAMAMATSU development: another way to improve the fill factor and therefore the PDE

Through Silicon Via Technology: each anode is connected by the shortest distance possible to the substrate

with wire bonding (traces to the bonding pads)

with TSV (No traces)

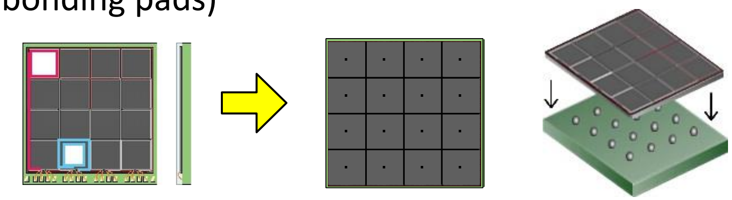

16x16 channels array

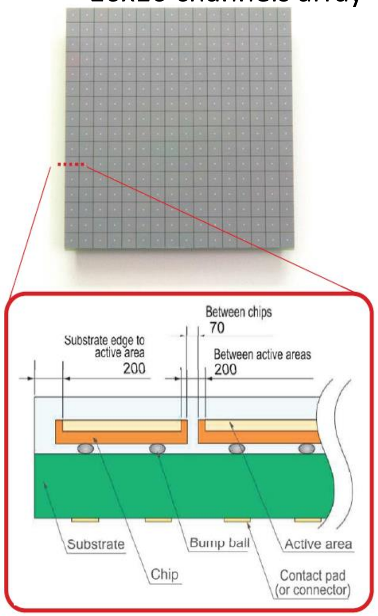

K. Sato, IEEE NSS 2013

+ high precision assembly → Discrete Array like monolithic array !

S12642-0808PA

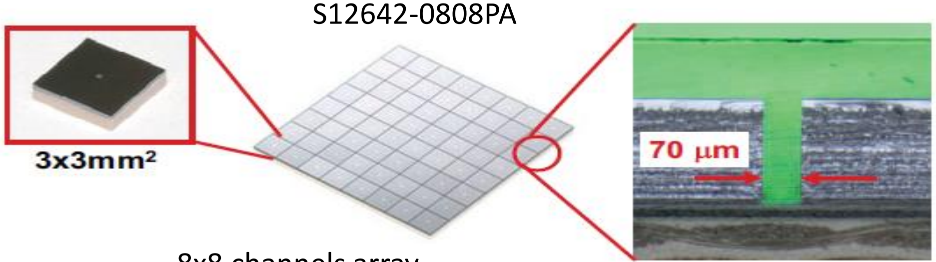

8x8 channels array

4 side tileable configuration with very narrow gap between neighboring active areas (200 µm) equivalent to the gap in traditional monolithic type devices

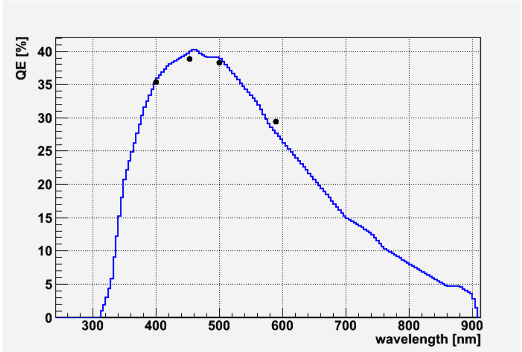

N. Otte, NDIP14

KETEK & PHILIPS are going to use TSV as well

Quick look on some other structures

Digital SiPM

Resistor embedded in the bulk

Array of G-APDs integrated in a standard CMOS process. The signal from each cell is digitized and the information is processed on chip:

- time of first fired cell is measured
- number of fired cells is counted
- active control is used to recharge fired cells

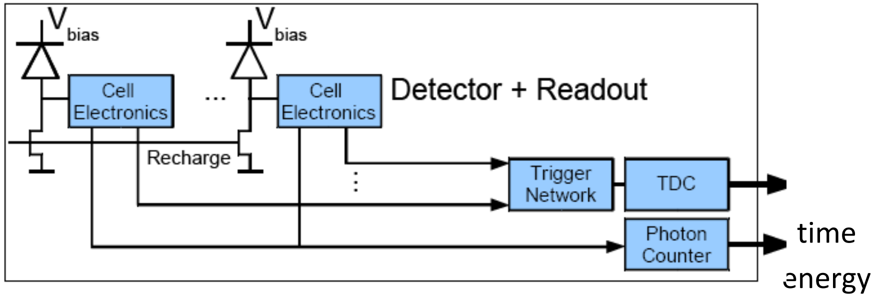

York Hämisch, TIPP 2011

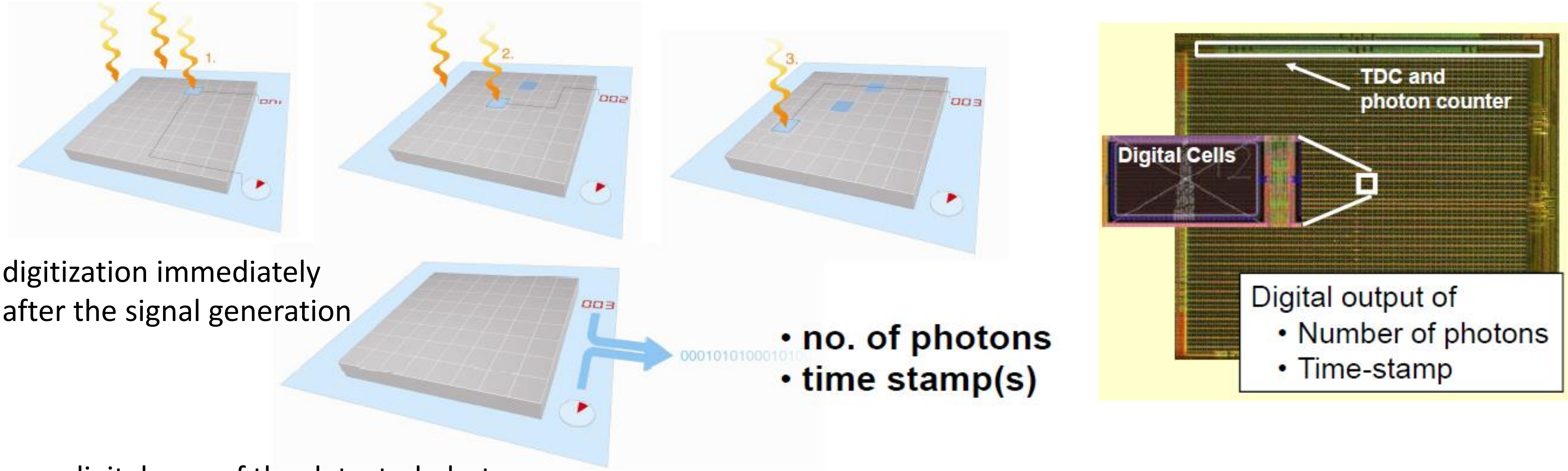

digitization immediately after the signal generation

digital sum of the detected photons

The Digital SiPM by Philips - DPC

Early Designs in 2005

DLS-3200-22-44

- 3200 cells
- 59 x 64 µm² cell size
- 78% fill-factor

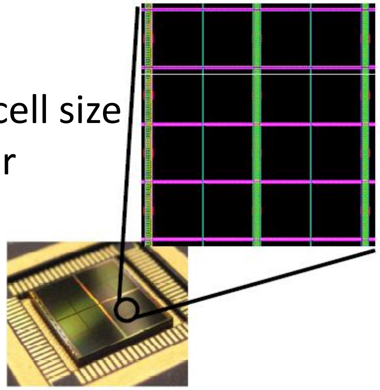

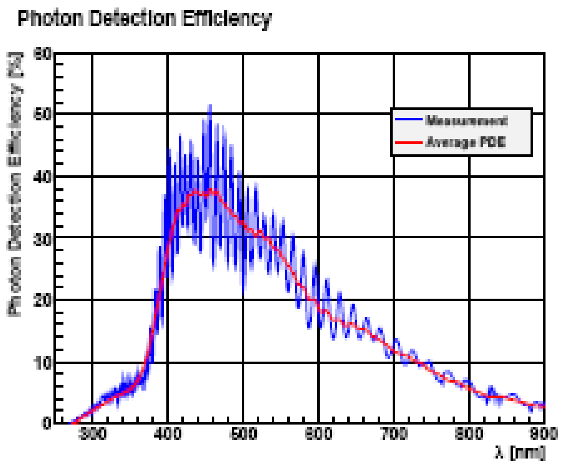

T. Frach, 2012 JINST 7 C01112

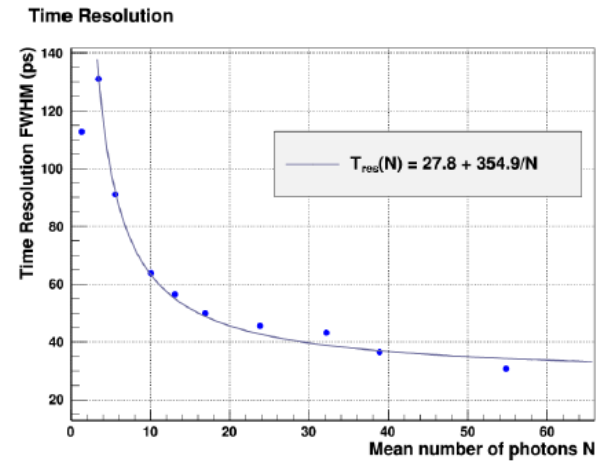

T. Frach, Hereaus seminar 2013

- *afterpulsing ~ 18% (20 °C)*
- *DCR = 200 kHz/mm² (20 °C)*
- *temperature sensitivity ~ 0.33 %/°C*
- *timing resolution (SPTR) = 140 ps (FWHM)*
- *recovery time : 5 – 40 ns*

<u>Radiation hardness ?</u>

→ still working for 10^{11} n/cm² (data to be published soon)

<u>Drawback:</u>

➢ requires a dedicated readout provided by Philips

Digital SiPM: other developments

FBK – ST micro – Edimburg University

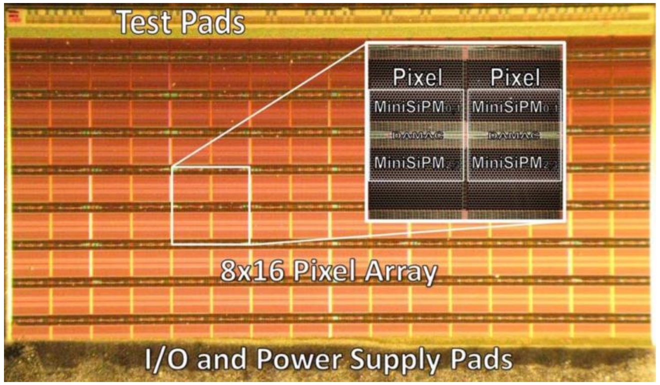

L. H. C. Braga, IEEE Journal of solid state circuit vol. 49, 2014.

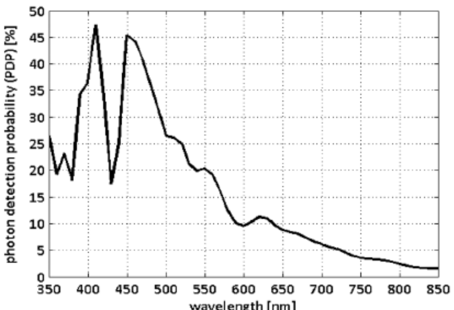

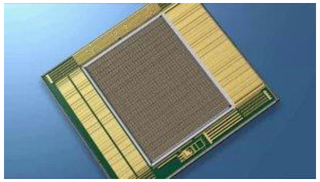

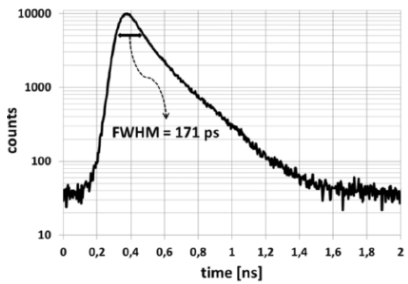

Faculty of Electrical Engineering, TU Delft

Area of the chip: 22.1 mm2 with a sensitive area of 3.2 x 3.2 mm²

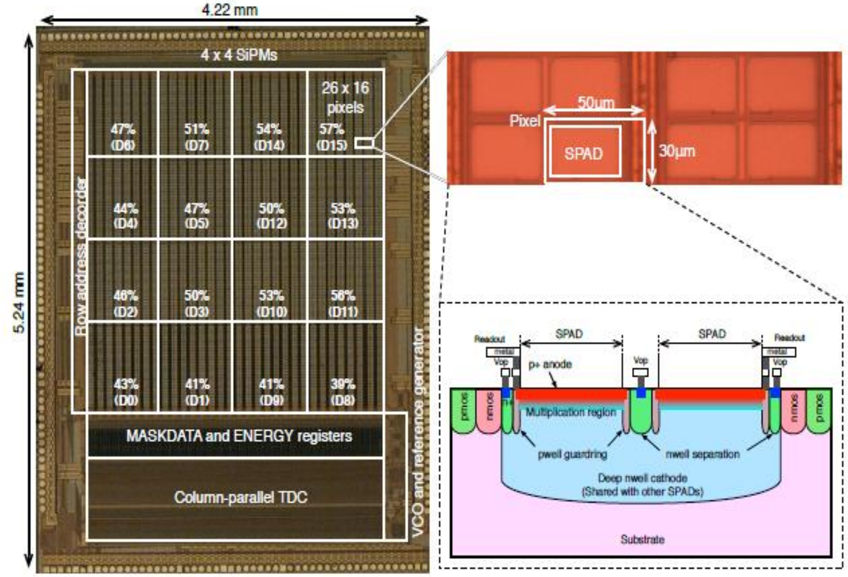

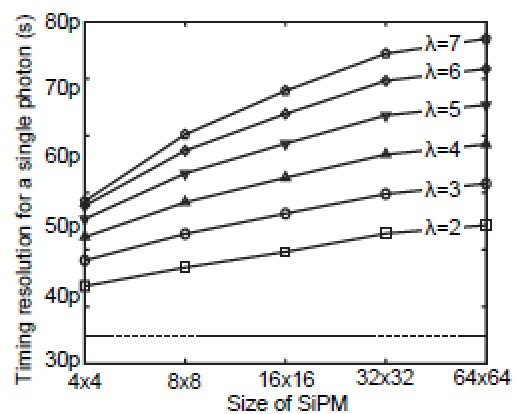

S. Mandai, 2013 JINST P05024

SiPMs with bulk integrated resistors

The quenching resistors are formed in the Si bulk rather than on the surface of the device

MPI

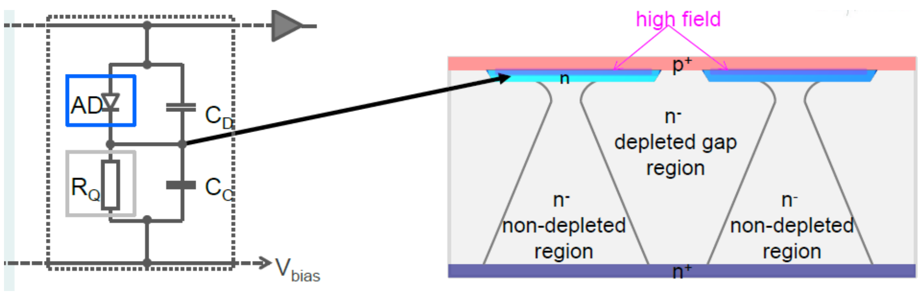

NDL

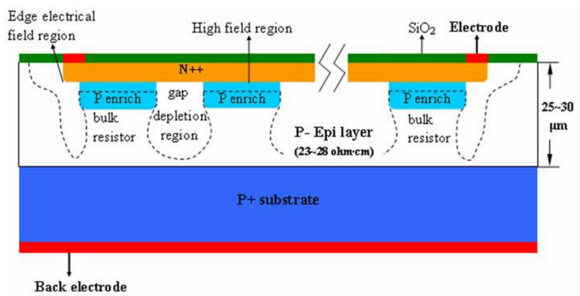

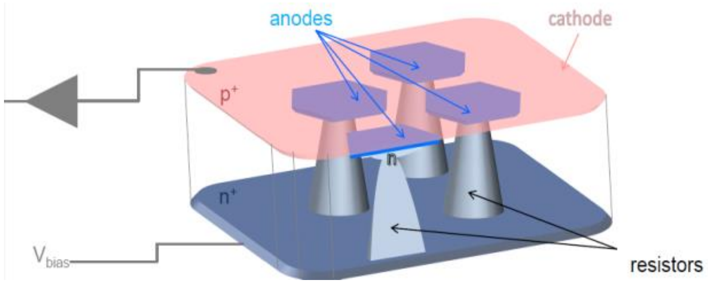

Advantages

- simple fabrication process
- no obstacles in entrance window
- possible high geometrical fill-factor
- possibility of antireflective coating
- possible high cell density

SiPMs with bulk integrated resistors

MPI

- Pitch : 100 – 160 µm
- Gap : 5 – 20 µm
- Gain = 2 – 10x10^6
- Cross-talk= 15 – 30 % (-20°C)
- DCR= 10 MHz/mm² (25 °C)
- PDE (440 nm) = 26 % (-20°C)

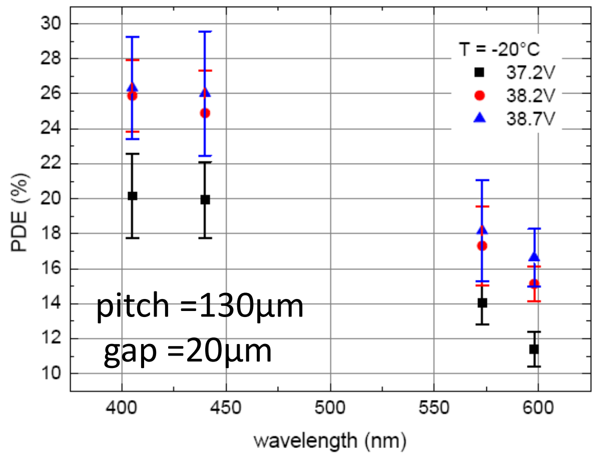

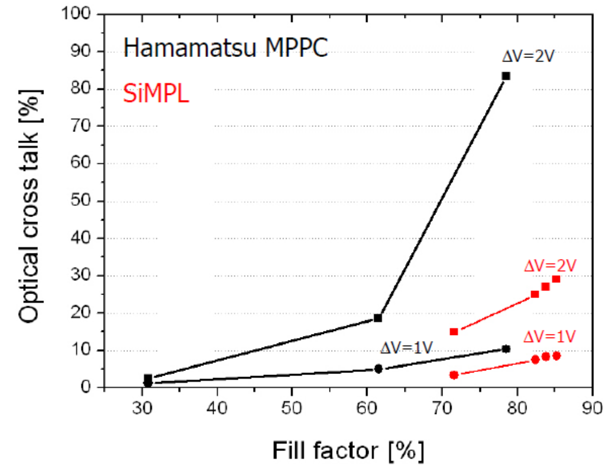

C. Jendrysik, NIM A 718 (2013)

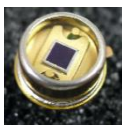

NDL

- 2.2 × 2.2 mm² cell size : 42 µm
- 43400 cells
- DCR = 8 MHz/mm² (21 °C)
- Gain = 2 10^5 (21 °C)
- PDE (460 nm) = 12 %
- recovery time : 5.8 ns

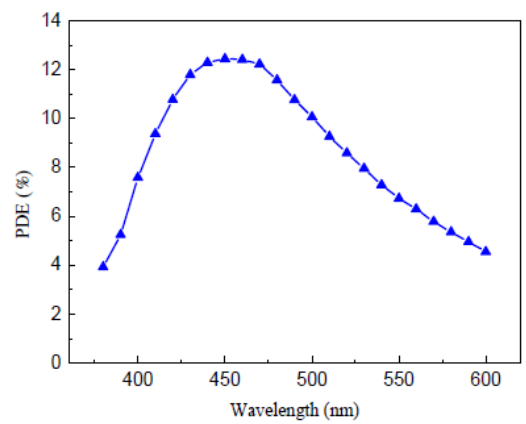

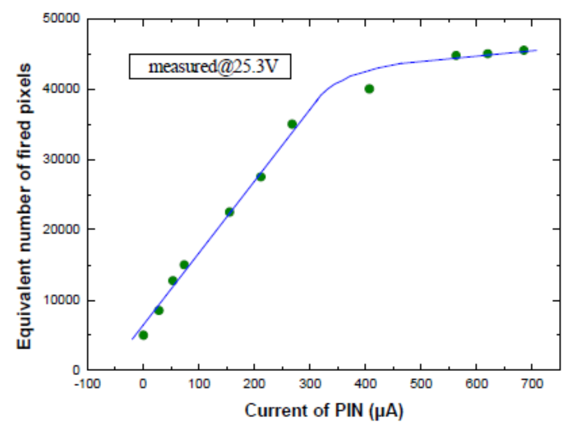

C. Li, IEEE NSS 2013

Promising results

R&D on going at MPI and NDL to improve the structure and the performances

Conclusion

Advantages and drawbacks of SiPMs

SiPM	• High gain (10^5-10^6) with low voltage (< 100 V) • Single photo detection • Good timing resolution (SPTR = 40 ps - sigma) • Insensitivity to magnetic field (up to 7 T) • High photon detection efficiency (35 % in blue) • Mechanically robust • A lot of R&D and different producers • Low cost mass production possible (ex: T2K)	• High dark count rate @ room temperature for large device (≥ 9 mm^2) • High temperature dependence of the breakdown voltage, the gain • Small devices • Few geometrical configurations available

New developments to discover during the NDIP14 Conference

Lectures and Revues :

- **Summer School INFIERI 2013, Oxford*:*** Intelligent PMTs versus SiPMs, ***Véronique Puill***
- **RICH 2013**: Status and Perspectives of Solid State Photo-Detector, ***Gianmaria Collazuol*** ← all you want to know about SiPM
- **SiPM workshop,** 16.02.2011, CERN: State of the art in SiPM's, ***Yuri Musienko***

Books:

- **Physics of semiconductor devices** – 3rd edition, ***S.M Sze*** (*John Willey & Sons*)

Reference articles:

- **Silicon Photomultiplier - New Era of Photon Detection** from Valeri Saveliev
- **Advances in solid state photon detectors** from D. Renker and E. Lorenz
- **Silicon Photo Multipliers Detectors Operating in Geiger Regime: an Unlimited Device for Future Applications** from G. Barbarino, R. de Asmundis, G.a De Rosa, C. M Mollo, S. Russo and D. Vivolo

Articles and presentations:

All quoted under the figures and plots of this presentation (my apologies if I forgot some of them)

Interactive SiPM demo

Do you want to play will a real SiPM before attending to session number 3 ?

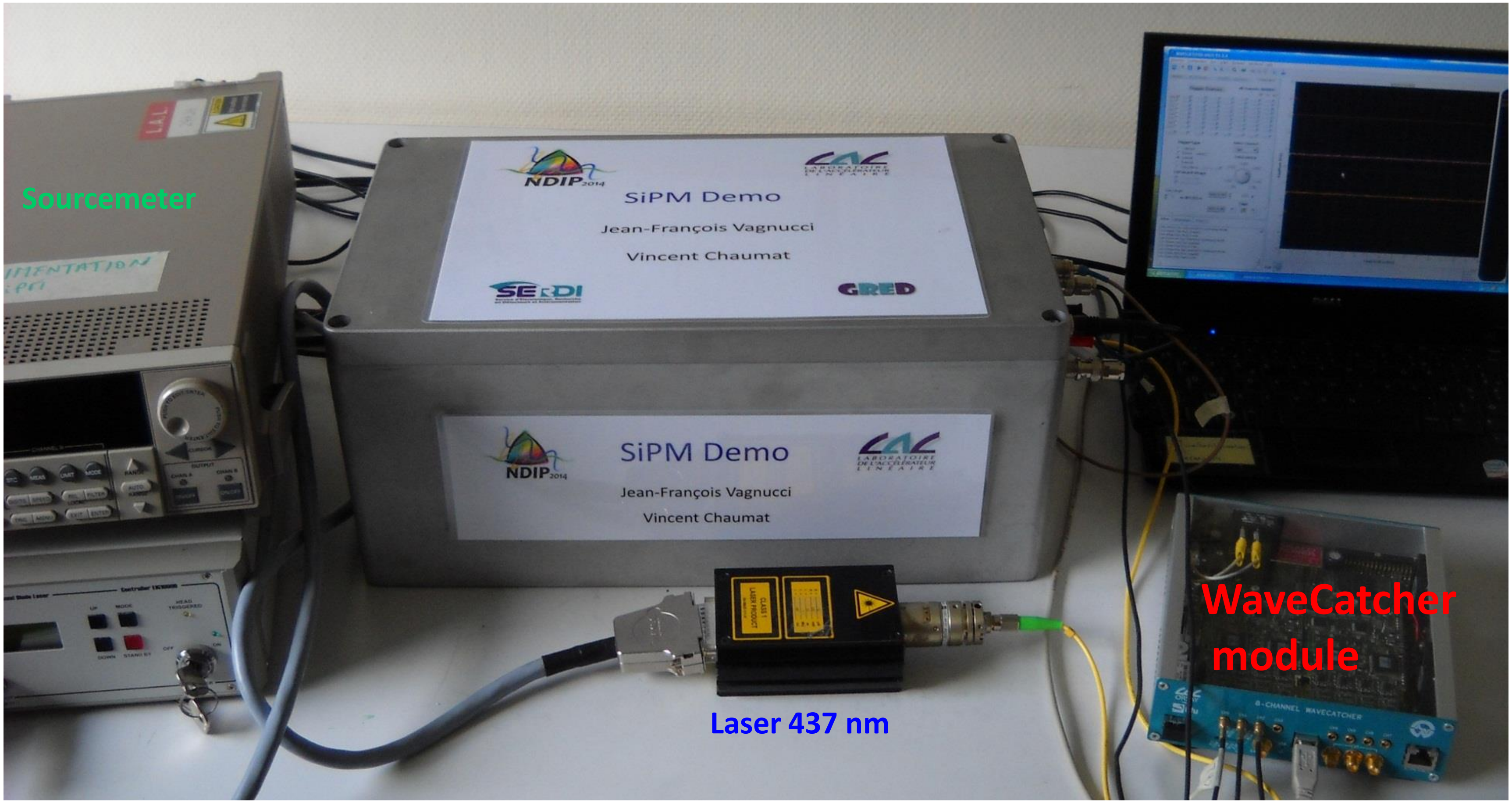

Drawing of the test bench

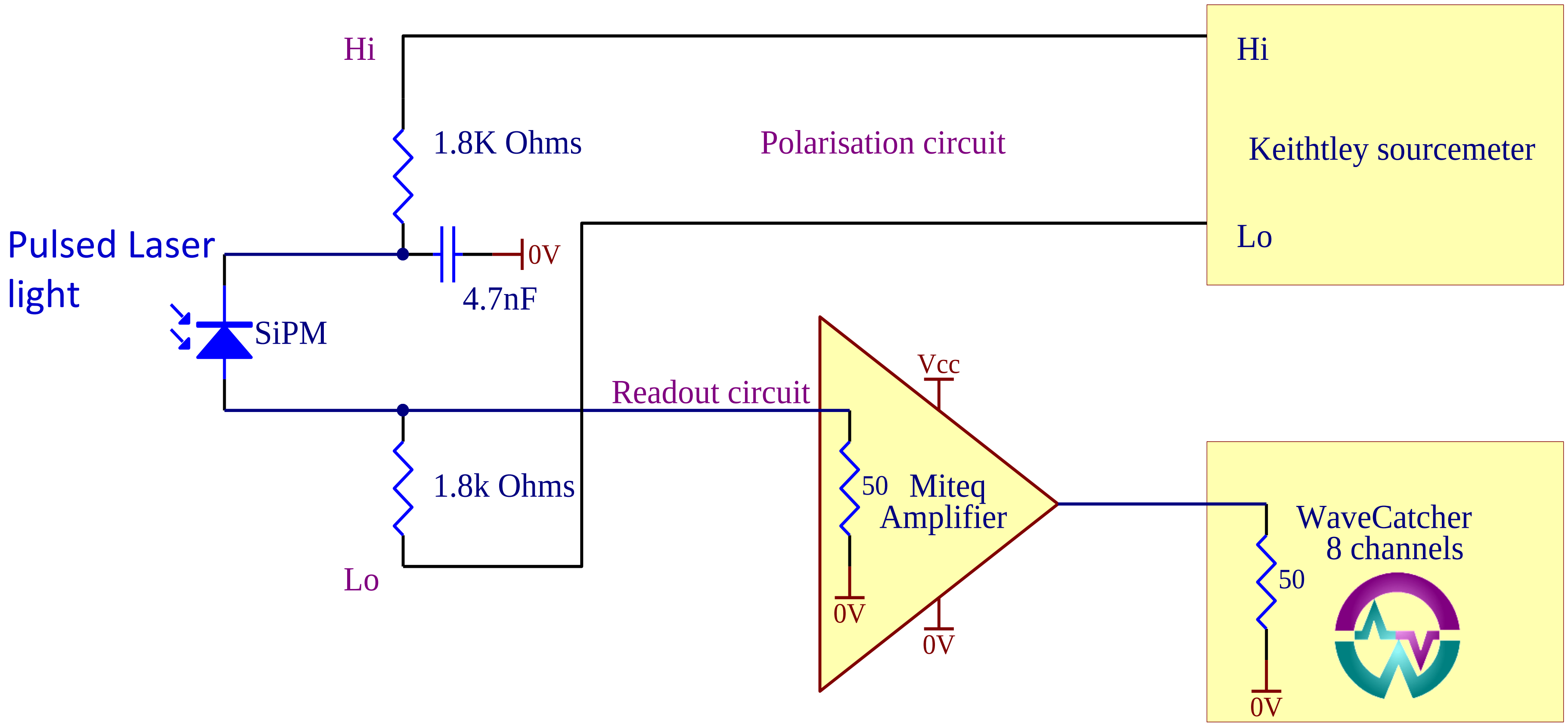

Drawing by V. Chaumat, LAL

Readout: WaveCatcher Module

- Based on the SAMLONG Analog Memory ASIC
- Sampling rate ranging between 400 MHS/s and 3.2GS/s.
- 1024 samples/channel
- 12 bits of dynamic range
- Small signal bandwidth > 500MHz
- Sampling jitter < 5 ps rms at the system level
- 8-channel synchronous system
- Advanced Oscilloscope-Like Software (Plug and Play)
- Embedded feature extraction: Baseline, Peak, Charge,CFD (TDC-like mode) …

Amplitude histogram

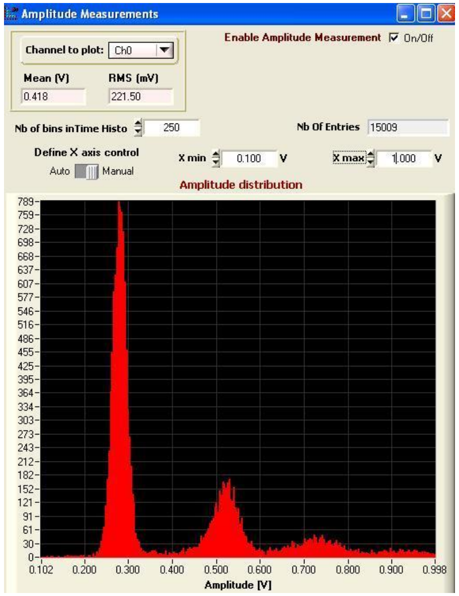

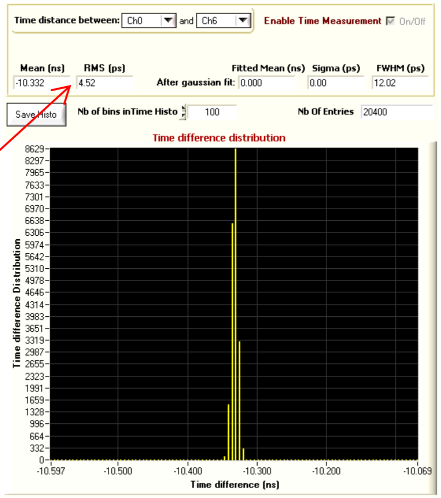

DCR as a function of the threshold

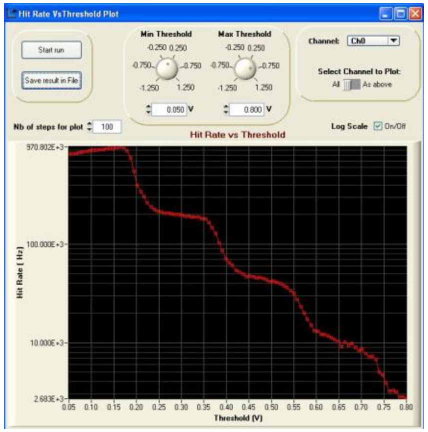

D. Breton, IEEE RT 2014

Thanks for your attention (even at 8 a.m after a night of football matches of the Word Cup in Brazil …)

Quarter-finale

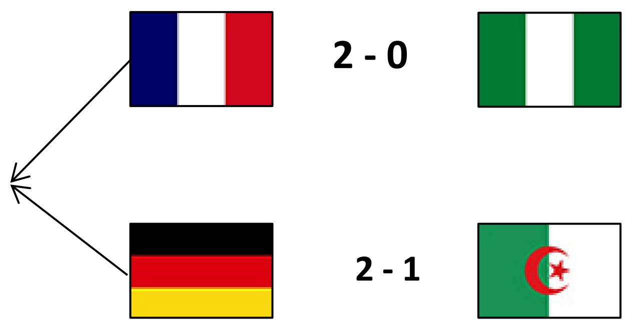

Backup material

Next generation Neutrino Experiment in China

60 km from Daya Bay and Haifeng

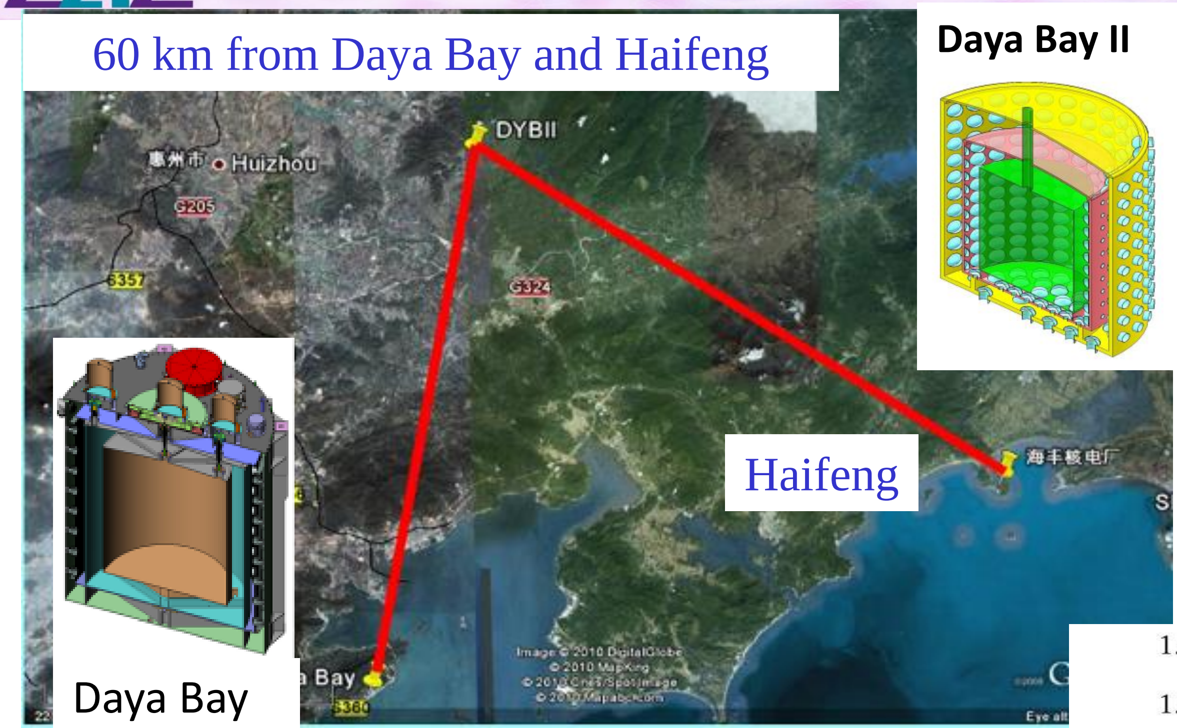

Daya Bay II

Huge Detector （LS + PMT

Energy resolution ~ 3%/√E

- Neutrino target: 30m(D)×30m(H)
- LS, LAB based : ~20kt
- Oil buffer: ~6kt
- Water buffer: ~10kt
- PMT (20”) :~20,000

Reactor experiments:

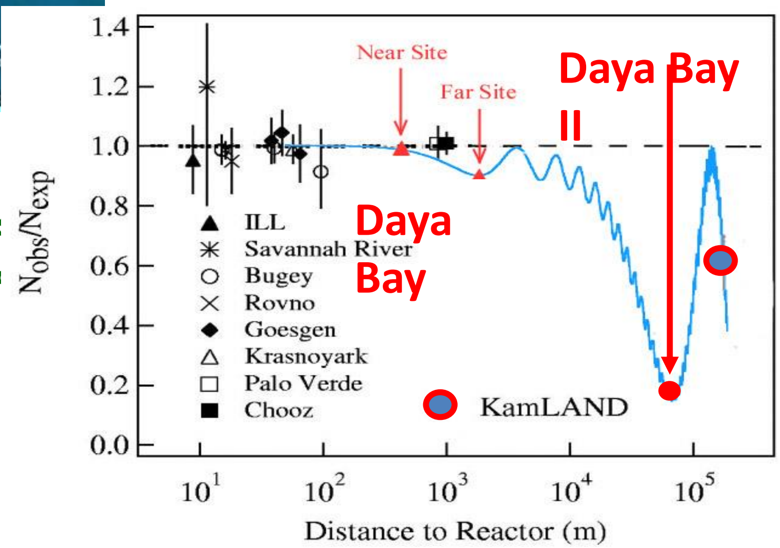

The Main Scientific goals:

⇨**Mass Hierarchy**

⇨Mixing matrix elements

⇨Supernovae

⇨geo-neutrinos

L. Zhan, et. al., Phys.Rev.D 78:111103,2008
L. Zhan, et. al., Phys.Rev.D 79:073007,2009

SiPMs for Calorimeters : CALICE AHCAL

High granularity hadronic calorimeter optimised for the Particle Flow measurement of multi-jets final state at the ILC

Photodetector requirements:

- insensitive to magnetic field (~ 4T)
- good sensitivity in blue-green
- cheap (10 millions channels)

studied SiPMs : MePHI/PULSAR, CPTA

HCAL prototype (from 2007 to 2011)

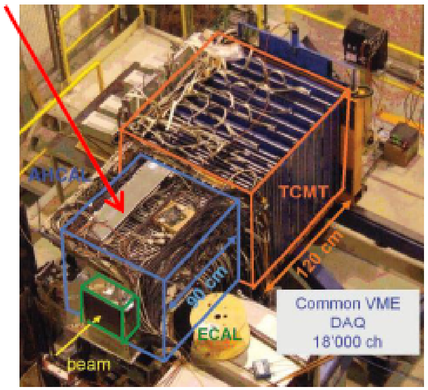

38 layers - ~ 7600 SiPMs from MePHI/PULSAR

scintillator tiles

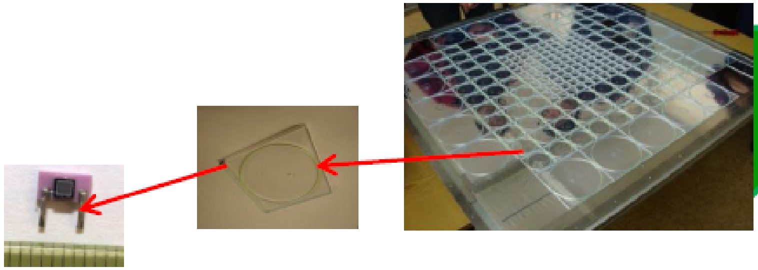

MePHI/PULSAR SiPM

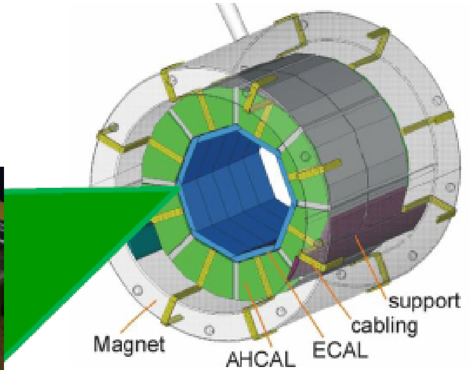

Michal Tesař, PhotoDet2012

HCAL test beams at SPS H8

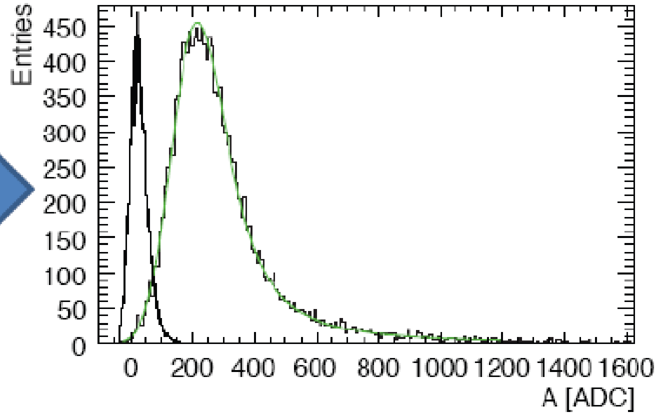

MIP distribution of muons

CALICE Collaboration, 2010 JINST 5 P05004

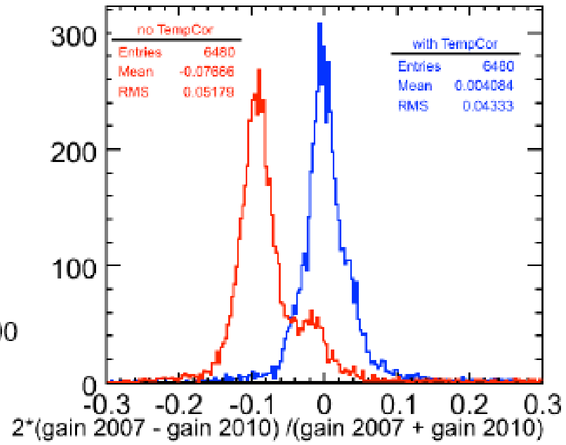

S. Lu, LCWS11

temperature dependance (variation of PDE x Gain : 3.7%/°C %)→ correction of response variations

Ongoing activity : engineering prototype is now under construction with SiPM from CPTA

SiPMs for Calorimeters : Upgrade of the CMS HCAL

HB & HE upgrade

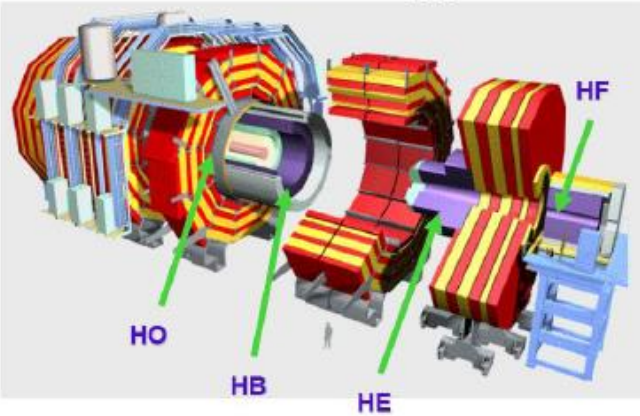

<u>Photodetector requirements (to replace the HPD)</u>:

- ➢ very large dynamic range: a few p.e → 2500 p.e
- ➢ high occupancy in front layers in SLHC → fast recovery time (5 – 100 ns)
- ➢ radiation hard up to 3.10^{12} 1 MeV neutrons/cm² for 3000 fb^{-1} (Gain*PDE change ≤ 20%)

<u>Studied SiPM</u> :
HAMAMATSU, ZECOTEK, FBK, CPTA , ST-Micro, Sensl, NDL, KETEK

Prototype HB RM used at 2011 Testbeam

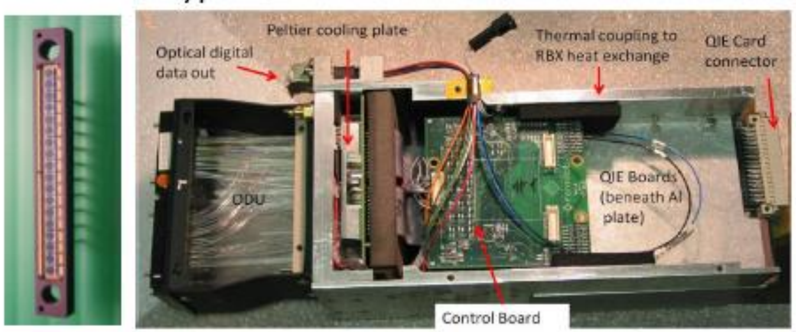

Y. Musienko, NDIP 2011

Temperature dependence → control @ 0.2 °C

Significant progress on the SiPM development over the last 2 years (HAMAMATSU , Zecotek, NDL) → the MPPCs from HAMAMATSU are close to satisfy most of the requirements.

Muon response in a single tower of CMS HO

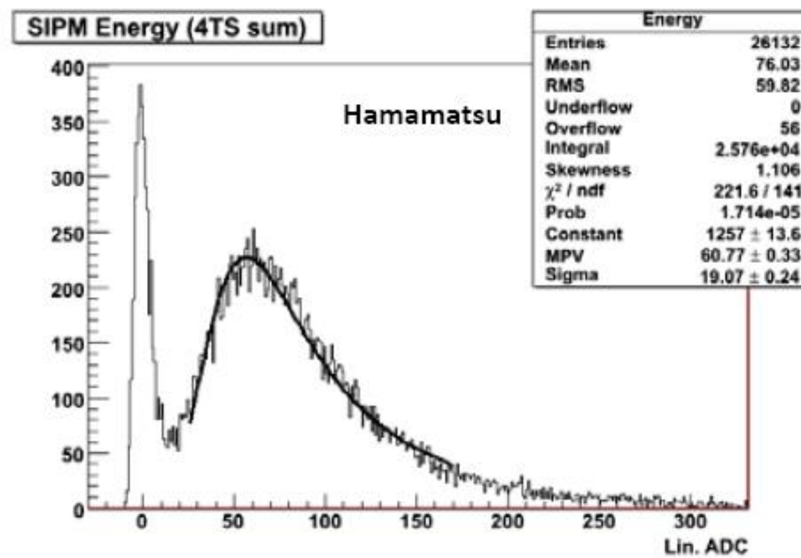

J. Freeman, FERMILAB-CONF-09-601-E

SiPMs for neutrino oscillation experiment: T2K

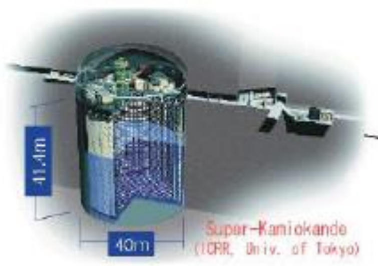

Far detector : Super Kamiokande

<u>ND280</u> : near detector complex - neutrino beam flux and spectrum measurements

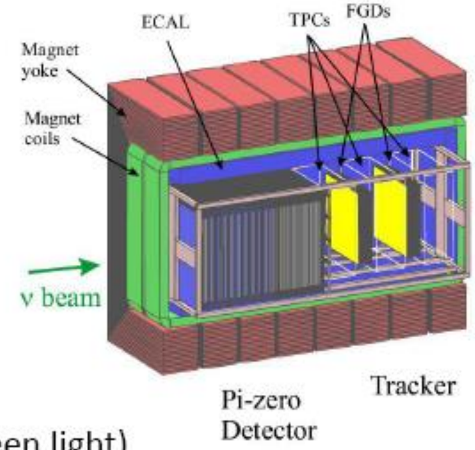

HAMAMATSU MPPC customized device

1.3 x 1.3 mm²

667 cells (50 x 50 μm²)

<u>Photodetector requirements</u>:

- insensitive to magnetic field
- coupling with a scintillator + WLS fiber (PDE > 20 % for green light)
- DCR < 1 MHz
- compact

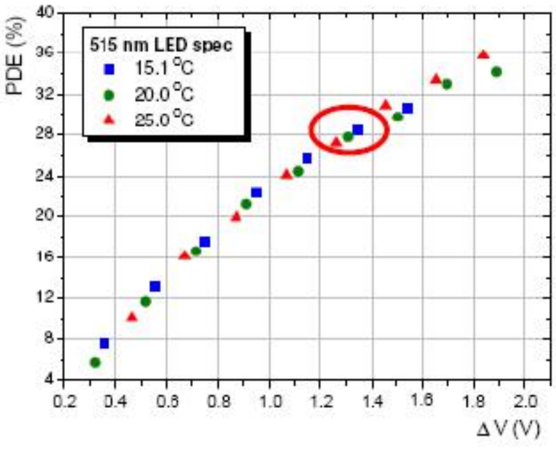

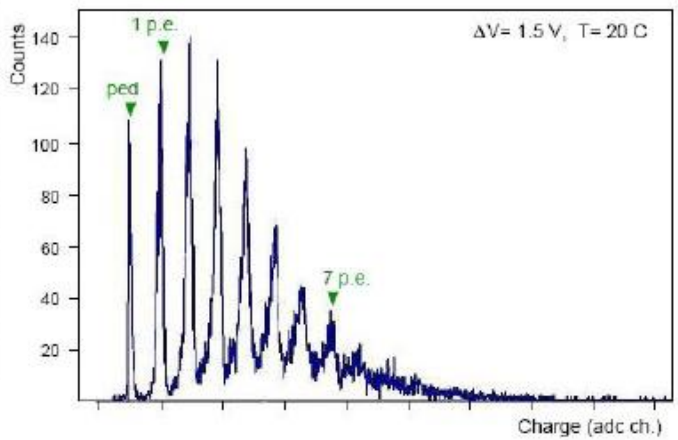

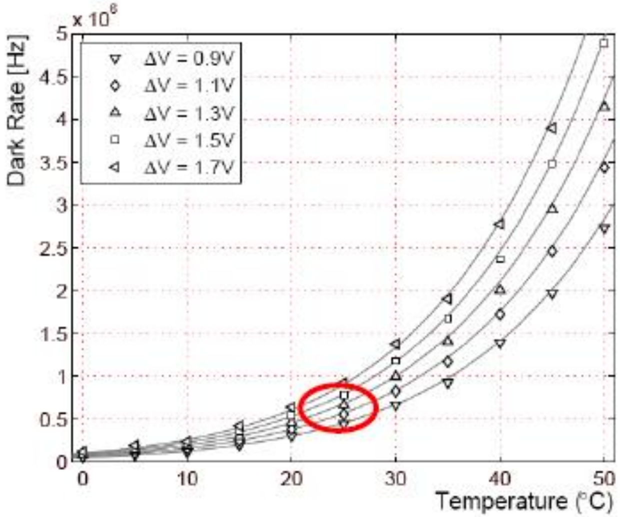

A. Vacheret, arXiv:1101.1996

<u>55996 MPPC tested</u> : only 0,16 % rejected

SiPMs for Cherenkov light detection (IACT)

FACT: First G-APD Cherenkov Telescope

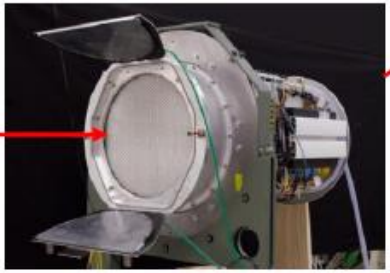

MPPC S10362-33-50C coupled to a cone light concentrator

1440 channels

Th. Krähenbühl, Photodet 2012

Photodetector requirements:

- PDE > 20 % for blue light
- ability to detect single photons
- stable
- robust
- compact

problem with the SiPM V_{BD} temperature dependance
→regulation of the bias voltage with a feedback system

First operation on the night of October 11, 2011

After one year of routine operation:

- no indication of any problem or ageing in any SiPM
- temperature as well as ambient-light dependence of SiPM well under control
- operation under very different ambient conditions shows no problem

an Event Seen by FACT

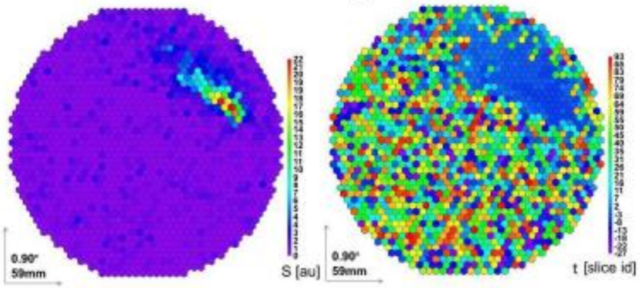

P. Vogler, TWEPP 2012

Small animal PET

miniature, high-resolution camera for a small-animal PET imaging system that is based on a combination of SiPM with a continuous scintillation crystal.

- LYSO continuous crystal (12 x 12 x 5 mm^3)
- monolithic matrices from FBK (DASIPM project)

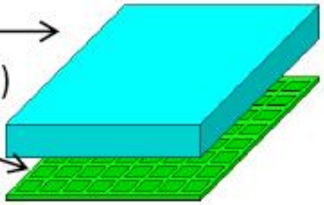

➢ $\Delta E/E$ ~ 15% FWHM (at 511 keV)
➢ $\Delta x = \Delta y$ ~ 0.7 mm FWHM

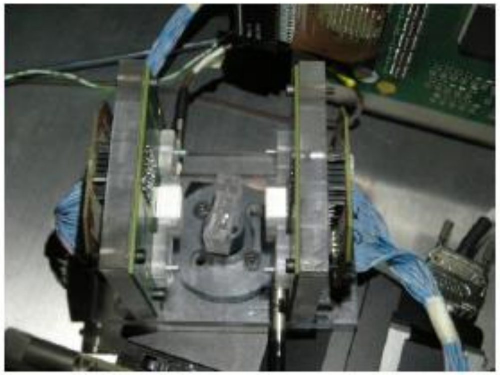

G. Llosa, PSMR 2012

AX-PET

from radial... ... to axial

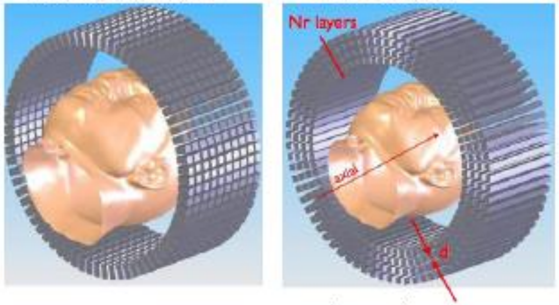

C. Joram, NIM A 654 (2011) 546-559

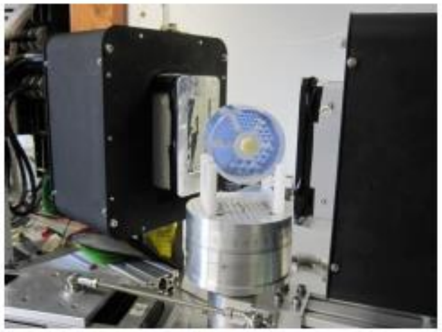

- long LYSO crystals (3×3×100 mm^3)
- orthogonal WLS strips
- readout by SiPMs from Hamamatsu
- 3D reconstruction of photons

Some results
➢ $\Delta E/E$ ~ 12% FWHM (at 511 keV)
➢ $\Delta x = \Delta y$ ~ 2 mm FWHM
➢ Δz (axial) = 1.8 mm FWHM

Latest development:
Use of Digital SiPM (Philips) for AX-PET with TOF → CRT < 200 ps FWHM.

Optimizing signal shape for timing

Single cell model → $(R_d||C_d)+(R_q||C_q)$
SiPM + load → $(||Z_{cell})||C_{grid} + Z_{load}$

Signal = slow pulse ($\tau_{d\,(rise)}, \tau_{slow\,(fall)}$) +
+ fast pulse ($\tau_{d\,(rise)}, \tau_{fast\,(fall)}$)

- $\tau_{d\,(rise)} \sim R_d(C_q+C_d)$ [intrinsic]
- $\tau_{fast\,(fall)} = R_{load}\,C_{tot}$ (fast; parasitic spike)
- $\tau_{slow\,(fall)} = R_q\,(C_q+C_d)$ (slow; cell recovery)

F.Corsi, et al. NIM A572 (2007) 416
S.Seifert et al. IEEE TNS 56 (2009) 3726

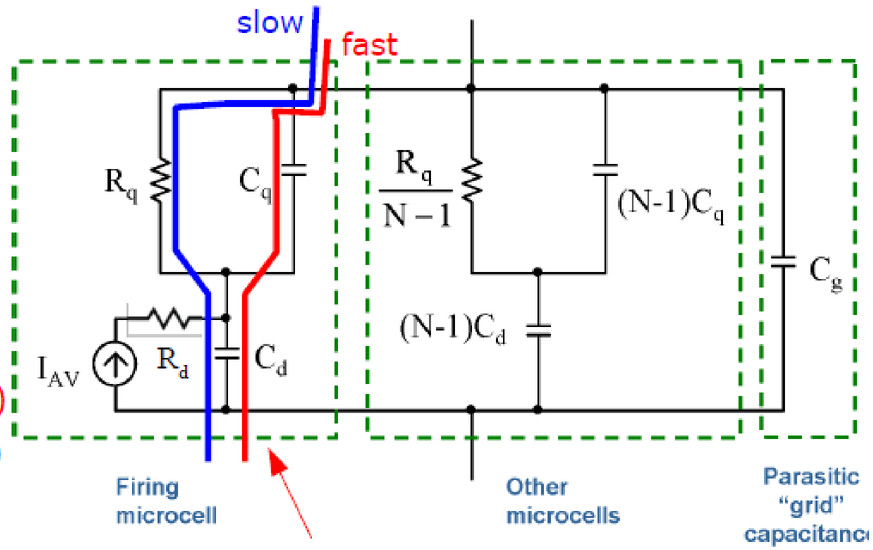

Cq → fast current supply path in the beginning of avalanche

Pulse shape

- Rise: Exponential
- Fall: Sum of 2 exponentials: transient + recovery

Sp.Charge Rd x Cd,q filtered by parasitic inductance, stray C, ... (Low Pass) → $O(R_{load}\,C_{tot})$

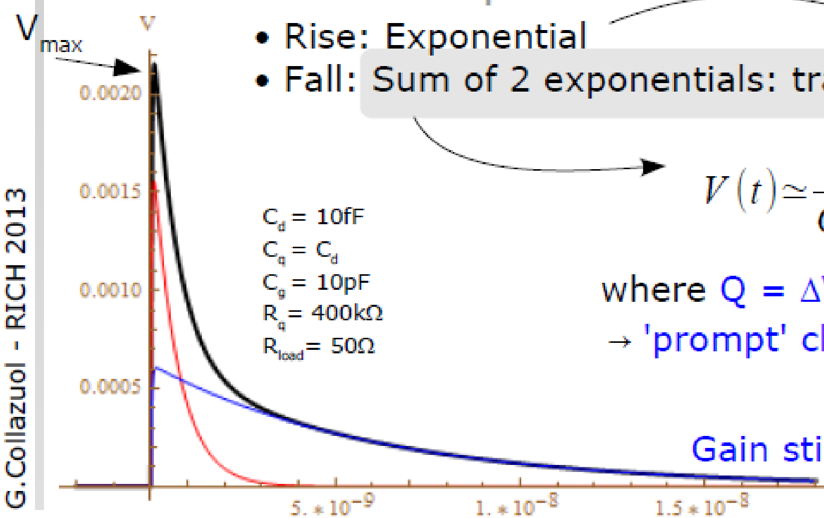

$$V(t) \simeq \frac{Q}{C_q+C_d}\left(\frac{C_q}{C_{tot}} e^{\frac{-t}{\tau_{FAST}}} + \frac{R_{load}}{R_q}\frac{C_d}{C_q+C_d} e^{\frac{-t}{\tau_{SLOW}}}\right) \text{ for } R_{load} << Rq$$

where $Q = \Delta V\,(C_q+C_d)$ is the total charge released by the cell
→ 'prompt' charge on C_{tot} is $Q_{fast} = Q\,C_q/(C_q+C_d)$

Gain still well defined: $G = \int dt \frac{V(t)}{q_e R_{load}} = Q/q_e = \frac{\Delta V (C_d+C_q)}{q_e}$

G.Collazuol - RICH 2013

SiPM – Electrical Model

[source: W. Shen]

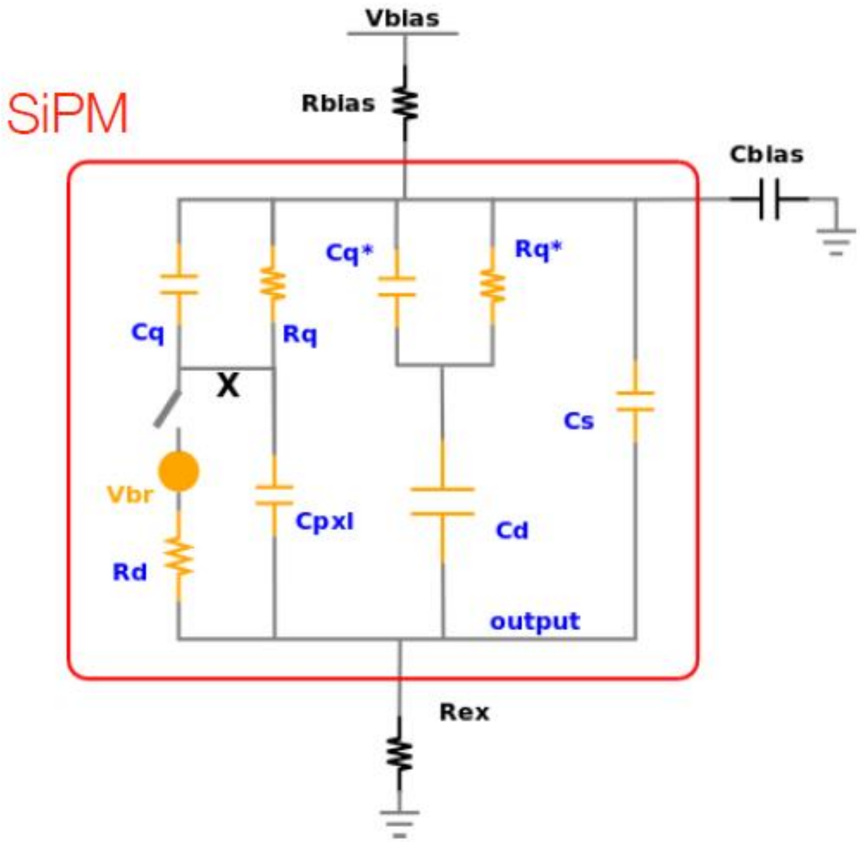

C_{pxl}	Pixel capacitance
C_q	Parasitic capacitance
C_d	Capacitance of inactive pixels
C_s	Stray capacitance
R_q	Quench resistor
R_d	Space charge resistance

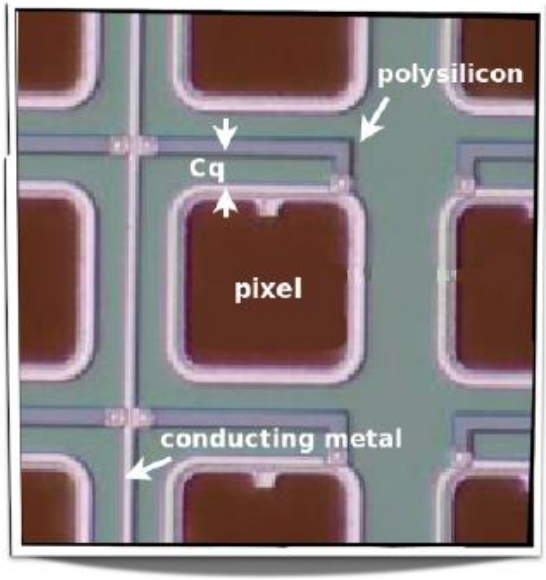

… and what about using just AC coupling …

SiPM std architecture

(a)

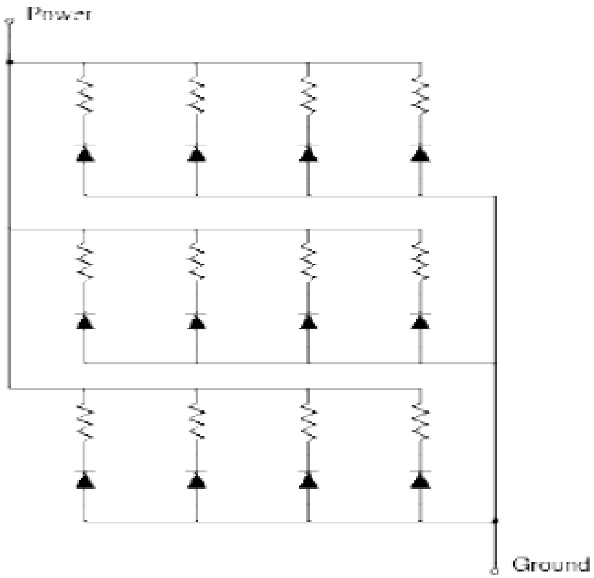

SensL new SiPM architecture for fast timing

(b)

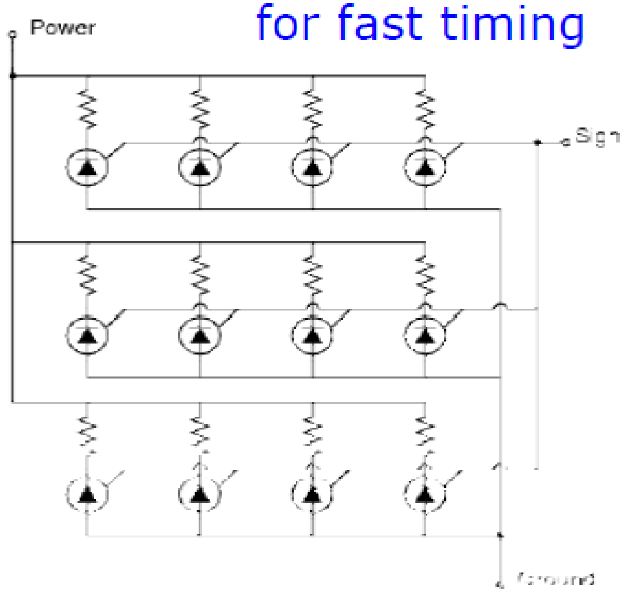

Figure 1: (a) traditional SPM architecture; (b) SPM architecture with inclusion of fast signal terminal.

The traditional SPM consists of a parallel array of avalanche photodiodes each in series with a quench resistor, as shown in Figure 1(a). In this configuration both bias and readout must occur on the same electrode. The introduction of a derivatively coupled electrode to each APD-resistor pair creates single-purpose signal line which delivers steeper rise-time pulses than the traditional SPM discharge which is inherently limited by the large output capacitance of each APD [3].

O'Neill et al " SensL New Fast Timing Silicon Photomultiplier " PhotoDet 2012 - proceedings

Prompt OC suppression using Si damaged by ion implantation

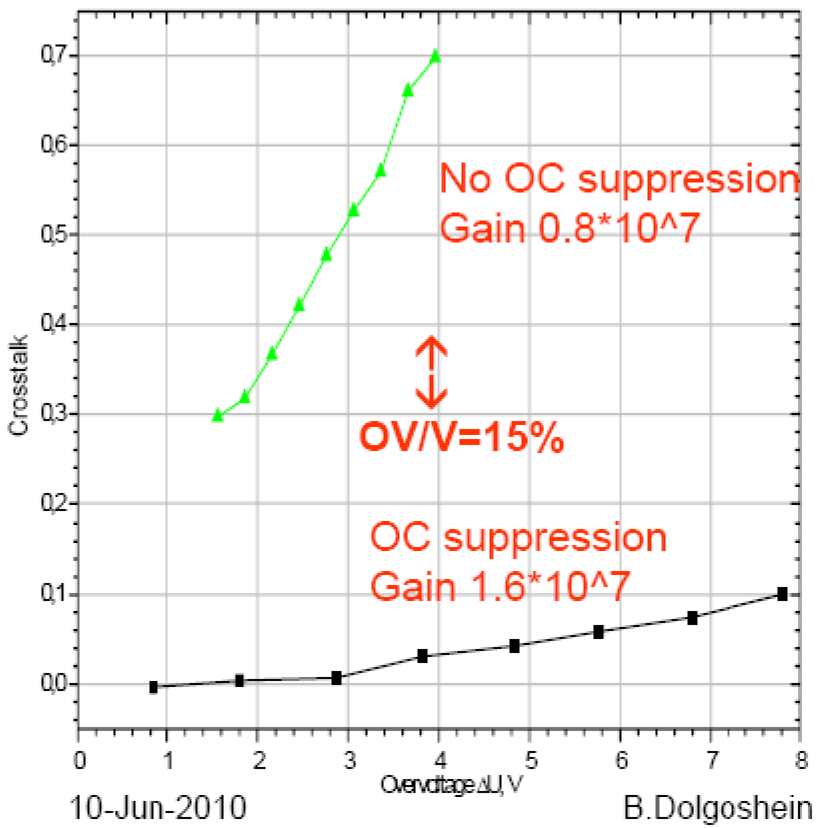

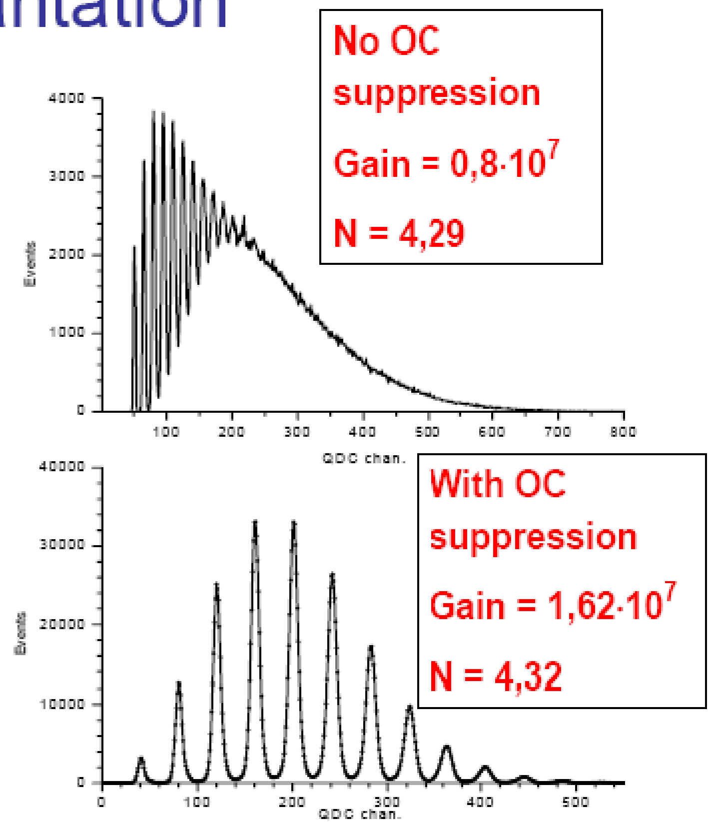

SiPM 1x1 mm^2

10-Jun-2010 B.Dolgoshein Silicon PM 27

MOS-SiPM (new "analog" SiPM structure)

Passive quenching + active recharge

Gola, Piemonte, Acerbi IEEE NSS 2013 (FBK-Advansid)

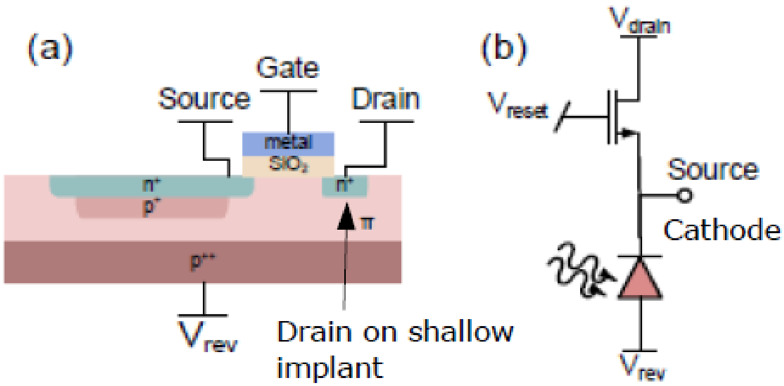

Fig. 1: (a) Structure of the MOS-SiPM cell, showing the transistor partially merged with the SPAD. (b) Schematic circuit of the microcell.

- **MOSFET transistor** replaces quenching R
- custom process
- **no losses** in Fill Factor
- **cheaper** than standard analog SiPM

- **Operation** : periodic reset

- **Features**

→ "hottest" cells self-disabled (like in d-SiPM)
  → low Dark Count device
→ After-pulsing suppressed almost completely
→ Very fast signal ~2ns width
  (AC coupling to Cathode)

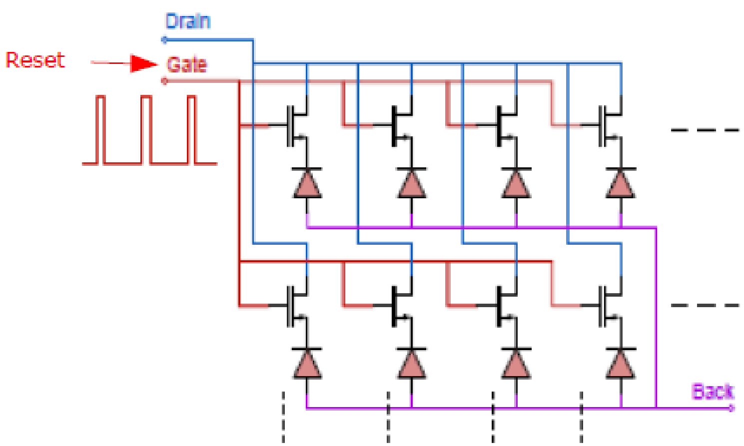

Fig. 2: Schematic circuit of the MOS-SiPM, showing the connections of the microcells.

!!! developement to be followed

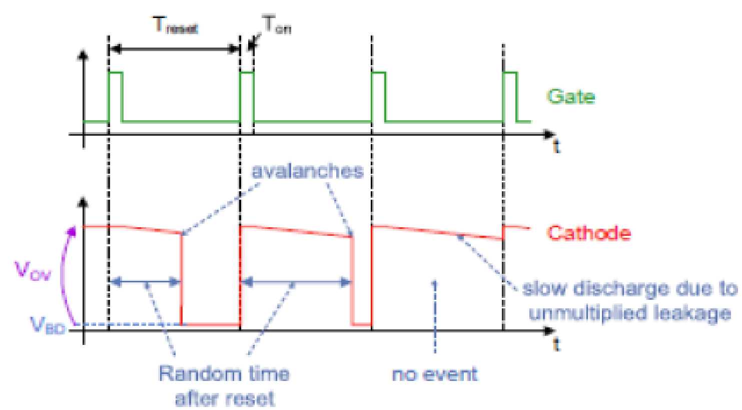

Fig. 3: Working principle of the MOS-SiPM, which is operated in a periodic pulsed reset mode.

SPTR: position dependence → cell size

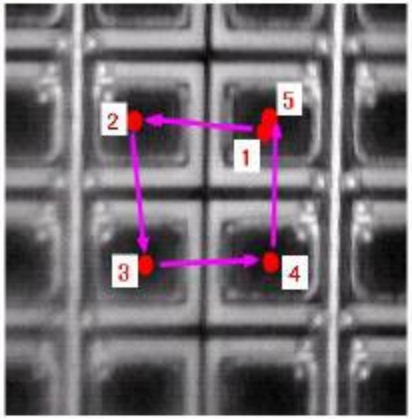

	FWHM (ps)	FWTM (ps)
1	199	393
2	197	389
3	209	409
4	201	393
5	195	383

K.Yamamoto PD07

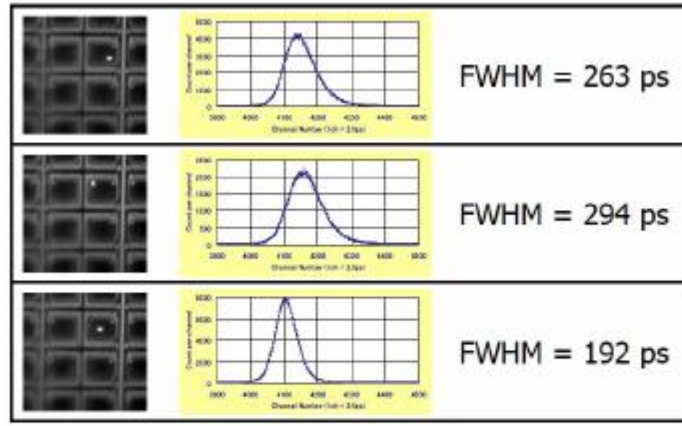

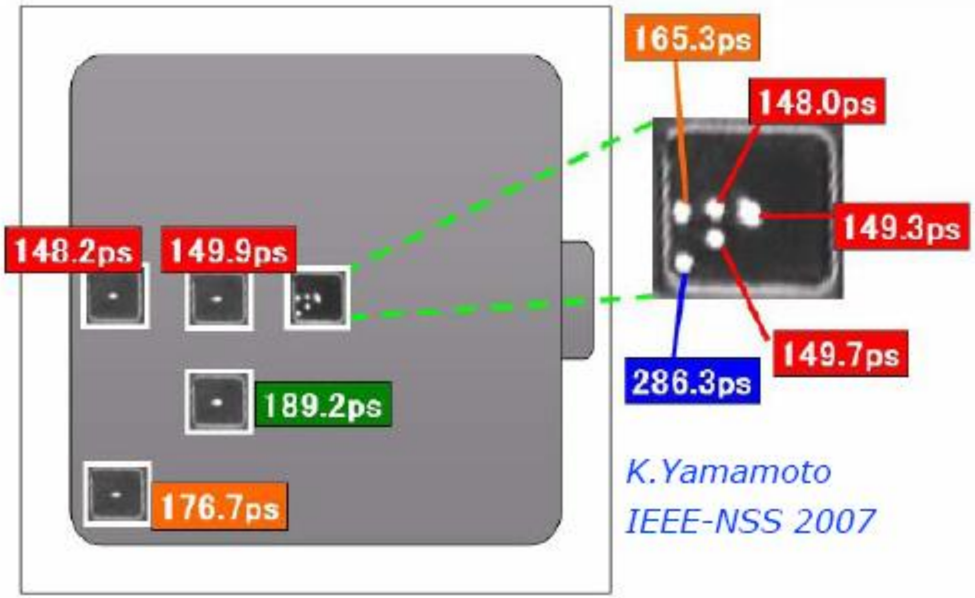

K.Yamamoto
IEEE-NSS 2007

Larger jitter if photo-conversion at the border of the cell

Due to:
1) slower avalanche front propagation

2) lower E field at edges

→ cfr PDE vs position

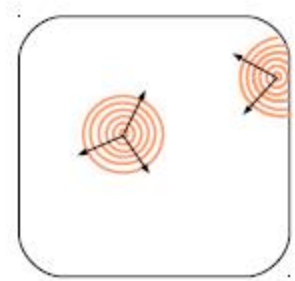

Data include the system jitter (common offset, not subtracted)

G.Collazuol - PhotoDet 2012

SiPM Single PhotoElectron timing Resolution

V. Puill et al, Single Photoelectron Timing Resolution of SiPM as a function of the bias voltage, the wavelength and the temperature, NIMA 54094, NDIP2011 Proceedings

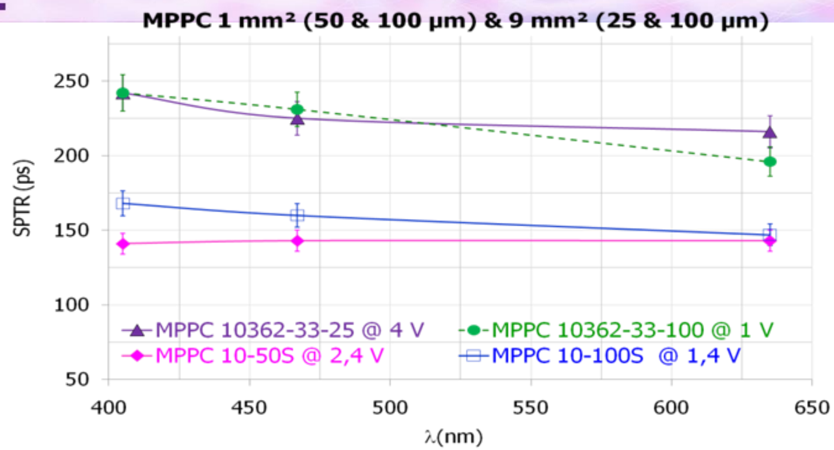

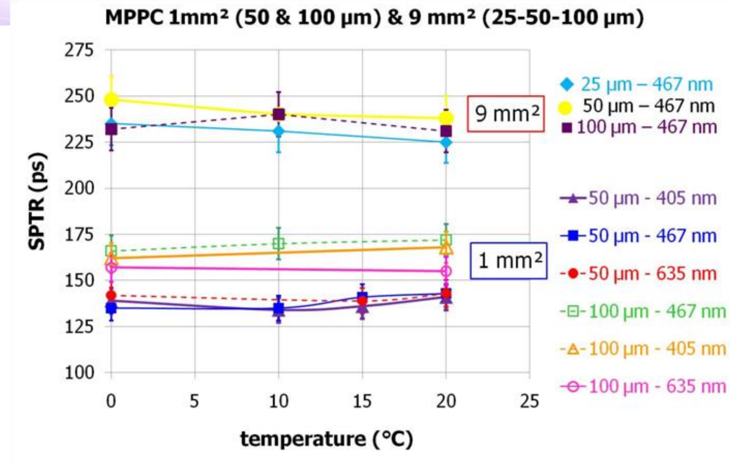

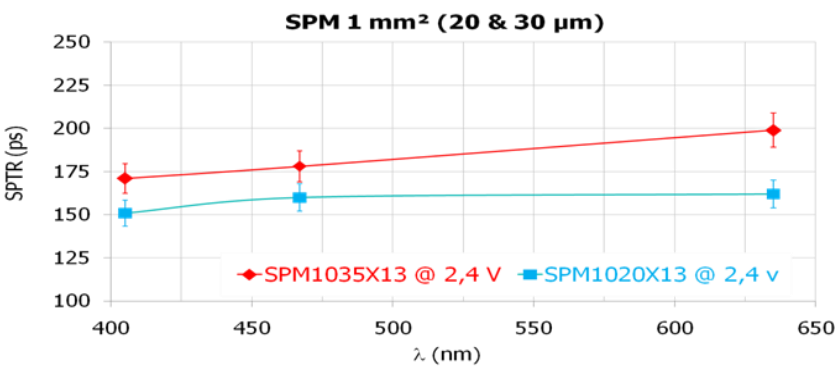

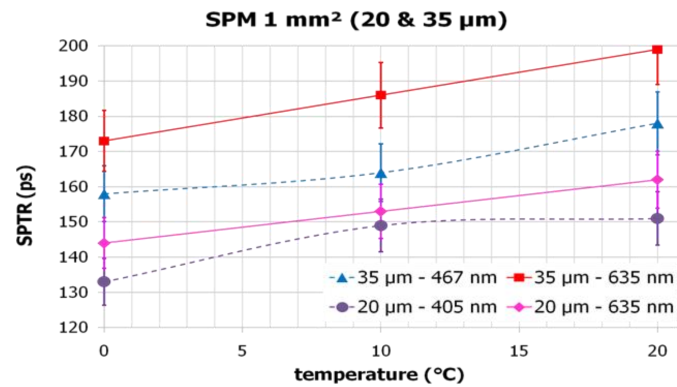

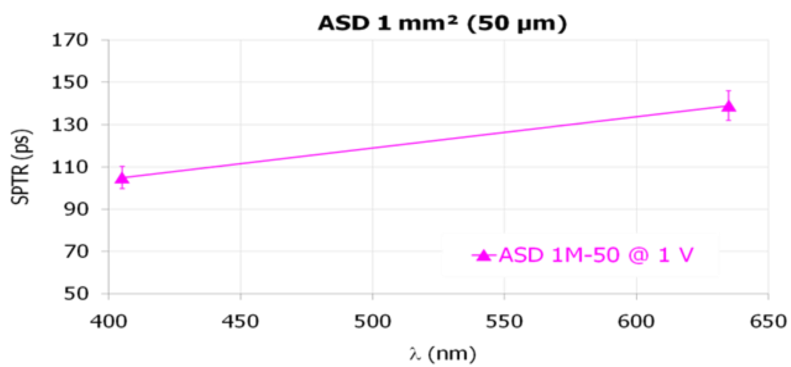

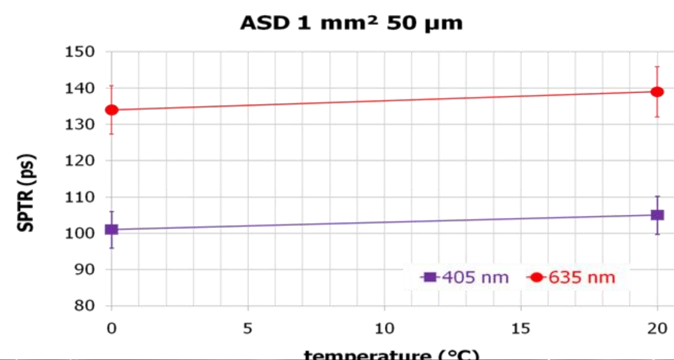

X-ray irradiation

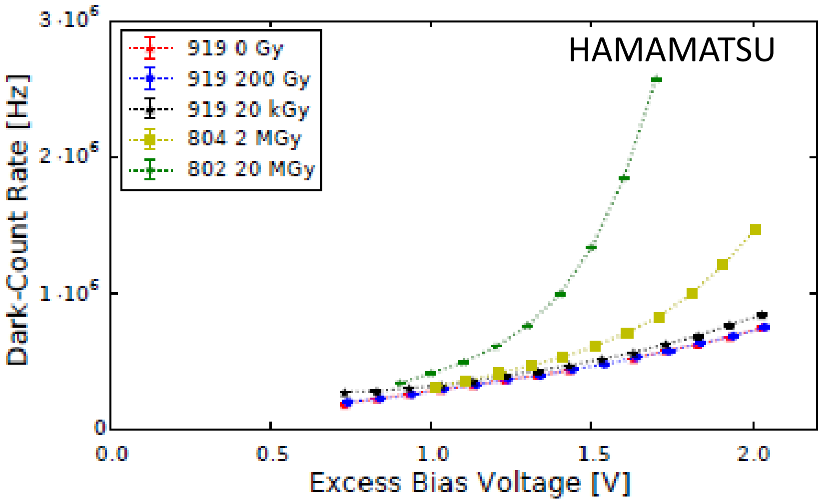

C. Xu, arXiv:1404.3206v2, 2014

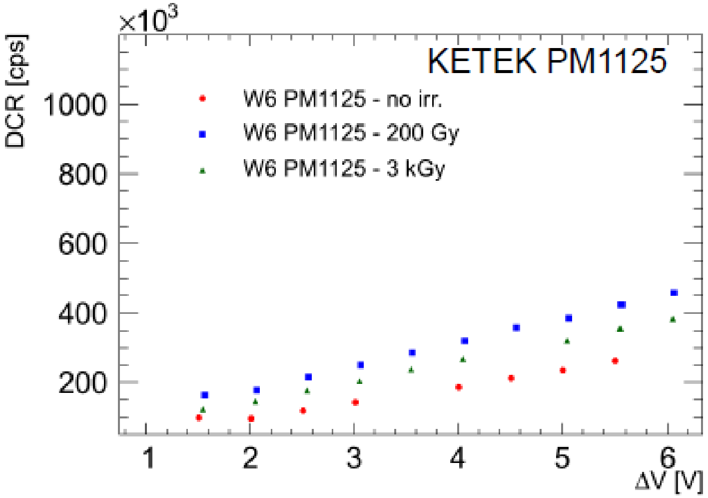

E. Garutti, IPRD13

Annealing

Proposal to Test Improved Radiation Tolerant Silicon Photomultipliers
F. Barbosa, J. McKisson, J. McKisson, Y. Qiang, E. Smith, D. Weisenberger, C. Zorn
Jefferson Laboratory

How to Extend the Lifetime?

SiPMs cooled to 5°C during the beam → reduction of the dark noise by a factor 3 and minimization of the effects of neutron irradiation

Beam down period : SiPMs heated to ~40°C (post-irradiation annealing) → bring the noise down to a residual level

SiPM Neutron Radiation Test

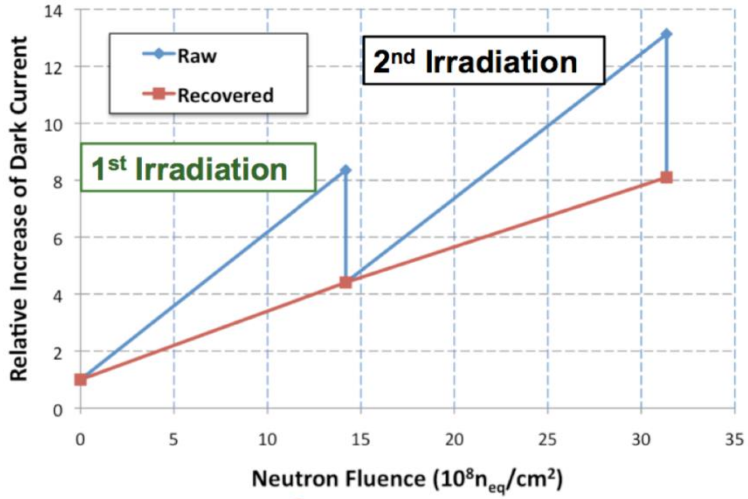

Neutron Fluence with 10^8 g/s on LH_2 Target with 1/3 efficiency
-> $3\times10^8\ n_{eq}/cm^2/year$

At 25°C, annealing requires at least 5 days

Heating to above 40°C can reduce the annealing time to less than 24 hours